AFWL-TR-
86-36

(2)

MECHANISMS OF PULSED LASER INDUCED DAMAGE TO OPTICAL COATINGS

Michael Ray Lange

The University of New Mexico
Albuquerque, New Mexico 87131

July 1986

Final Report

Approved for public release; distribution unlimited.

AIR FORCE WEAPONS LABORATORY
Air Force Systems Command
Kirtland Air Force Base, NM 87117-6008

AFWL-TR-86-36

This final report was prepared by the University of New Mexico, Albuquerque, New Mexico, under Contract F29601-84-K-0092, Job Order ILIR8412. Craig Hammond (CCN) was the Laboratory Project Officer-in-Charge.

When Government drawings, specifications, or other data are used for any purpose other than in connection with a definitely Government-related procurement, the United States Government incurs no responsibility or any obligation whatsoever. The fact that the Government may have formulated or in any way supplied the said drawings, specifications, or other data, is not to be regarded by implication, or otherwise in any manner construed, as licensing the holder, or any other person or corporation; or conveying any rights or permission to manufacture, use, or sell any patented invention that may in any way be related thereto.

This report has been authored by a contractor of the United States Government. Accordingly, the United States Government retains a nonexclusive, royalty-free license to publish or reproduce the material contained herein, or allow others to do so, for the United States Government purposes.

This report has been reviewed by the Public Affairs Office and is releasable to the National Technical Information Service (NTIS). At NTIS, it will be available to the general public, including foreign nations.

If your address has changed, if you wish to be removed from our mailing list, or if your organization no longer employs the addressee, please notify AFWL/CCN, Kirtland AFB, NM 87117-6008 to help us maintain a current mailing list.

This technical report has been reviewed and is approved for publication.

CRAIG HAMMOND
Project Officer

FOR THE COMMANDER

CARL E. OLIVER
Lt Col, USAF
Deputy Chief Scientist

ARTHUR H. GUENTHER
Chief Scientist

DO NOT RETURN COPIES OF THIS REPORT UNLESS CONTRACTUAL OBLIGATIONS OR NOTICE ON A SPECIFIC DOCUMENT REQUIRES THAT IT BE RETURNED.

REPORT DOCUMENTATION PAGE

1a. REPORT SECURITY CLASSIFICATION Unclassified	1b. RESTRICTIVE MARKINGS
2a. SECURITY CLASSIFICATION AUTHORITY	3. DISTRIBUTION / AVAILABILITY OF REPORT Approved for public release; distribution unlimited.
2b. DECLASSIFICATION / DOWNGRADING SCHEDULE	
4. PERFORMING ORGANIZATION REPORT NUMBER(S)	5. MONITORING ORGANIZATION REPORT NUMBER(S) AFWL-TR-86-36
6a. NAME OF PERFORMING ORGANIZATION University of New Mexico 6b. OFFICE SYMBOL (If applicable)	7a. NAME OF MONITORING ORGANIZATION Air Force Weapons Laboratory
6c. ADDRESS (City, State, and ZIP Code) Bandolier Hall West Albuquerque, New Mexico 87131	7b. ADDRESS (City, State, and ZIP Code) Kirtland AFB, NM 87117-6008
8a. NAME OF FUNDING / SPONSORING ORGANIZATION 8b. OFFICE SYMBOL (If applicable)	9. PROCUREMENT INSTRUMENT IDENTIFICATION NUMBER F29601-84-K-0092
8c. ADDRESS (City, State, and ZIP Code)	10. SOURCE OF FUNDING NUMBERS PROGRAM ELEMENT NO. 61101F; PROJECT NO. ILIR; TASK NO. 84; WORK UNIT ACCESSION NO. 12

11. TITLE (Include Security Classification)
MECHANISMS OF PULSED LASER INDUCED DAMAGE TO OPTICAL COATINGS

12. PERSONAL AUTHOR(S)
Lange, Michael Ray

13a. TYPE OF REPORT	13b. TIME COVERED	14. DATE OF REPORT (Year, Month, Day)	15. PAGE COUNT
Final	FROM _____ TO _____	1986 July	138

16. SUPPLEMENTARY NOTATION
Submitted in partial fulfillment of the requirements for the Degree of Docto. of Philosophy in Optical Sciences.

17. COSATI CODES		
FIELD	GROUP	SUB-GROUP
20	05	
11	03	

18. SUBJECT TERMS (Continue on reverse if necessary and identify by block number)
Pulsed Laser Induced Damage; Optical Thin Film Coatings; Temperature Dependent Absorption

19. ABSTRACT (Continue on reverse if necessary and identify by block number)

report addresses this problem
Laser induced damage in optical components is the limiting factor in the design of high power lasers. This ~~problem is addressed in this present work~~ with special emphasis placed on the optical coatings used upon the components. A theoretical model is developed assuming basic mechanisms which lead to damage of the coatings. Numerical results are generated which are compared with experimental data.

The basic procedure applied to this problem is that of the solution of inhomogenous field equations representing classical heat and electron diffusion in solids. The technique used is integral transform mathematics. The results are supported by modeling with a numerical finite element program. Findings

Findings from this work include several sets of scaling relations which give insight into the relationship of the damage threshold of optical coatings to the material and laser→(over)

20. DISTRIBUTION / AVAILABILITY OF ABSTRACT ☒ UNCLASSIFIED/UNLIMITED ☐ SAME AS RPT ☐ DTIC USERS	21. ABSTRACT SECURITY CLASSIFICATION Unclassified
22a. NAME OF RESPONSIBLE INDIVIDUAL Craig Hammond	22b. TELEPHONE (Include Area Code) (505) 844-9856 22c. OFFICE SYMBOL CCN

DD FORM 1473, 84 MAR — 83 APR edition may be used until exhausted. All other editions are obsolete.

19. ABSTRACT (Continued)

parameters involved. These are plotted versus experimental data for support of the assumed processes. The specifics of these findings include the fact that the rate at which thermal diffusion occurs in optical components is important, and that there is a fundamental difference in the damage process between oxide and fluoride coatings. In addition, basic mechanisms are suggested as the source of damage in these coatings.

Further research directions are suggested in the conclusions, including some possible experiments.

ACKNOWLEDGMENTS

The list of persons and institutions for which I am indebted in relation to this work is somewhat lengthy. I will list a few of the more significant ones here, and state that this list is by no means complete.

I would first like to acknowledge the Chairman of my committee, my advisor and friend Dr. John K. McIver for the seemingly endless and flawless guidance. I can make the same statement about Dr. Arthur H. Guenther, another member of my committee and Chief Scientist of the institution which supported all of my work, the Air Force Weapons Laboratory.

Furthermore, I would like to thank Col. Tom Walker for providing the challenging problem, Dr. Alan Stewart for his stimulating discussions, Jeanne Williams for the manuscript preparation, Pat Whited for handling the bureaucracy and Nancy Slate for tolerating me through the whole experiance.

TABLE OF CONTENTS

LIST OF ILLUSTRATIONS

LIST OF ILLUSTRATIONS—Continued.

LIST OF TABLES

CHAPTER 1

INTRODUCTION

Laser induced damage in optical components is the limiting factor in the design of high power lasers. This statement applies particularly to coated optical components due to the coatings' lower damage thresholds. The problem has existed since the beginning of the laser and is exhibited through the research published in this field. A prime example of this is the National Bureau of Standards' Special Publication of the Proceedings of the Symposium on Optical Materials for High Power Lasers, or Boulder Damage Symposium which has been held annually for the past seventeen years (since 1969).

Understanding of this phenomena has been limited because of the complexity of the many processes involved and the lack of the ability to model intense field interactions. In addition, material technology is just beginning to reach a stage where adequately pure materials can be produced for high intensity optical applications. The deposition of optical coatings lags in this area due to the extreme complexity of producing a quality optical thin film. The characteristics (packing density, porosity, purity, stoichiometry, uniformity, etc.) of optical coatings seldom approach their bulk counterparts. The particular interest in optically thin films is because of their relative sensitivity to intense fields and the fact that most optical components are coated to suppress or enhance reflection.

The conditions of deposition (partial vacuum, temperature, molecular energies, etc.) along with substrate processing (polishing, etc.) used in the production of optical quality coatings are also conducive to film imperfections. Furthermore, molecular growth of films not only tends to allow trapping of undesirable substances, but may even promote it [Barna, Radoczi and Reicha 1985]. Imperfectly cleaned substrates may also cause misalignments of growth (nodules) [Guenther 1981] with poorly bonded boundaries and defects of various sorts. There is significant evidence [Hurt and Decker, 1984] that these imperfect regions are sources of the initiation of laser induced damage in optically thin films.

In practice, optical components are often coated with many layers of films. This multilayer system introduces many new problems which are not related to the basics of the interaction of the field and the film. For example, the field distribution within a stack of films must be computed; the difficulties of controlling the quality and parameters increases significantly with an increase in the number of layers; furthermore, the many interfaces (a weak point of coatings) of different materials adds to the complication. For this reason, these studies are restricted to a single layer film.

There are several good data bases for laser induced damage in single layer optical coatings [Walker, Guenther and Nielson 1981; Bettis 1975; Rainer, et al. 1982]. Due to the difficulty of controlling and characterizing all of the parameters (film and laser) involved, a large data base is desirable to minimize the effect of statistical fluctuation in the damage threshold.

The goal of this research is the development of a model of laser induced damage in optical coatings, based upon thermodynamic considerations, and the correlation with of the observed trends in the data. From the model a microscopic theory is then developed which produces the required conditions for the thermodynamic model.

Most analytic research in this field has been restricted to laser interaction with ideal intrinsic materials. These unfortunately bear no resemblance to real world optical coatings. The theoretical projections, when compared to data, make this glaringly apparent. Most other works concerned with extrinsic processes have either concentrated upon mechanisms of absorption or thermodynamic treatments. Several models have been developed based upon absorption and thermal diffusion that takes place in the optical materials [Bloembergen 1972; Walker, et al. 1981; Komolov 1982]. None, to this point, have demonstrated a relationship between the films thermal properties and the damage that takes place. In addition, none of the thermal models have described mechanisms for the absorption that takes place other than that there must be an absorbing impurity of some sort.

That is not to say that the ultimate solution of laser induced damage in optical coatings has been found. A physically feasible process has been described and justified, however, which is completely consistent with the most thorough data sets of laser induced damage of optical coatings.

The only previous relationship found for laser induced damage to optical coatings with material properties was that of Bettis' [1975] scaling with index of refraction. Though Bettis' model was simple, it

scaled quite well with some bulk damage data, in addition to some coatings. It did not , however, scale well with much of the data used in this present study. Furthermore, it was based upon the classical analog of the transition probability intrinsic to the respective coatings and should not apply well to the extrinsic damage observed in the coatings of interest. Furthermore it does not explain the observed morphology in the optical coatings of interest.

It is clear to this author that there are many processes of laser induced damage in optical materials that apply to many different situations. The processes described within may be more or less applicable than described. The calculations demonstrate that they must at least be a contributing factor.

The morphology of damage in fluoride and some oxide films dictate that damage, and thus anomalous absorption, occurs at isolated microscopic sites [Walker, et al. 1981]. Therefore, a natural model is that of a localized site absorbing at many times the rate of the surrounding film. Due to the localization of the damage and the scales involved (diameter of damage site $2a \sim 0.1$ microns, pulse length 5 to 40 ns) significant thermal diffusion of energy must take place (i.e. $\delta = \sqrt{Dt_p} > a$). Here D is the thermal diffusivity in cm^2/s and t_p is the laser pulse length. Thus, it is likely that thermal diffusion of the absorbed energy is an important factor in the determination of the required incident laser energy which causes damage.

The morphology of damage suggests that an appropriate model to try is that of a spherical region which absorbs radiation. The scales involved necessitate that the dominant process in the localized energy

deposition leading to damage is diffusion. This mathematical model is developed in the following chapter. The requirement of a spherical region is unnecessary. The spherical geometry is primarily used because of the mathematical tractability.

Thermal heat balance demonstrates that for a given distribution of absorbing region sizes there is one size of region most likely to damage. The characteristic size of the most easily damaged region is determined by the material parameters and the pulse length. This concept is applied in a broad sense because even if the regions evolve in time they have some average size over the duration of the pulse which determines the quantity of energy absorbed. This concept is consistent with the observed morphology [Walker, et al. 1981]. In particular, the damage regions observed are larger at longer pulse lengths. The reasonable criterion chosen for damage is that the boundary of the region reaches some characteristic phase change temperature. The melting temperature is chosen for these studies due to the observation of a region bordering the pits where material flow seems to have occured.

The appropriate heat conduction equations are then formulated and solved via LaPlace Transform [Goldenberg and Tranter 1952], or via the more general integral transform [Ozisik 1980]. The quantity of interest is the incident laser energy density which causes the localized region to heat up to the damage criterion point. This quantity is exhibited in the non-homogeneous source term of the thermal diffusion equation. It is multiplied by an absorption cross section for the

absorbing region and indicates what portion of the incident beam is absorbed and deposited in the localized volume.

The classical absorption cross section is computed from electromagnetic theory (Mie Theory) [Born and Wolf 1980] assuming an highly absorbing localized region (a sphere). The size of the sphere used is that of the size of the region most likely to damage due to thermal considerations.

With this model all parameters of import may be specified with the exception of the properties of the absorbing region. It is shown in the following chapter that for regions and properties of interest (i.e., those of the data) the thermal properties of the absorbing region are not important, while those of the surrounding film are. The optical properties of the absorbing region, however, are important. This applies particularly to the imaginary part of the index of refraction which is a direct measure of the energy that is absorbed in the region.

Both observation [Bliss, Milam and Bradbury 1973] and theory [Meyer, Bartoli and Kruer 1980] indicate that the evolution of the imaginary part of the index of refraction is fast with respect to the incident pulse length. Further theoretical evidence of this will be presented in Chapter 6. It is not likely that these highly absorbing regions exist before the incident pulse.

In addition to the effects of the surrounding film on the laser damage threshold for a single incident pulse, the mathematical generality of integral transform technique of solution allows the investigation of other effects. One such effect is that of the

substrate and its conductivity on the rate at which an absorbing site heats up. Another such effect is that of thermal build up due to a repetitively pulsed laser. The models and results of these studies will be presented in Chapters 3 and 4. It is shown that the substrate conductivity can be important and that thermal build up in repeated pulses is usually negligible. Experimental comparison of the work described there will be given in Chapter 5. The comparison with available experiments lends validity to this model. It also provides an order of magnitude estimate of the range of the otherwise unknown optical absorption coefficient and its behavior.

Chapter 6 addresses the evolution of the electron density which is the source of the imaginary part of the index of refraction in the optical absorption. It is shown that common absorbing centers in optical materials used for coatings can provide significant localized absorption adequate for the evolution of the localized sites which lead to damage. It is also likely that these centers exist in high densities in optical coatings due to the conditions of deposition and polishing.

Chapter 7 addresses the role of temperature dependence in the absorption and diffusion leading to damage in optical films. The findings are that temperature dependent absorption can (but doesn't necessarily) contribute to damage in small band gap oxide films, but cannot have any significant effect in the larger band gap fluoride films. Temperature dependence of material parameters can be important quantitatively for the diffusion processes, but the dependence is very

complicated and often unknown. The dependence, however, should not affect qualitatively the findings of this work.

CHAPTER 2

THE LOCALIZED ABSORPTION-DIFFUSION MODEL

The localized absorption-diffusion model incorporates a small localized region within the film that absorbs the incident laser radiation at a rate far above that of the surrounding film. The absorbed energy subsequently diffuses through the surrounding film. The cross section of the absorbing center available to the radiation together with the diffusion capability of the film determine the rate at which the region approaches the critical temperature at which damage ensues.

In this section an analytical expression for the damage threshold is described which is valid for arbitrary shapes of an incident pulse. The particular example of a single flat-top-pulse is then discussed.

The derivations are shown in Appendix A and the predictions of this model are compared to experimental data in Chapter 5.

A general description of the problem is illustrated in Fig. 1. A spherical absorbing region of radius a is embedded in a surrounding material of different optical and thermal properties. Only the region is permitted to absorb radiation. The size of the region is assumed to be much smaller than the laser spot size so that absorption can be thought of as occuring in a field with a constant radial intensity.

The thermal properties of the system are described by the thermal conductivity K and the thermal diffusivity D of each region.

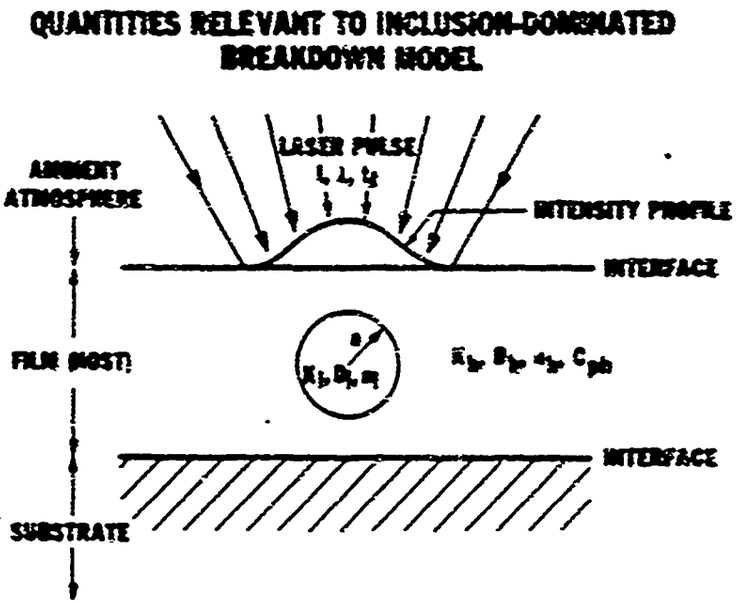

Fig. 1. Quantities relevant to inclusion-dominated breakdown model.

These properties in concert with the rate at which radiation is absorbed are taken to be independent of temperature. This does not mean that absorption is assumed to be constant. The assumption is that the change in absorption is sudden (i.e., of small duration compared with the pulse length). The system is said to be damaged when the interface between the two regions reaches some critical temperature (e.g., the melting temperature of the film). This condition is chosen because an interface between a film and an absorbing region would be a stressful point, and melting has been observed.

Mathematically the temperature distribution in the system is described by the following thermal diffusion equations [Ozisik 1980]:

$$\frac{1}{D_i}\frac{\partial T_i(r,t)}{\partial t} = \frac{1}{r}\frac{\partial^2}{\partial r^2}(rT_i) + \frac{A}{K_i} \qquad r \leq a \ , \tag{1}$$

$$\frac{1}{D_h}\frac{\partial T_h(r,t)}{\partial t} = \frac{1}{r}\frac{\partial^2}{\partial r^2}(rT_h) + \frac{A}{K_i} \qquad a < r \ , \tag{2}$$

$$T_i(r,0) = T_h(r,0) = 0 \ , \tag{3}$$

where the subscripts i and h refer to the inclusion and the host respectively and A is the source term. The interface condition between the impurity and the host is assumed to be

$$T_i(a,t) = T_h(a,t) \ , \tag{4}$$

$$K_i \left.\frac{dT_i}{dr}\right|_a = K_h \left.\frac{dT_h}{dr}\right|_a \ . \tag{5}$$

The solution for this system may be found using the LaPlace (temporal) transform or by an integral (spatial) transform as is presented here. The integral transform technique is more general because no specific form of the absorption profile need be assumed.

The general solution, for a sphere in an infinite medium, which is is derived in Appendix A, is found to be

$$T_i(r,t) = \frac{D_i b}{2\pi^2 r a K_i} \int_0^\infty dy \quad \frac{y^2 \sin(yr/a) \exp(-y^2 t/\gamma) \hat{\bar{A}}(y,t)}{(C \sin y - y \cos y)^2 + b^2 y^2 \sin^2 y}, \quad (6)$$

where

$$\hat{\bar{A}}(y,t) = 4\pi \int_0^t dt' \exp(\lambda^2 t') \int_0^a dr\, rA(r,t') \sin(\alpha r), \quad (7)$$

with $y = \lambda a/D_i^{1/2} = \alpha a$. Now, if it is assumed that $A(r,t) = A(t)$ (i.e., absorption within the region is independent of the radius), and $A(r,t')$ is proportional to the incident pulse which is assumed to be a square wave, a very simple solution can be found.

Since the quantity of interest is the energy of the incident pulse which results in an assumed critical temperature, the following integrations are performed.

$$\int_{V_i} dr^3 A(r,t) = Q\left(\frac{2\pi a}{\lambda}, n'\right) I(t), \quad (8)$$

where Q is the absorption cross section computed from electromagnetic theory and n' is the imaginary part of the index of refraction. The damage threshold is then defined as

$$E = \int_0^{t_p} dt I(t) \, (J/cm^2). \quad (9)$$

where t_p is the pulse length required to reach the critical temperature T_c at the radius a of the absorbing region. Thus $T_c t_p = f(r,Q,E)$ is inverted to give $E = g(T_c, t_p, r, Q)$ for the damage threshold in Joules per centimeter squared.

For a single square pulse such that $t_p/\gamma > 1$, where $\gamma = a^2/D$, in an absorbing region where Q is proportional to πa^2 an appropriate expression for the integral solution may easily be computed. The damage in Joules per centimeter squared is then found to be

$$E_0 = \frac{16T_c}{\pi} (\rho_h C_h K_h t_p)^{1/2}. \tag{10}$$

This derivation is shown in Appendix A. Note that the thermal properties of the absorbing region do not show up here. This is an approximation which is demonstrated in Appendix A. The comparison of this relation to experimental data is given in Chapter 5.

It is mentioned above that relation (10) is derived based upon the fact that the absorption cross section Q is proportional to πa^2. Although this is usually thought of as the large radius limit of an absorbing sphere, this is not necessarily the case. A numerical [Wiscombe 1979] study of the Mie theory of the interaction of an electromagnetic wave and a generalized dielectric sphere clarifies this point.

In general, the absorption cross section of a sphere takes on the appearance of Fig. 2. The index of refraction of the host material and the sphere for this case are $n_h = 1.6$, $n_i = 1.9 - i0.005$ respectively. The complicated structure results from internal electric

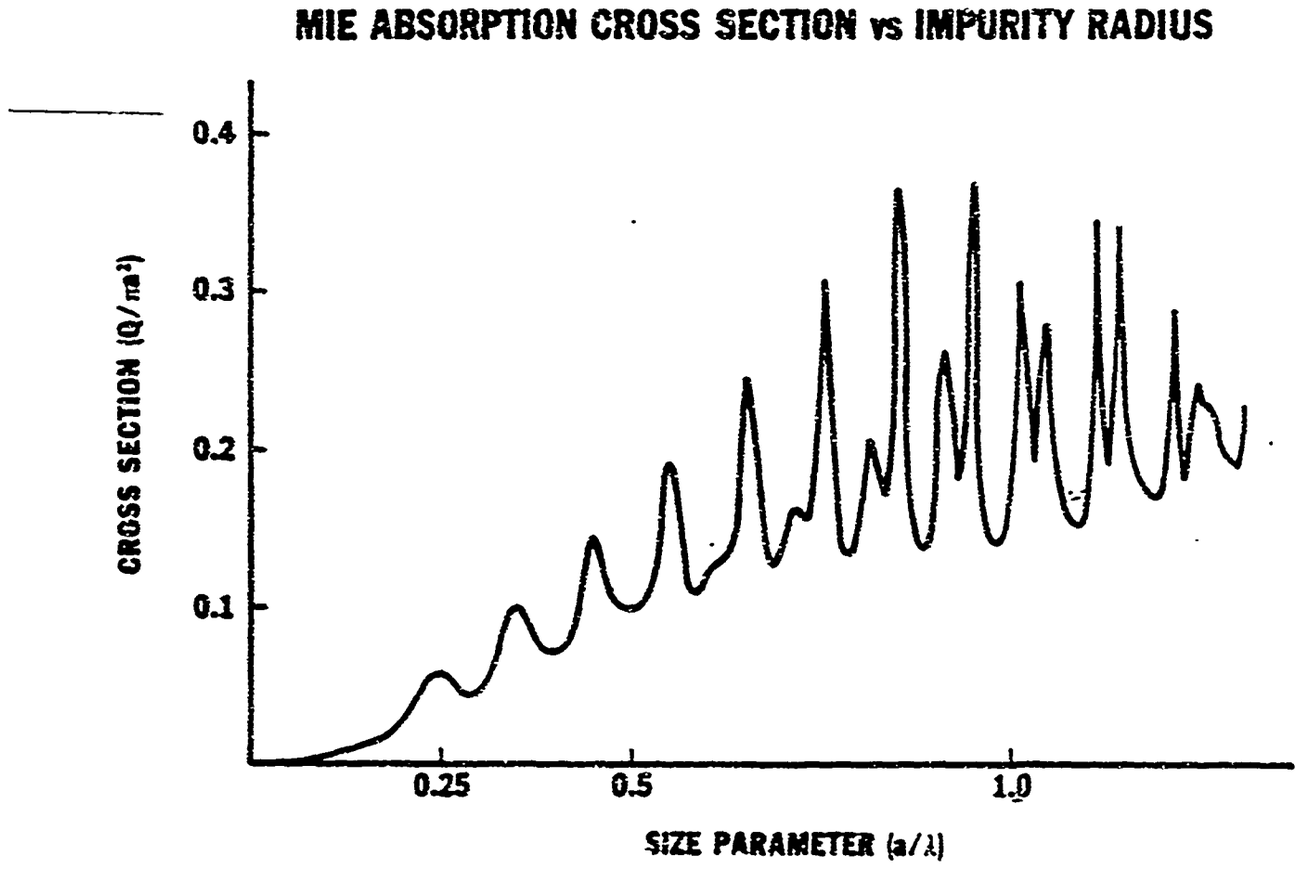

Fig. 2. Mie absorption cross-section as a function of the size parameter q.

and magnetic multipole resonances which are set up in the interaction region. Energy considerations (to be discussed in Chapter 6) dictate that for adequate absorption to cause damage within the pulse absorption must be orders of magnitude greater. Data fits of the absorption-diffusion model in fact show that the absorption must be such that the imaginary part of the index of refraction is greater than one.

A study of regions with an index of refraction such as this gives results illustrated in Fig. 3. The important point to note is that spheres that are only a fraction of a wavelength in size tend to behave as large spheres. This behavior results from the fact that the energy is attenuated within the bounds of the sphere.

As long as the regions are strongly absorbing (as above) relation (10) holds. If the region is very small compared to the wavelength, or weakly absorbing, the scaling relation may be shown to be

$$E_c = \frac{4\pi T_c}{Q} \frac{aK_h t_p}{1 - \frac{a}{(\pi D_h t_p)^{1/2}}} . \qquad (11)$$

This relation has not been shown to fit any of the data. Furthermore the conditions under which it holds true do not allow sufficient energy to be transferred to the region to damage it. Relation (10) therefore evolves from thermodynamic considerations of energy transfer requirements to explain the observed morphology in some of the optical coating damage data. The morphology of pitting which is the source of this model is primarily observed in the fluoride data. It will be shown in Chapter 5 that relation (10) best describes the

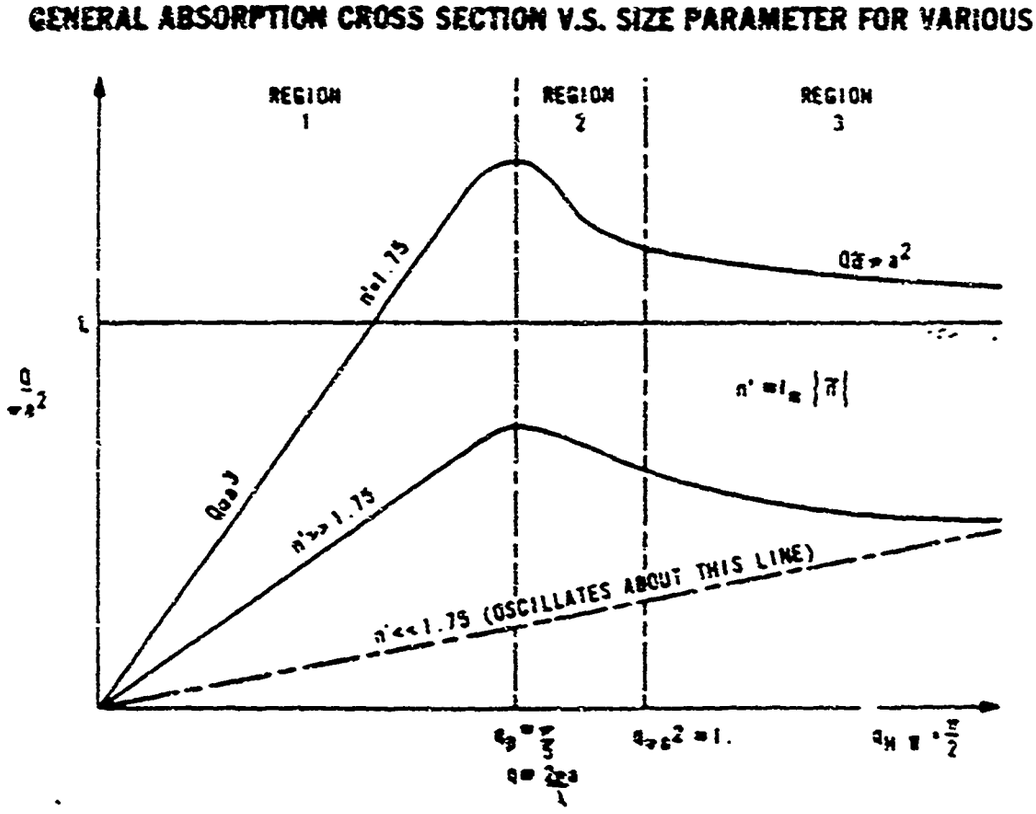

Fig. 3. General absorption cross section versus size parameter for various imaginary indices of refraction.

behavior of the fluoride data. The behavior of the oxide data will be explored more in Chapter 7.

Although relation (10) describes the behavior of some of the data remarkably well, it is a proportionality scaling of the thermal properties. Relation (10) says very little about the optical properties other than the fact that the imaginary part of the index of refraction must be large for it to be valid. Also, although in the region in which relation (10) is applied, it is shown to be valid, relation (10) is still an approximate solution. For these reasons, an integrated computer program which solves the electromagnetic field equations for the exact classical absorption cross section and integrates the thermal diffusion equations for the exact solutions of them has been developed. Comparison of the scaling with the exact solution is shown in Figs. 4 through 7. The program is used to find the required value that the imaginary part of the index of refraction must assume in order for damage to occur in the films for which damage data exists. Comparison of this data with the predictions of the program is given in Chapter 5. The scalings are shown to agree remarkably well with the data. This point reinforces the concept that very large localized ionization must occur in a very short time compared with the pulse length to explain the data. This concept is further reinforced by theoretical computation carried out in Chapter 6.

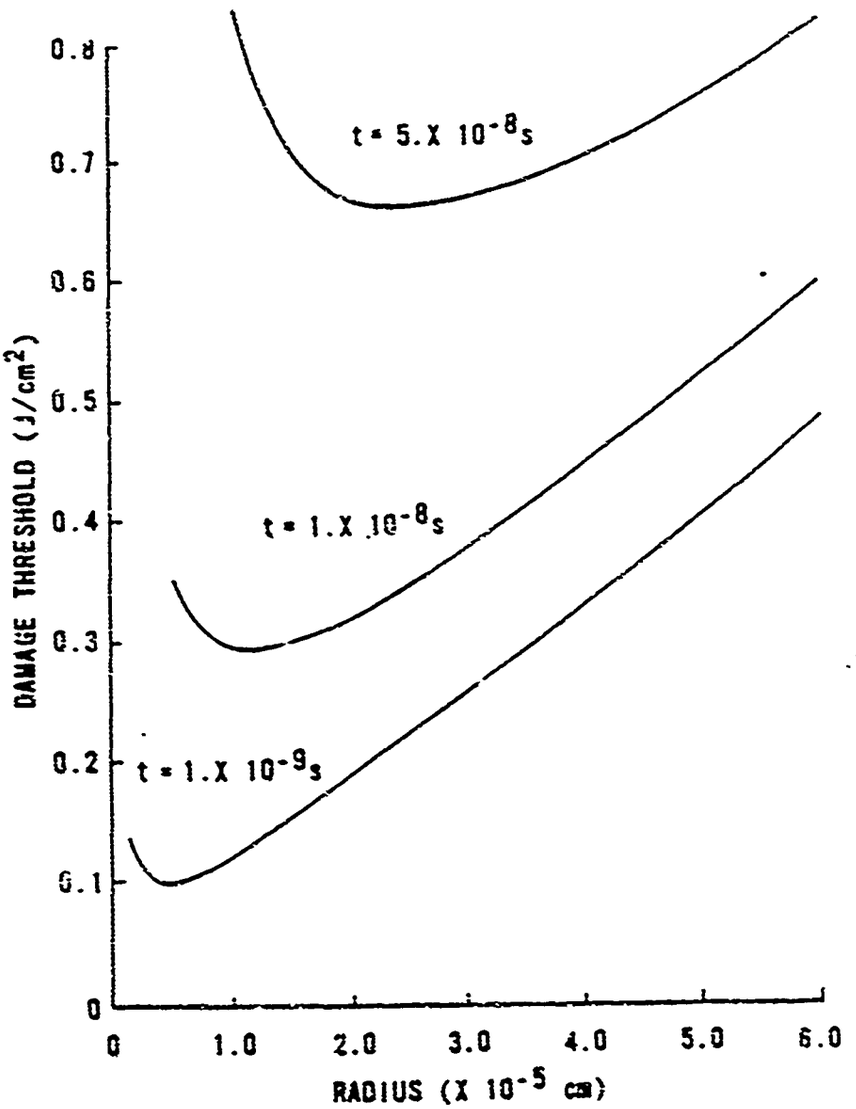

Fig. 4. Damage threshold as a function of impurity radius for various pulse lengths, the host is glass while the inclusion is platinum.

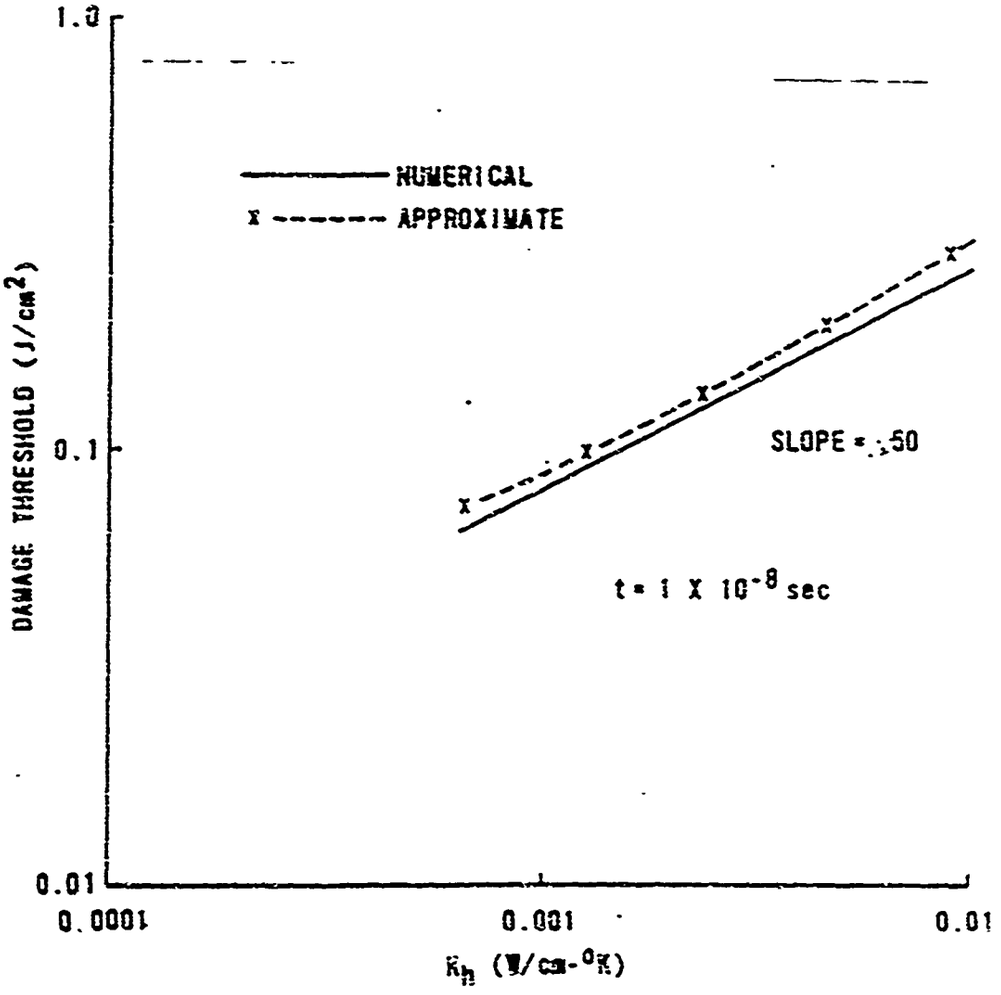

Fig. 5. Damage threshold as a function of host conductivity: platinum - impurity.

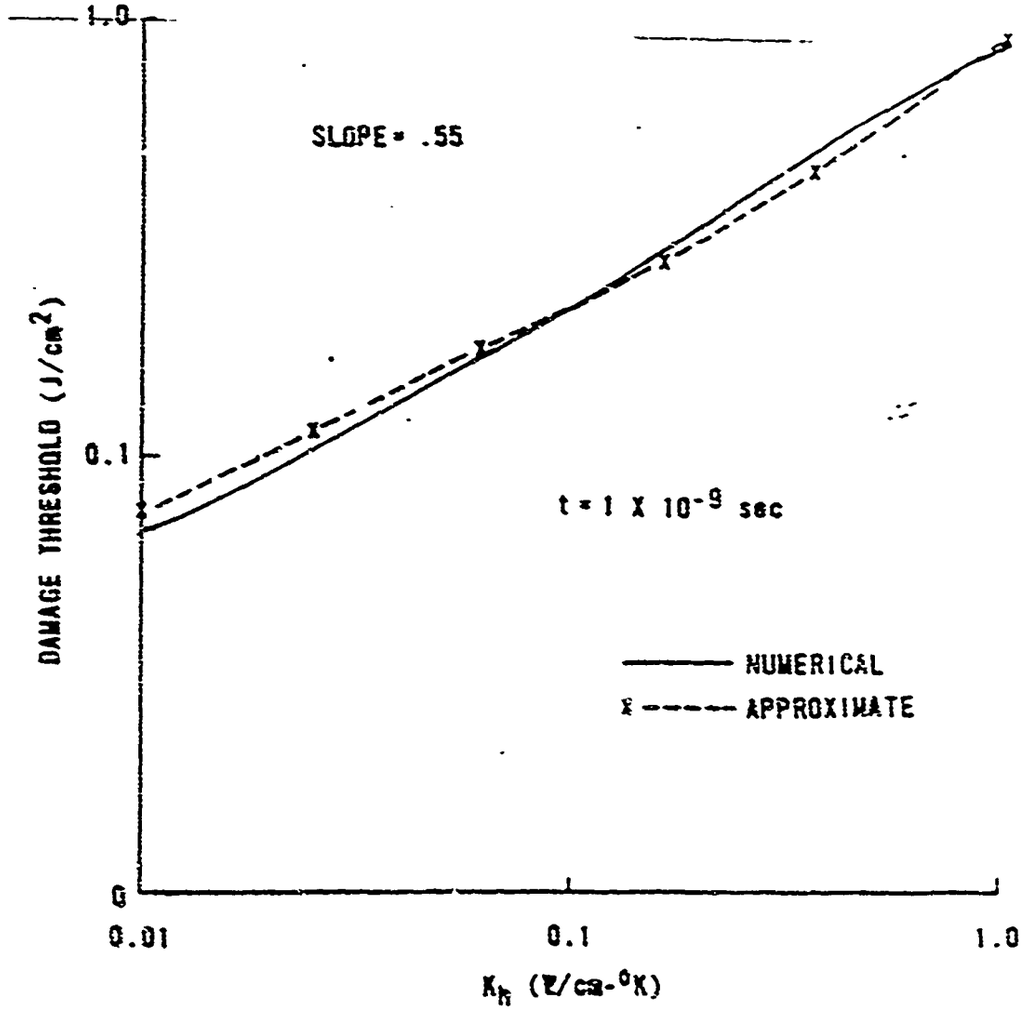

Fig. 6. Damage threshold as a function of host conductivity: ThO_2 - impurity.

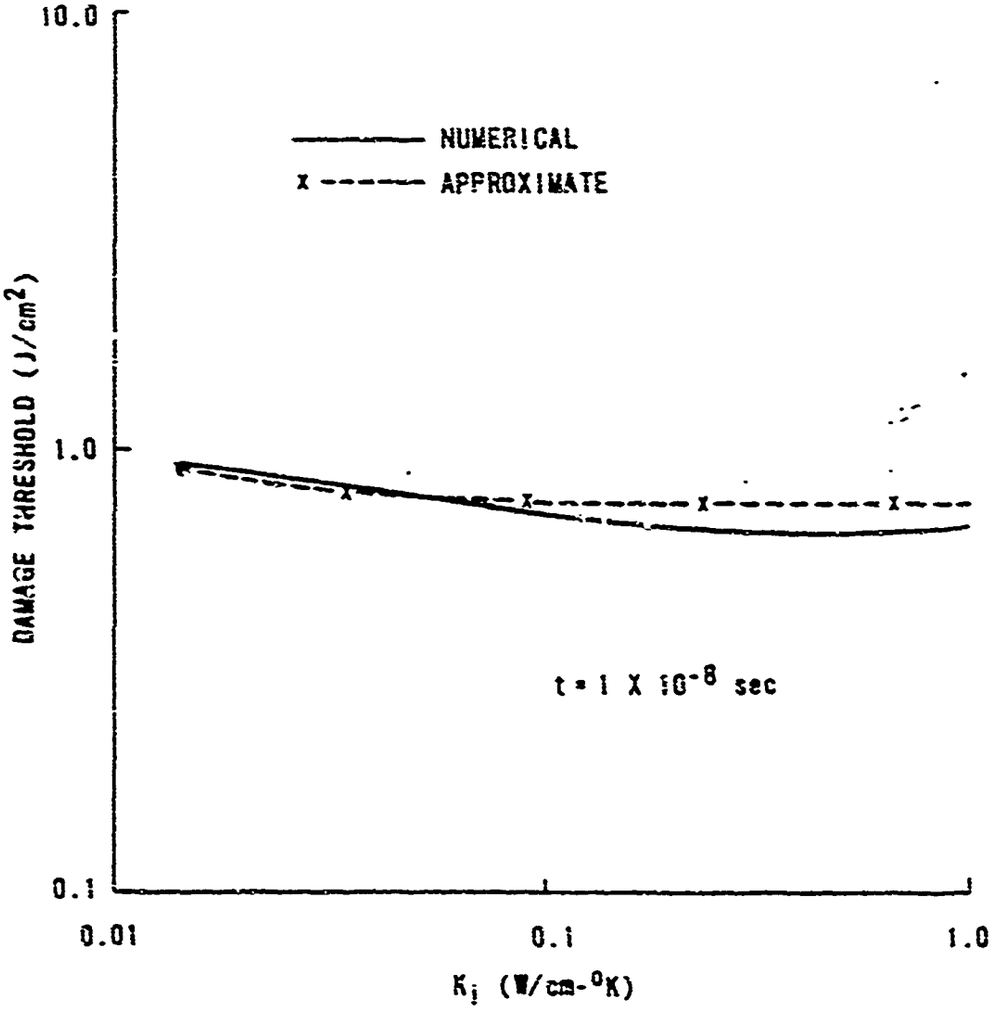

Fig. 7. Damage threshold as a function of impurity conductivity: ThF$_4$ - host.

Table 1. Quantities employed in the analysis of an absorbing impurity embedded in a host.

Thermal Properties for ThF_4 (Host) and ThO_2 (Impurity)

K_h	=	0.1(J/cm-s- K)
K_i	=	0.142 (J/cm-s- K)
D_h	=	0.15 (cm^2/s)
D_i	=	0.0594 (cm2/s)

Thermal Properties for Glass (Host) and Platinum (Impurity)

K_h	=	0.013(J/cm-s- K)
K_i	=	0.67 (J/cm-s- K)
D_h	=	0.003 (cm^2/s)
D_i	=	0.24 (cm^2s)

Damage Condition

T_c	=	2000. K

CHAPTER 3

FILM SUBSTRATE CONSIDERATIONS

In Chapter 2 the dependence of the damage threshold on the thermal and optical properties of the system is discussed. The present chapter specifically addresses the thin film aspects. These are included by using a cylindrical impurity embedded within the film. A description of the model is shown in Fig. 8.

The work presented here is a study of a cylindrical inclusion embedded in a single layer thin film with an underlying substrate whose thermal character ranges from nonconductive to highly conductive. The reason for choosing a cylindrical impurity is threefold: cylindrical or columnar-like inclusions do occur in thin films [Lewis, et al. 1985], the effect of the substrate is maximized (providing an upper bound) by having a large contact area (as opposed to a point contact such as with a sphere); and finally, it affords a mathematical simplicity through the matching of boundary conditions.

In reference to Fig. 8 a cylindrical impurity of radius a is embedded in a thin film of physical thickness l with different thermal and optical properties. The diameter of the inclusion is assumed to be much less than the spot size of the laser illuminating the sample so that the impurity is subject to a uniform intensity in the radial direction. The film and absorbing region are in perfect thermal contact with an underlying substrate. The thermal conductivity $K(J\ cm^{-1}s^{-1}K^{-1})$ and the thermal diffusivity $D(cm^2-s^{-1})$ are labeled by

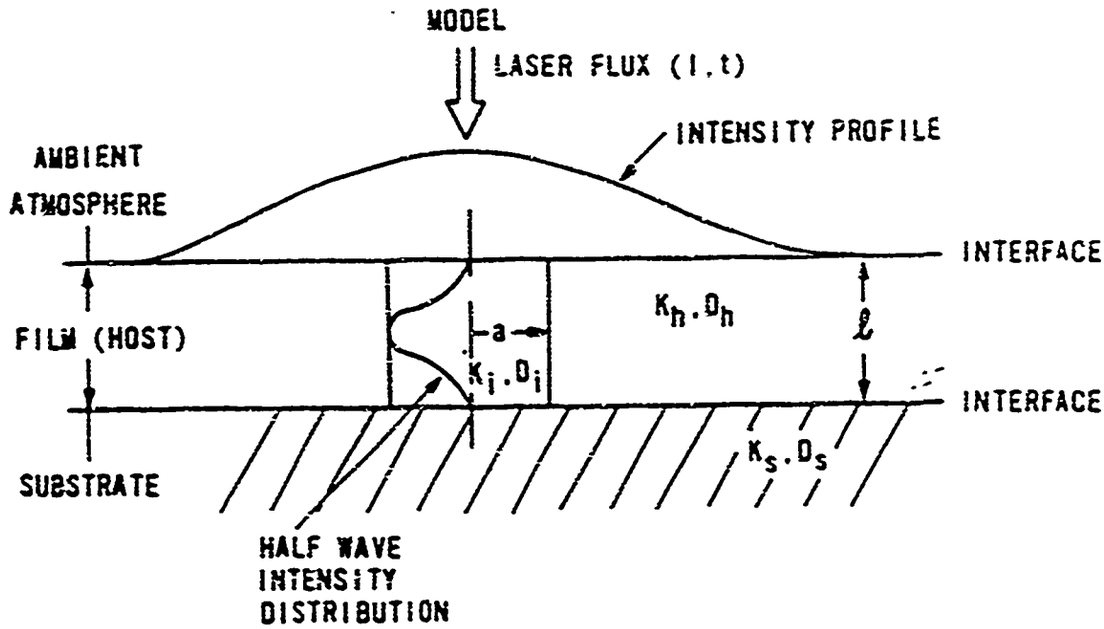

Fig. 8. A Description of the General Film-Substrate Model

A cylindrical impurity of radius a is embedded in a thin film of thickness l and interfaces with a substrate. The thermal properties of the impurity, host and substrate are subscripted with i, h, and s respectively. The diameter of the inclusion is assumed to be much smaller than the spot size of the laser illuminating the sample. Radiation is absorbed in the inclusion and the diffusion governs the temperature field that results.

the subscript i, h, or s referring to the impurity, film (host) and substrate respectively. The thermal properties of the system along with the absorption cross section are taken to be independent of temperature and the impurity is the only part of the system that absorbs incident radiation. As is the case for the previously studied spherical model, damage is assumed to occur when the surface of the impurity reaches some critical material-dependent temperature T_c.

Mathematically the model is described by the following thermal diffusion equations [Ozisik 1980]:

$$\frac{1}{D_i}\frac{\partial T_i}{\partial t} = \frac{1}{r}\frac{\partial}{\partial r}\left(r\frac{\partial T_i}{\partial r}\right) + \frac{\partial^2 T_i}{\partial z^2} + \frac{A}{K_i} \qquad 0 \leq r < a, 0 \leq z < l \ , \tag{12}$$

$$\frac{1}{D_h}\frac{\partial T_h}{\partial t} = \frac{1}{r}\frac{\partial}{\partial r}\left(r\frac{\partial T_h}{\partial r}\right) + \frac{\partial^2 T_h}{\partial z^2} \qquad a < r, 0 \leq z < l \ , \tag{13}$$

$$\frac{1}{D_s}\frac{\partial T_s}{\partial t} = \frac{1}{r}\frac{\partial}{\partial r}\left(r\frac{\partial T_s}{\partial r}\right) + \frac{\partial^2 T_s}{\partial z^2} \qquad 0 \leq r, l < z \ , \tag{14}$$

$$T_i(r,z) = T_h(r,z) = T_s(r,z) = 0 \qquad t = 0 \ , \tag{15}$$

where A is the source term in watts per cubic centimeter.

The boundary conditions are assumed to be

$$T_i = T_h, \ K_i \frac{dT_i}{dr} = K_h \frac{dT_h}{dr} \qquad r = a, \ 0 \leq z < l \ , \tag{16}$$

$$T_i = T_s, \ K_i \frac{dT_i}{dz} = K_s \frac{dT_s}{dz} \qquad 0 \leq r < a, \ z = l \ , \tag{17}$$

$$T_h = T_s, \; K_h \frac{dT_h}{dz} = K_s \frac{dT_s}{dz} \qquad a < r, \; z = 1 , \tag{18}$$

and

$$\frac{dT}{dz} = 0 \qquad \text{at } z = 0 . \tag{19}$$

Exact solutions are found for the extreme cases of a nonconducting substrate and an infinitely conducting substrate with either uniform or standing wave absorption distributions. As before the solution may be found via Laplace or integral transform. An approximate solution is also found for the important realistic case of a finite valued thermally conducting substrate. All of these cases are compared with numerical finite element analyses via the thermal/structural analysis code NASTRAN for consistency. The derivation of the results are presented in Appendix B. The Laplace derivation is mentioned, but not presented due to its extraordinary length and its lack of generality. It does not apply to arbitrary absorption functions in space or time. It is found consistent with the integral transform solution.

For the special cases of the infinite and nonconducting substrates the problem reduces to Eqs. (12) and (13) together with Eq. (15) where Eqs. (17) and (18) reduce to $T = 0$ at $z = 1$ for an infinitely conducting substrate and $dT/dz = 0$ at $z = 1$ for a nonconducting substrate.

The general solution for the boundary temperature is presented in Appendix B. Any arbitrary spatial dependence for absorption may be used. Any such function may also be repetitively pulsed as is shown in the next chapter.

For the purpose of demonstrating trends, the realistic case of a single-pulsed sine squared standing wave (half-wave film) is investigated. The source term may be written as

$$A(z,t) = A_0 \sin^2 \frac{\pi z}{l} = \frac{A_0}{2}\left(1 - \cos \frac{2\pi z}{l}\right) . \tag{20}$$

The source term $A(z,t)$ can also be written in terms of the incident laser intensity $I(Wcm^{-3})$ and the absorption cross section $Q(cm^2)$ by realizing that

$$\int_{v_i} dr^3 A(r,t) = QI(t) \qquad 0 < t < t_p , \tag{21}$$

$$A = 0 \qquad t_p < t , \tag{22}$$

where t_p is the duration of the laser pulse. In this case

$$\frac{A_0}{2} \pi a^2 l = IQ. \tag{23}$$

As before, the above relation is integrated over t and inverted to find

$$E(J/cm^2) = g(T_i, t_p, r, Q) . \tag{24}$$

The absorption cross section used in this solution is $Q = Cr^2$ where C is some constant. This is based upon the Mie scattering results from Chapter 2.

Once the solutions for the damage threshold (in Joules per square centimeter) for a given pulse length are known, the thin film character and substrate effects in extreme limiting cases can be

determined. In order to isolate the substrate effects from radial diffusion, the limit as $a \to \infty$ is taken. Expressions for the damage threshold scaling are found, for the case of $K_s \to 0$, to be

$$E \propto T_c t K_i \left(\frac{2D_i t}{l} + \frac{1}{4\pi^2}\left\{1 - \exp\left[-\left(\frac{2\pi}{l}\right)^2 D_i t\right]\right\}\right)^{-1} , \tag{25}$$

and furthermore as $t \to 0$

$$E \propto \frac{T_c l K_i}{D_i} . \tag{26}$$

For the long pulse limit, i.e. $t \gg l^2/(4D_i\pi^2)$ we find

$$E \propto \frac{T_c t K_i}{2D_i t/l + 1/4\pi^2} . \tag{27}$$

By comparison, for a substrate which is infinitely conducting, as $t \to 0$

$$E \propto \frac{T_c l K_i}{D_i} , \tag{28}$$

which is the same as is found for the nonconducting substrate above. Finally, for the long pulse limit with an infinitely conducting substrate, i.e. $t \gg 4l^2/(9D_i\pi^2)$,

$$E \propto \frac{T_c t K_i}{l} . \tag{29}$$

The important scaling trends of the damage threshold are the linear dependence on temperature T , the linear dependence on the thickness l of the film for very short pulse lengths ($t \to 0$), the inverse thickness dependence on l for long pulses with an infinitely conducting substrate, and the various pulse length dependences (e.g. none as $t \to 0$ and linear in t for long pulses with infinitely conducting substrates). Some of these dependences begin to appear in Fig. 9 for the range of pulse lengths plotted. For example, we begin to see an inverse thickness dependence for long pulses and a highly conducting substrate.

It should be noted that these scalings are in extreme limits and are not intended to be realistic design relations. For example, no host dependence appears because of the limit $a \to \infty$. These relations are intended to give insight into the effects or lack of effects of thin film/substrate system parameters.

The general thermal parameter dependences of the problem due to radial heat diffusion are determined by insulating the substrate and varying the host film and impurity thermal conductivities. As with previous spherical impurity studies, the damage threshold increases with increasing host thermal conductivity, while the damage threshold is essentially insensitive to the thermal conductivity of the inclusion.

A more illuminating exercise is to set $l = (4/3)a$ so that the length of the inclusion varies with the radius of the inclusion. This forces the volume to be proportional to 'a' cubed and the

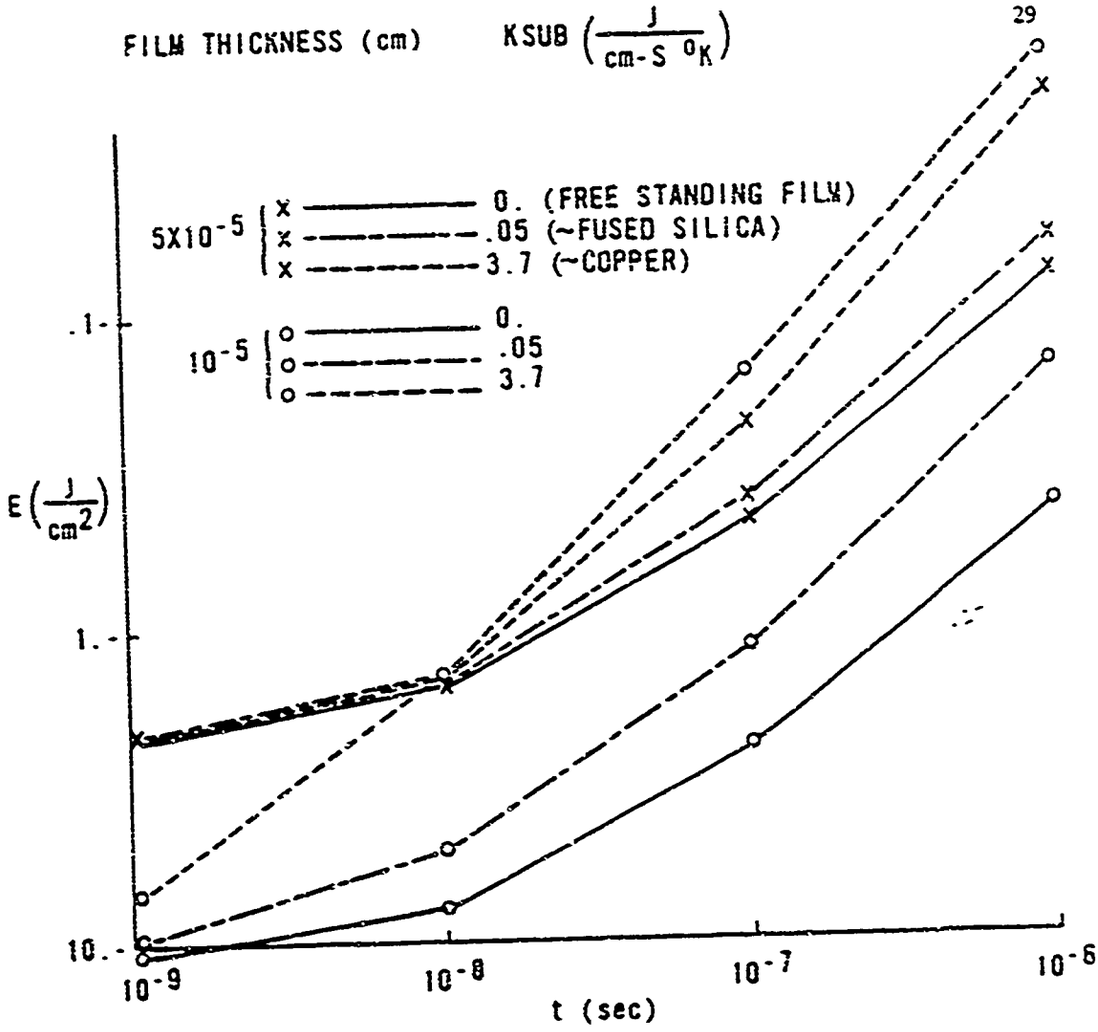

Fig. 9. Calculated Damage Threshold Vs. Pulse Length.

This is calculated for two different film thicknesses l and three different substrate conductivities K_S: —— x ——, $l = 5x10^{-5}$ cm, $k_s = 0$ J $cm^{-1}s^{-1}K^{-1}$ (free standing film); - —— x ——- , $l = 5x10^{-5}$cm, $K_S = 0.05$ J $cm^{-1}s^{-1}K^{-1}$ (fused silica); —— x ——, $l = 5x10^{-5}$ cm, $K_S = 3.7$ J $cm^{-1}s^{-1}K^{-1}$(copper); —— 0 —— , $l = 10^{-5}$ cm, $K_S = 0$ J cm^{-1} $s^{-1}K^{-1}$;- — 0 —-, $l = 10^{-5}$cm, $K_X = 0.05$ J $cm^{-1}K^{-1}$; —— 0 ——, $l = 10^{-5}$ cm, $K_S = 3.7$ J $cm^{-1}s^{-1}K^{-1}$.

cross section to be proportional to 'a' squared. When this is done a minimum value of the damage threshold is found (i.e. a radius at which damage is easiest) and scaling laws for host conductivity and pulse length are found much like those predicted for spherical impurity particles. The end result of this analysis is that the details of the geometry are not very important to the thermal aspects of the problem as long as the volume of the impurity is proportional to some mean radius cubed and the absorption cross section is proportional to some mean radius squared. So, if the absorbing regions are irregularly shaped volumes, as may be the case, then the thermal scaling laws derived from an ideal geometry model should still apply.

The final aspect of the problem studied is the effect of the intensity distribution within the film. It is easily seen from Fig. 10 that high intensity I(J cm^{-2}s^{-1}) short pulses can lead to very high temperature gradients. If the intensity is high (Fig. 10, curve 3) with a sine squared half-wave, and the pulse length short enough, very high temperatures can be reached in the center of the film while the boundaries remain nearly at their initial temperature. In this case a substrate will have very little effect regardless of how highly conducting it may be.

The descriptors short, long, etc. refer to a comparison with scales determined by the diffusivities D involved. For example, the diffusion length $\delta = (D_i t)^{1/2}$ for I_s is approximately 1/40 of the thickness of the film. At this depth in the film the temperature is still quite low. Thus, this rough measure of the range of the effect of one point on another indicates that the boundary temperature will

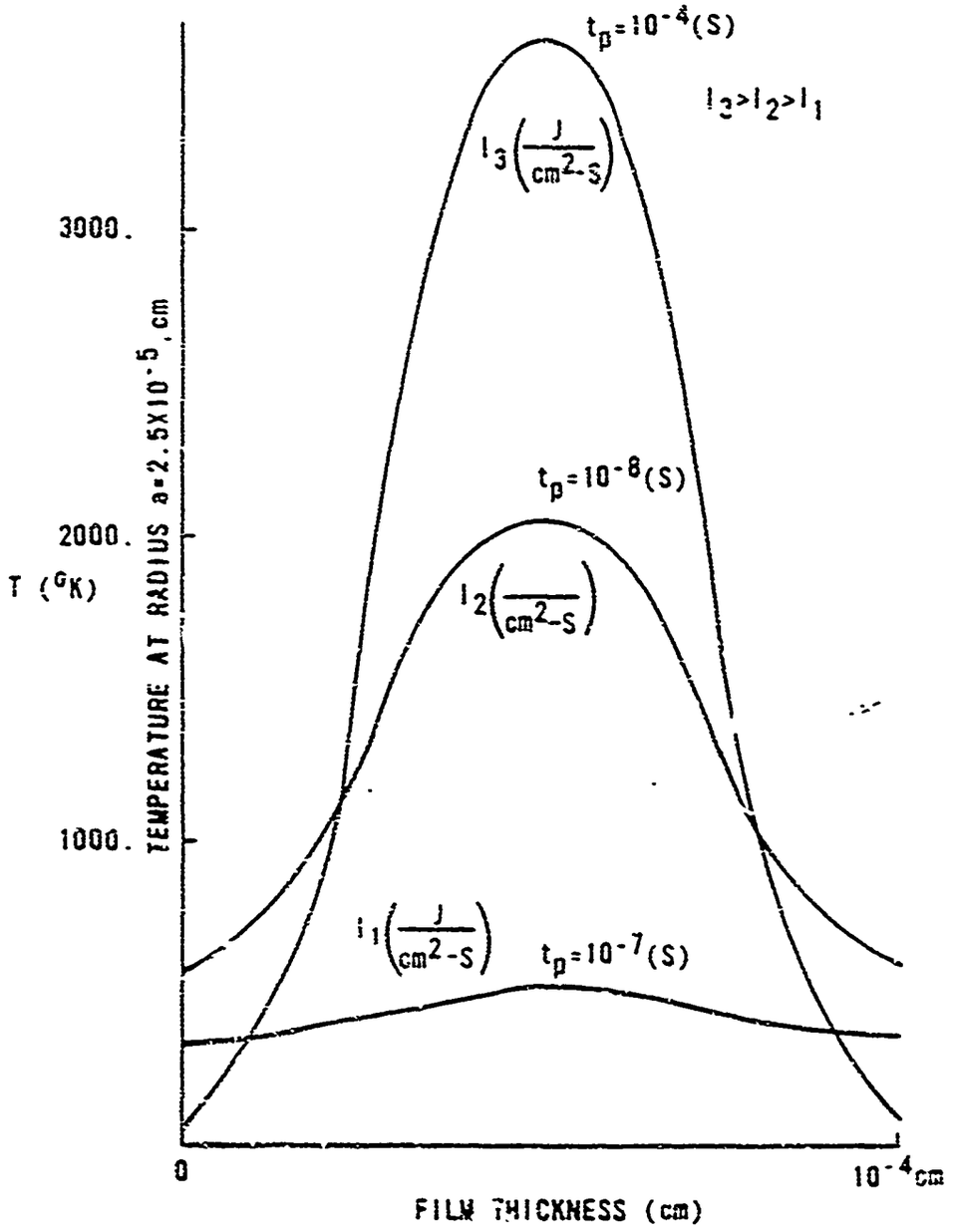

Fig. 10. Plot of Temperature vs. Film Depth - I.

The absorbed energy is proportional to a standing wave for three different intensities I_1, I_2, I_3 ($I_3 > I_2 > I_1$), three pulse lengths and a fixed energy density E = 0.9 J cm^{-2}: curve 1, I_1, $t_p = 10^{-7}$ s; curve 2, I_2, $t_p = 10^{-8}$ s; curve 3, I_3, $t_p = 10^{-9}$ s. The same total energy is deposited in all three cases (i.e. It = constant).

not be affected significantly. However, if we decrease the thickness of the film by a factor of ten with the same pulse length, δ is approximately 1/4 of the film thickness. Referring to Fig. 11 we see a significant effect on the temperature profile of substrates with various conductivities.

If instead of a half-wave intensity distribution, we have a wave such that the maximum intensity is at the interface with the film and substrate, there would be a considerable effect for good conducting substrates at much smaller δ parameters.

The results presented here imply various conclusions. At least one of the conclusions presented is easily verified. That is, if substrates of high thermal conductivity are used, the damage threshold may increase. Experimental results pertinent to this are presented in Chapter 5.

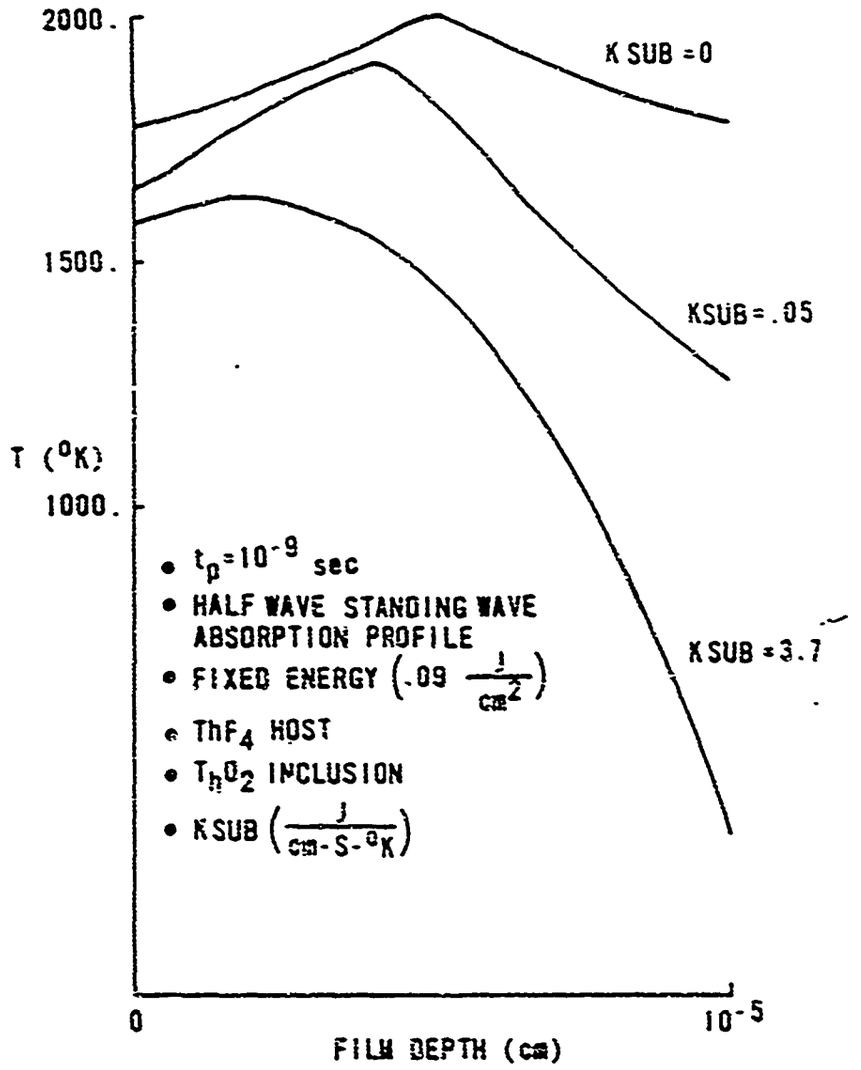

Fig. 11. Plot of Temperature Vs. Film Depth - II.

The absorbed energy is proportional to a standing wave showing the effect of three different substrate thermal conductivities ($t_p = 10^{-9}$ s, half-wave standing wave absorption profile, fixed energy density (0.09 J cm^{-2}); ThF host; ThO_2 inclusion): curve 1, K_S = 0 J $cm^{-1}s^{-1}K^{-1}$ (free-standing film); curve 2, K_S = 0.05 J $cm^{-1}s^{-1}K^{-1}$ (fused silica); curve 3, K_S = 3.7 J $cm^{-1}s^{-1}K^{-1}$ (copper).

CHAPTER 4

REPETITIVELY PULSED LASER CONSIDERATIONS

The problem of multiple pulse laser induced damage in optical components is a very important and general one. It is a significant problem that reflects the durability of optical elements. This stems from the fact that multiple pulsed damage addresses the use of optical elements that are subjected to more than one cycle regardless of the time delay between pulses.

In a review of this area one encounters a large array of seemingly contradictory data. For example in some instances there is no apparent effect of prior pulses [Bass and Barrett 1972] (i.e., no memory), while in other cases there is unmistakable evidence of a build-up or accumulation of damage [Merkle, Bass and Swimm 1982]. Some situations demonstrate clear evidence of thermal build-up effects [Koumvakalis, Lee and Bass 1982; Wood, Sharma and Wate 1982] while others [Bordelon, et al.] show no evidence of this effect. A pulse repetition frequency dependence in some cases [Koumvakalis, et al. 1982; Wood, et al. 1982; Balitskas and Maldutis 1981] exhibits reversible effects in some materials while others [Bordelon, et al 1982] show no evidence of this effect. It is also known that low level irradiation can condition elements such that they can ultimately withstand higher fluences [Gorshkov, et al 1983; Becker, et al. 1983]. This wide diversity of responses may also depend upon the configuration of the

material (i.e. bulk. film, crystalline, amorphous, metallic, polymer, etc.)

The morphology of multi-pulsed damage is just as varied, not only between different materials, but between different configurations of the same material (i.e., anti-reflecting films and highly-reflecting films) [Foltyn and Jolin 1983]. One mode of damage for films, both with and without some sort of accumulation mechanism, is for a small pit to form and no subsequent damage to occur [Foltyn and Jolin 1983]. Another mode is for damage to grow with subsequent pulses to a diameter that is consistent with points in the incident field that are $\sim$ 25% of the damage threshold [Foltyn and Jolin 1983]. Clearly there is no simple universal multipulse laser induced damage scenario. There, in fact, may be as many effects as there are materials or classes of materials.

What is done herein is to once again exploit the thermal model of laser induced damage and apply it to multipulsed lasers. The justification for this is that absorption and diffusion must occur in all cases of laser damage and laser induced damage is thermally dominated in certain single pulse cases. There is, in addition, evidence that the mechanism for some cases of laser induced damage is the same for the first pulse as the subsequent pulses [Balitskas and Maldutis 1981; Bass and Barrett 1973; Kovalev, et al. 1980] (though, for other cases [Koumvakalis, et al, 1982] this is evidently not true). Even cases where damage is not thermally dominated a change of state necessarily accompanies a change in temperature (e.g. a change in band gap) and thus, it is desirable to know the temperature field.

The thermal model is generalized to facilitate any sort of general absorption that may occur in various materials. However, the absorption function must be determined for each different situation. The determination of the temporal and spatial dependence of the absorption function for each situation, as for the single pulse case, is the primary difficulty. For certain single pulse situations a very simple absorption function can prove adequate. However, due to irreversible changes (i.e. memory) of some sort, this is not true for most multiple pulse interactions.

In this section a general model of arbitrary multi-pulse absorption is derived. The arbitrary form of the absorption applies not only to localized absorption, but allows application to laser windows with macroscopic gaussian beam absorption [Wood, et al. 1982]. In addition, it allows application to an opaque material with absorption of any general form. The problem is then simplified to the case of a uniform, nonexpanding absorption, without irreversible processes as an illustration of the effects purely due to thermal build-up.

The results are as expected, in that thermal build-up in itself cannot be responsible for the observed decrease in damage threshold in most cases of isolated absorbing inclusions. Other mechanisms must couple with the diffusion process to provide the observed behavior. The key to understanding the many observations and mechanisms involved is to determine specific pulse to pulse behavior of the absorption function. Any correct theory of the interaction involved must predict the spatial, temporal, pulse repetition frequency and pulse number dependence of the absorption term in the diffusion equations.

Theory

In previous chapters a spherical model, valid for the region where the pulse length is not larger than the diffusion time to the boundaries of the film, and a cylindrical model, valid for much longer times, are described.

In general the diffusion equation is used to describe the distribution of temperature within the system. In the absorbing region

$$\frac{1}{D_i}\frac{\partial T}{\partial t} = \nabla^2 T + \frac{A(r,t)}{K} \quad , \tag{30}$$

where T, D, K are temperature, diffusivity (cm^2/s) and conductivity (J/ K-s-cm) and A is the absorption function in (J/cm^3-s) while

$$\frac{1}{D_h}\frac{\partial T}{\partial t} = \nabla^2 T \quad , \tag{31}$$

outside of the absorbing region. Here, perfect thermal contact is assumed at the boundaries of the absorbing region and the subscripts i and h refer to the inclusion and host film respectively. The two geometries give specific solutions within the impurity of

$$T_i = \frac{1}{r}\int_0^\infty \frac{d\alpha}{N(\alpha)} \sin(\alpha r)\ \hat{A}\ (\alpha,t) \quad , \tag{32}$$

for the spherical case, and

$$T_i = \int_0^\infty \frac{d\alpha}{N(\alpha)}\ \alpha\ J_0\ (\alpha r) \sum_{j=0}^{\infty} \cos\left(\frac{j\pi z}{l}\right)\ \hat{A}(\alpha,t) \quad , \tag{33}$$

for the cylindrical case.

Here A is the transformed absorption function (defined below), $N(\alpha)$ is a normalization factor, α the radial eigenvalue and l is the length of the cylinder (i.e. the thickness of the film). The expression for the source term in the above equations is

$$\dot{\bar{A}} = \exp[-\xi t] \int_0^t dt' \exp[\xi t'] \int_{Vol} dr^3 \psi_j(r,\alpha) A(r,t') \quad . \tag{34}$$

Here ξ is the composite eigenvalue of the system, $\psi_j(r,\alpha)$ is the eigenfunction of the composite region and $A(r,t)$ is the general absorption function with "Vol" referring to the volume of the absorbing region. The subscript j on ψ applies to axial modes of the cylindrical geometry. Expressions for these parameters are given in Table 2 for specific geometries. The absorption function written in the form

$$A(r,t) = \sum_{n=1}^{N} A_n(r,t) \quad , \tag{35}$$

contains the complete evolution of the absorption including irreversible or long lived changes to the material with each pulse from 1 to N. There is data [Bliss, et al 1973; Bordelon, et al 1982] indicating that in some cases the change in absorption occurs within a time that is small compared to the delay time 't_d' between pulses. In some cases it may occur within a time that is small compared to the pulse length t_p itself. For an idealized case where the absorption evolves early into the pulse and the absorption that follows is proportional to the field, or the case where the evolution transient occurs completely in between the pulses

Table 2. Eigenfunction parameters for a spherical and a cylindrical inclusion

	Sphere	Cylinder in a Film
ξ	$= \frac{\gamma^2 D_i}{a^2}$, $\gamma = \omega a$	$= D_i (\alpha^2 + i(\frac{j\pi}{t})^2)$
$\psi(\vec{r},\omega)$	$= \frac{\sin(\alpha r)}{r}$	$= J_o(\alpha r) \cos(\frac{j\pi z}{t})$
$\nu(\omega)$	$= 2\pi^2 \frac{K_i}{b r^2 D_i} \{(C\sin\gamma - \gamma\cos\gamma)^2 + S^2\gamma^2\sin^2\gamma\}$	$= \frac{t}{2}(\lambda^2 + S^2) \frac{K_h}{D_i}$
	$D = \frac{K_h}{K_i}\sqrt{\frac{D_i}{D_h}}$	$\lambda = \frac{\pi a}{2K_h} \{K_i \alpha J_1(\alpha a) Y_o(\beta a) - K_h \beta J_o(\alpha a) Y_1(\beta a)\}$
	$C = 1 - \frac{K_h}{K_i}$	$S = a\sqrt{\frac{D_i}{D_h}}$
		$B = \frac{\pi a}{2K_h} \{K_h \beta J_1(\beta a) J_o(\alpha a) - K_i \alpha J_1(\alpha a) J_o(\beta a)\}$

$$A(r,t) = \sum_{n=1}^{N} A_n(r)\{\theta(t-[n-1)t_p + (n-1)t_d]) - \theta((t-[nt_p + (n-1)t_d])\}. \quad (36)$$

Here the nth pulse turns on at $t = (n-1)t_p + (n-1)t_d$ and turns off at $t = nt_p + (n-1)t_d$ with t_p being the pulse length and t_d being the delay time between pulses and θ being the step function.

Thus, the spatial dependence of absorption from pulse to pulse is all that is important. In other cases [Foltyn and Jolin 1983] multipulse damage has been observed to occur after some number of pulses, but not grow spatially. In fact, no further damage is observed after the initial pitting. In this case

$$A(r,t) = f(r) \sum_{n=1}^{N} A_n\{\theta(t-[(n-1)t_p + (n-1)t_d]) - \theta(t-[nt_p + (n-1)t_d])\}, \quad (37)$$

so that only the magnitude of absorption varies with the pulse number.

In all of these cases the absorption evolution is unknown and is observed to be material and laser parameter dependent with an unknown physical mechanism.

Whatever the driving source, a measured empirical or theoretically derived form of A must be found before any specific situation can be treated adequately.

An illuminating exercise as a first step, however, is to assume A is constant and develop the solution. There are some cases where

this seems to apply. This exercise also serves to demonstrate purely thermal effects for repetitively pulsed lasers. For this case

$$A(r,t) = f(r)\, A_0 \sum_{n=1}^{N} \{\theta(t-[(n-1)t_p + (n-1)t_d]) - \theta(t-[nt_p + (n-1)t_d])\}\,, \tag{38}$$

so that

$$\hat{A} = \exp[-\xi t] \int_0^t dt' \exp[\xi t'] F(\alpha) A(t')\,, \tag{39}$$

where

$$A(t') = A_0 \sum_{n=1}^{N} \{\theta(t,(n-1)t_p,(n-1)t_d) - \theta(t,nt_p,(n-1)t_d)\} \tag{40}$$

$$F(\alpha) = \int_{Vol} d^3r\, \phi\,(r,\alpha) f(r)\,. \tag{41}$$

Various $F(\alpha)$'s are listed in Table 3 for different geometries and situations. The time integration in Eq. (39) is carried out term by term and the resulting series is summed to a result of

$$\hat{A} = A_0 \frac{F(\alpha)}{\xi} (1-e^{-\xi t_p}) \frac{(1-e^{-N\tau\xi})}{(1-e^{-\xi\tau})}\,, \tag{42}$$

where $\tau = t_p + t_d$. This is a particularly simple and elegant result first realized by Walker, et al. [1981] in connection with the Goldenberg and Tranter [1952] solution using the LaPlace transform and now proven here for that case and any general related case. Though this solution does not apply in general to catastrophic repetitively

Table 3. Transform coefficients for various absorbing regions.

	Spherical Absorption	Cylindrical Absorption
Uniform Absorption	$\cdot 1 \frac{\pi a^2}{Y^2}(\sin Y - Y\cos)$ $Y = \alpha a$	$J_1 \frac{(\alpha a)\, \ell a}{\alpha}$
Standing Wave $p\lambda/2$		$J_1 \frac{(\alpha a)a}{\alpha} \frac{\ell}{2} (\delta_{j,o} - \delta_{\frac{j,2p}{2}})$
Uniform Depth Gaussian Beam Cross Section (Weakly absorbing window)		$\frac{\sqrt{\pi}\, \alpha\alpha}{(l\ell/a^2)^{3/2}} e^{-\alpha^2 a^2/16} [I_{-1/2}(\alpha^2\frac{a^2}{16}) - I_{1/2}(\alpha^2\frac{a^2}{16})] l\ell \delta_{j,o}$ where a is the Gaussian spot size radius and $It_{1/2}$ is the exponentially increasing modified Bessel function
Gaussian Cross Section Standing Wave (Weakly absorbing thin film)		$\frac{\sqrt{\pi}\, \alpha\alpha}{(l\ell/a^2)^{3/2}} e^{-\alpha^2 a^2/16} [I_{-1/2}(\alpha^2\frac{a^2}{16}) - I_{1/2}(\alpha^2\frac{a^2}{16})] \frac{\ell}{2} (\delta_{j,o} - \frac{\delta_{j,2p}}{2})$

pulsed laser induced damage, it is likely that it does apply to some cases and may be informative for others for which it is not strictly valid. It is informative because it illustrates the purely thermal effects.

Results

Numbers are applied to the previous expression providing a sense of the effect of thermal build-up in optical materials subjected to repetitive laser pulses. For example, for a one-half micron thick thorium fluoride film using the isolated spherical absorbing impurity model with a 0.1 nanosecond pulse, if no growth of the absorbing region occurs a repetition frequency of greater than 10^8 Hz would be needed to see any significant decrease in damage threshold due to thermal build-up. The criterion that is used for damage there is for the edge of the absorbing region to reach the film melting temperature. Note on Fig. 12 the increase in radius most likely to damage with increased number of pulses. So, if no growth of the inclusion occurs (i.e. disc like growth into the film) and growth is limited by the film thickness then the effect of thermal build-up is even less. Note also in Fig. 13 of pulse repetition frequency equal to 10^8 Hz, that essentially no thermal build-up occurs. Thus thermal build-up could not be a factor in damage for this idealized case. This does not take into account a possibly dense distribution of particles so that the diffused heat of nearby absorbing regions could build-up in the surrounded region.

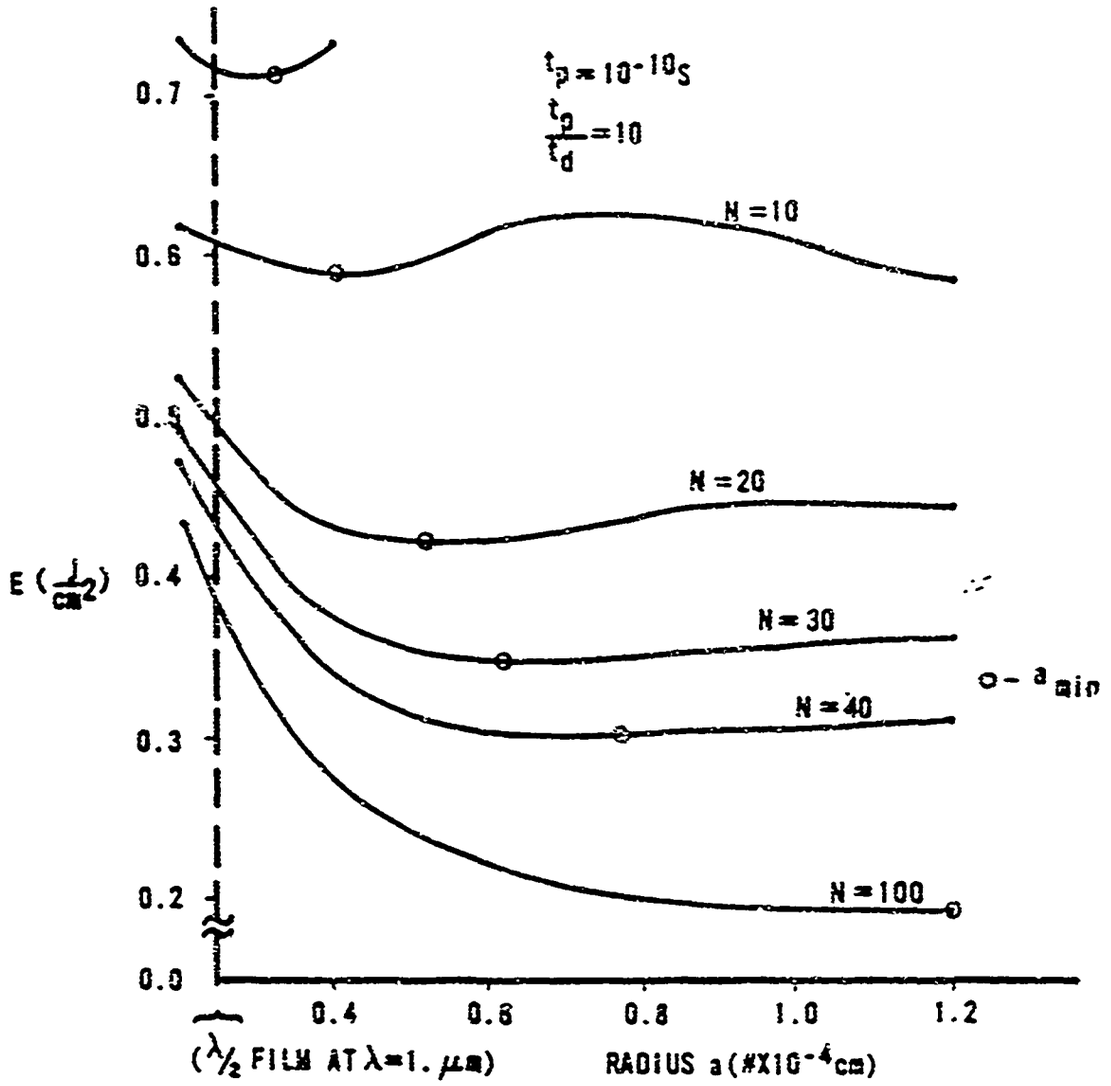

Fig. 12. Computed damage threshold in (J/cm^2) versus radius of the absorbing inclusion - I

This is a plot of one example of computed damage threshold in (J/cm^2) versus radius of the absorbing inclusion for various numbers of pulses. The pulse repetition frequency is 10^3 Hz.

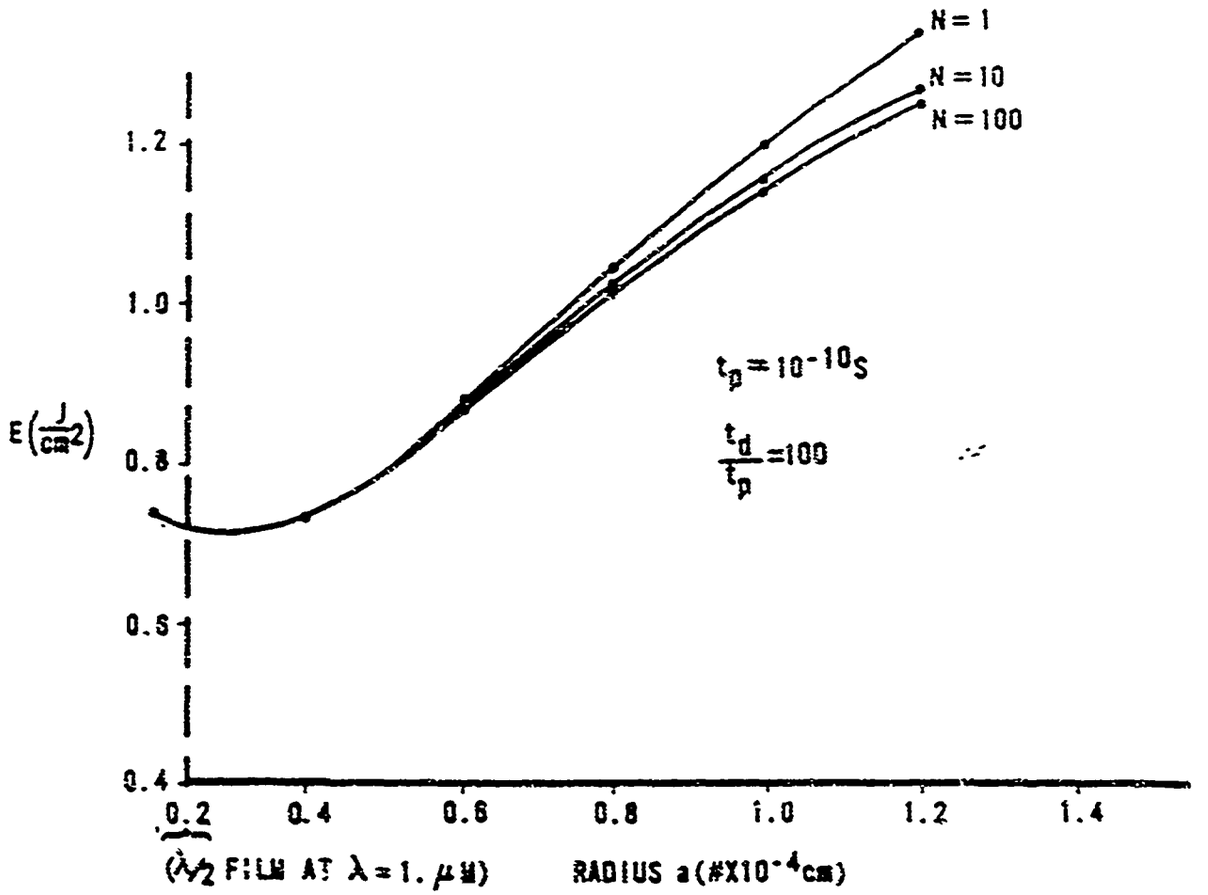

Fig. 13. Computed damage threshold in (J/cm^2) versus radius of the absorbing inclusion - II

This is a plot of computed damage threshold in (J/cm^2) versus radius of the absorbing inclusion similar to Fig. 1, but with a pulse repetition frequency of 10^8 Hz.

Detailed experimental determination of the distribution and strength of absorbers would be required for this calculation.

The largest possible effect of thermal build-up for a single isolated absorber would be for a free standing film (allowing only two dimensional heat diffusion) of very low thermal conductivity with a large strongly absorbing inclusion and a long pulse length. So, assume a free standing film of SiO_2 (k = 0.014 J/cm- K-s) ten microns thick with a 10 microsecond incident pulse repeated at 1000 Hz. The largest inclusion that could initially be embedded in the film would be one with a diameter equal to the film thickness. Again, assuming no growth of the absorbing region a decrease in damage threshold of only ten percent for 1000 pulses due to thermal build-up occurs. For a substrate of greater than zero conductivity this value would be further decreased. These extreme conditions should indicate that thermal build-up by itself is not a factor in these models. However, there are conditions with and without the assistance of additional mechanisms when it is imaginable that thermal build-up would be a factor.

Suffice it to say, a dense distribution of absorbing impurities, irreversible changes or temperature dependent absorption that is initiated at an absorbing inclusion are a few such cases. The latter suggestion is not a new idea. Komolov [1982] has investigated nonlinear temperature dependent absorption of the form

$$X(T) = X_i + X_0 e^{-u/T} . \tag{43}$$

Where X is the impurity absorption and $X_0 e^{-u/T}$ is an intrinsic film absorption. This is addressed in Chapter 7.

Also Manenkov, et al. [1982] have suggested irreversible mechano-chemical reactions with a rate constant of

$$K_{mch} = e^{-(u-\gamma\alpha)/k_b T} \tag{44}$$

where u is an activation energy and is the stress proportional factor driven by temperature gradients assisting in the damage.

With one of these mechanisms the region that is absorbing expands into the film from its origin at an inclusion or impurity. Another such process is investigated in Chapter 6. This expansion to macroscopic dimensions then necessarily involves thermal build-up. In fact according to the theories mentioned above, the expansion in turn is driven by the thermal build-up.

Another situation involving thermal build-up is the case where absorption occurs on a macroscopic scale (on the order of the diffusion length between pulses). This occurs, for example, in semiconductor grade windows [Wood, et al 1982] and on metallic mirrors [Koumvakalis, et al. 1982]. Table 2 lists the spatial part of the solutions for some of these cases. In particular the case of a weakly absorbing window such that absorption is uniform with depth into the window and the case of a standing wave in a thin film are shown. Many other similar solutions are possible (surface absorption or absorption which has essentially any arbitrary depth dependence). These are just mentioned to point out the tremendous generality of the integral transform technique.

As with microscopic absorption, most cases of observed macroscopic absorption observed are also dependent on the number of pulses and/or the pulse repetition frequency. So once again a function versus time, temperature, pulse number and pulse repetition frequency must be known or assumed to properly model this situation.

Some work by Nathan, Walker and Guenther [1983] has indicated that a multi-pulse damage decrease can occur by thermal build-up and various relations involving multipulse parameters are realized. Together these lead to

$$E_d \sim \left(\frac{t_p}{N_{min}}\right)^{1/2} . \tag{45}$$

The terms above are defined as follows: E_d is the damage threshold in (J/cm^2) and N_{min} is the number of pulses at which damage is most likely to occur given some pulse length and frequency. As in Chapter 2 this was found based upon the fact that the heat balance gives some particle radius a_{min} most likely to damage. Here a_{min} is the radius of the particle most likely to damage at this pulse length and pulse repetition frequency. These authors mention that relation (45) also applies to uniformly absorbing semi-infinite surfaces.

The numerical work of Nathan, et al. [1983] was verified and the basic trends are shown in Fig. 12. In addition, approximate relations for E (K,ρ,C_v,t_p,t_d,N) and a_{min} (K,ρ,C_v,t_p,t_d,N) were derived exactly as in Chapter 2 further verifying the numerics. Unfortunately, as also indicated in Fig. 12, the minimum radius for damage to occur quickly becomes very large. In fact, it becomes several orders of

magnitude larger than most thin films for reasonable laser parameters. Nathan's relations therefore primarily apply to bulk materials with extremely large inclusions, or more reasonably to surface absorption on a semi-infinite absorber.

The derived relations mentioned above are not given because of their extreme complexity yielding little additional insight into the problem. However, as with most real lasers, if one assumes that $t_d >> t_p$ and that impurity radii are small (limited to a thin film thickness) the relations simplify to the ones given in Chapter 2 for the single pulse case. This simply indicates that no thermal build-up can occur (i.e. in thin films, if inclusions damage thermally, it must be on the first shot instead of the Nth). It also indicates that multipulse thermal damage scales against the thermal parameters in a similar manner to the single pulse case. This has not been investigated for pulse dependent absorption.

The results of this chapter are certainly not conclusive. The problem is as initially stated that there is no simple universal effect in multipulse damage that we have ascertained.

CHAPTER 5

COMPARISON WITH EXPERIMENTAL DATA

The number of quality sets of experimental laser induced damage of optical coatings data are few. Comparison of data points from different data sets is probably not valid. This is due to the range of incomparable techniques, differences in conditions and criteria for damage and differences in coating sets. Thus, it is necessary to have large sets of parameter variation in a given experi- ment. There is one particularly thorough set of data in the literature at present [Walker, et al 1981].

This data set is compared with the scaling relation derived in Chapter 2 for similar films. The term similar films refers to the comparions of a half-wave film with a half-wave film, a full-wave film with a full-wave film, etc. The reason for this similarity is that the wavelength dependence in Mie theory appears in the form of a size parameter $q = 2\pi a/\lambda$. Where a is the radius of the absorbing region. Although the radius of the absorbing region is of a size most likely to be damaged according to thermodynamic considerations, for very thin films it is roughly determined by the thickness of the film. Thus, if the film thickness is halved and the incident wavelength is halved the size parameter q remains the same and so should the ratio of the absorption cross section to the geometric cross section. This in fact is not observed. A wavelength dependence still remains in the experimental data.

When the data are plotted against the scaling (Eq. 10) for half-wave, quarter-wave and full-wave films, a clear splitting by wavelength occurs in each of the three types of film. The wavelength dependence can be realized by comparing Figs. 14-16 with Figs. 17-19. The only free parameter between Figs. 17-19 is the imaginary part n' of the index or refraction. That is, a value of n' is chosen that normalizes the analytical curves to an experimental data point. Since the absorption (1/cm) = $4\pi n'/\lambda$, the nonlinear dependence of n' on indicates that the absorption is a function of the wavelength. This is not unreasonable. Absorption is a function of wavelength in most theories of absorption that may apply here. The specifics of the wavelength dependence cannot be hypothesized though unless the precise mechanism or mechanisms are known. It should be noted that the imaginary part of the index of refraction is simply a phenomenological measure of absorption and does not give any information on the absorption mechanism.

For oxides (Fig. 20) there is a splitting of the scaling for both wavelength and material, although HfO_2 scales on the same line as Al_2O_3. If oxides are scaled against $t_p^{1/2}T_c(K_0C_v)^{1/2}$ multiplied by some additional material-dependent term (other than $(K_0C_v)^{1/2}$ the oxides also scale as in Eq. (10). According to data [Walker, et al. 1981] this constant is highly material dependent. It does not seem to depend upon the film thickness, but it does appear to depend on the incident wavelength to some fractional power (about 1/2), i.e. the magnitude of the splitting of each material at each wavelength varies roughly as $\lambda^{1/2}$. All this indicates that oxides also scale as the

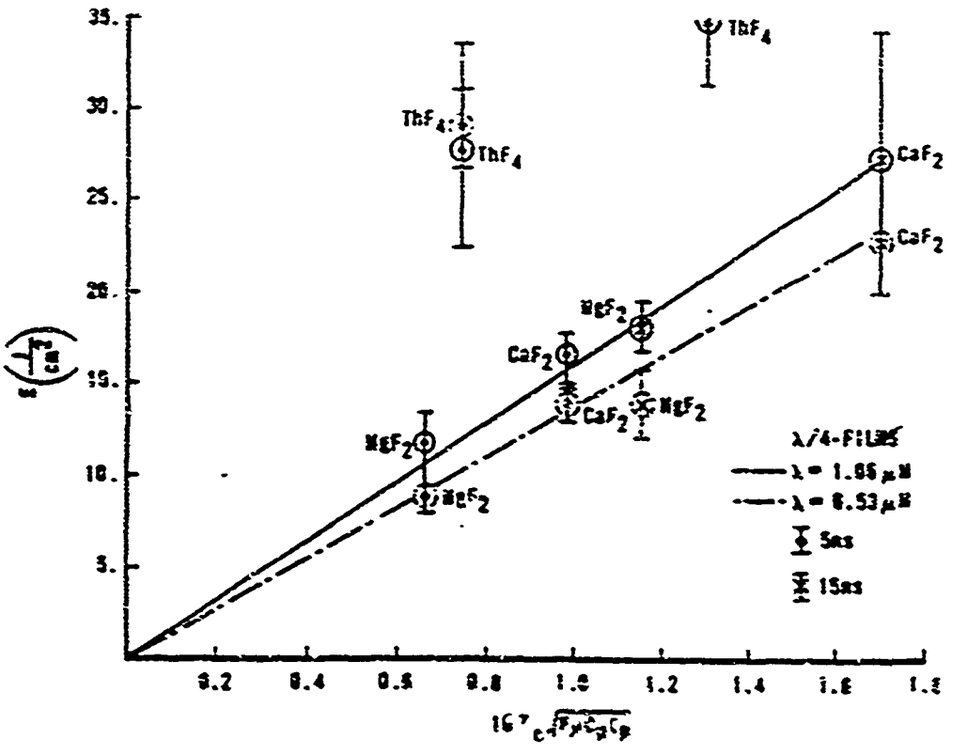

Fig. 14. Scaling of the experimentally measured damage threshold of fluorides vs. a theoretically derived parameter - I.

The parameter contains the thermal properties and the data is for quarter-wave films at two different wavelengths (the anomalously high ThF_4 points should be noted) measured at 5 ns (i) and 15 ns (ǂ): ——— , λ = 1.06 microns; — - —, λ = 0.53 microns. The material properties for the work in this chapter come from Goldsmith [1961], Sparks [1977] and Touloukain [1970]. Room Temperature values are chosen.

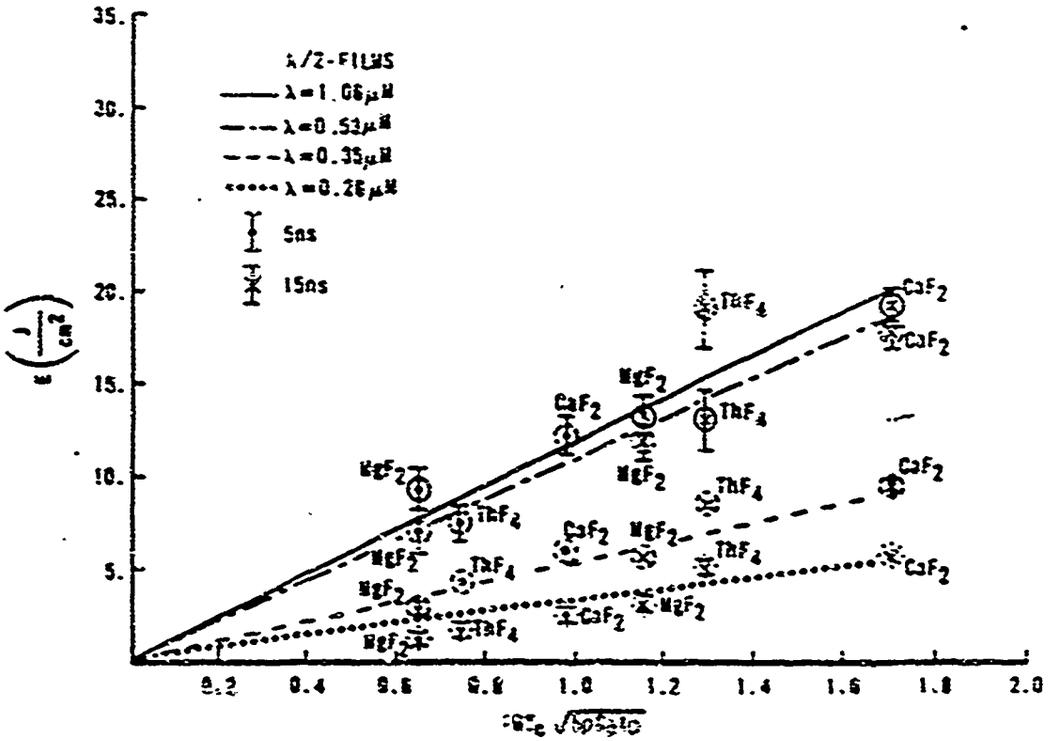

Fig. 15. Scaling of the experimentally measured damage threshold of fluorides vs. a theoretically derived parameter - II.

The parameter contains the thermal properties and the data is for half-wave films at four different wavelengths measured at 5 ns (I) and 15 ns (I): ——— , λ = 1.06 microns; — - —, λ = 0.53 microns; - - -, λ = 0.35 microns; ·····, λ = 0.26 microns.

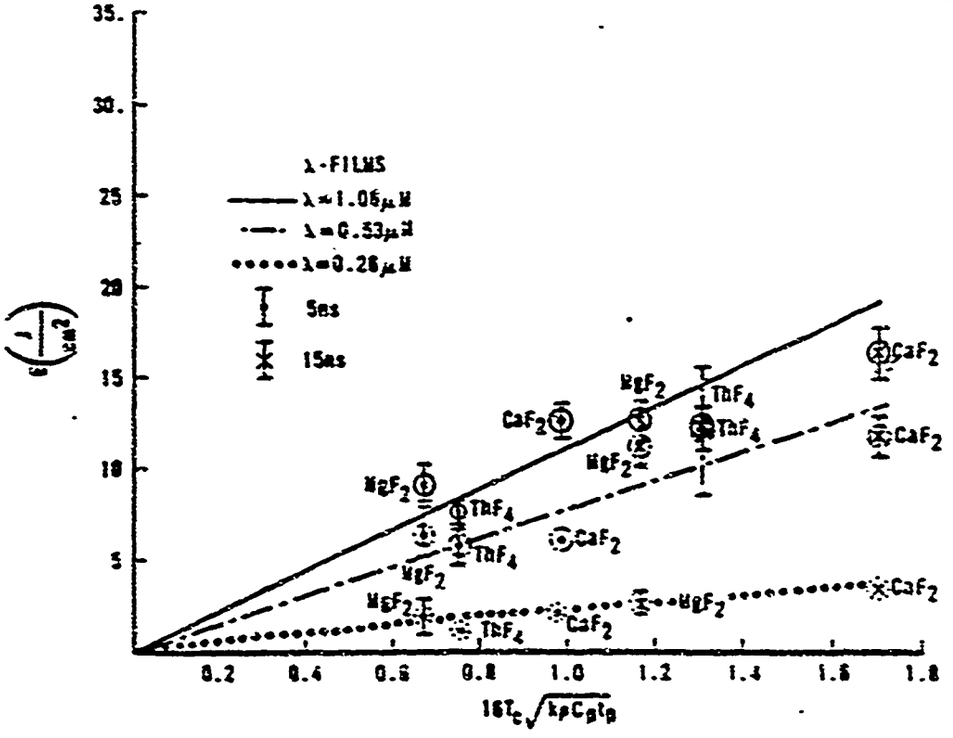

Fig. 15. Scaling of the experimentally measured damage threshold of fluorides vs. a theoretically derived parameter - III.

The parameter contains the thermal properties and the data is for full-wave films at three different wavelengths measured at 5 ns (I) and 15 ns (‡): ——, λ = 1.06 microns; — - —, λ = 0.53 microns; ·····, λ = 0.26 microns.

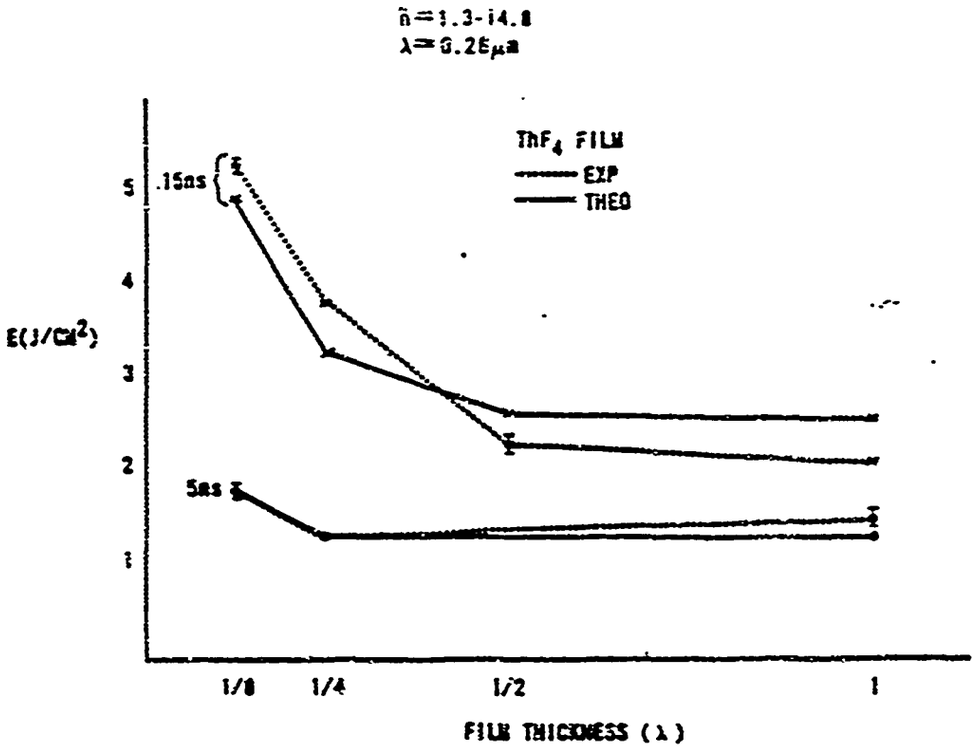

Fig. 17. Damage threshold data and theory vs. film thickness - I.

λ = 0.26 microns (measured in units of λ at 1.06 microns) (ThF_4 film; n = 1.3–i4.8): - - -, experimental data; ——, theoretical curve.

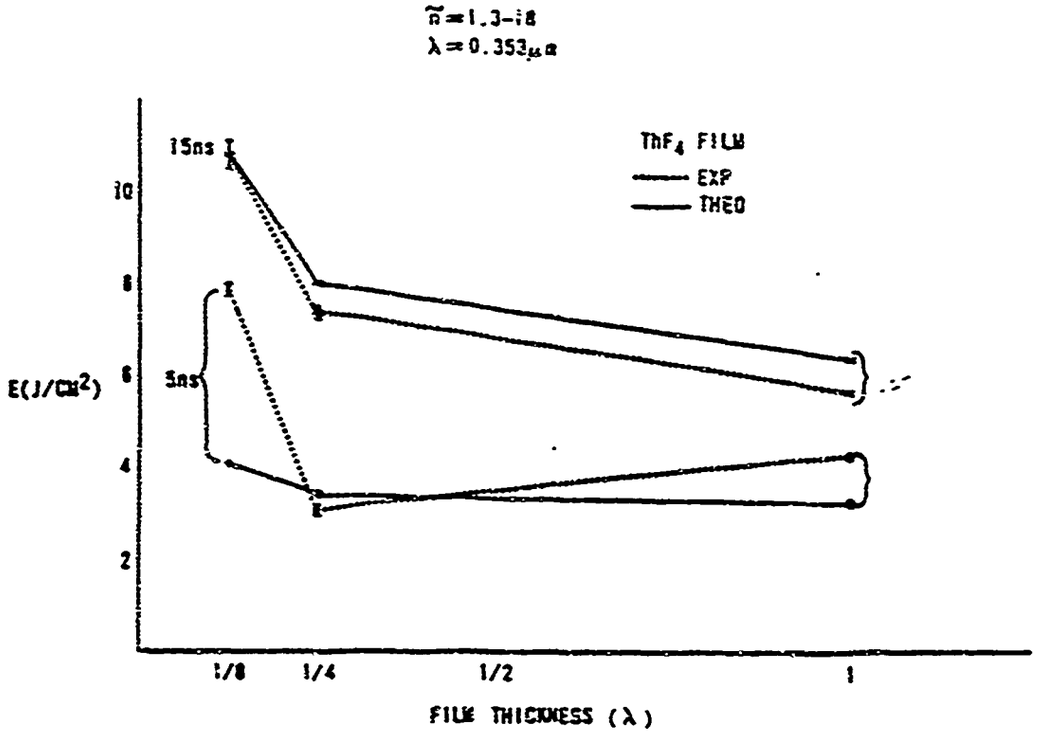

Fig. 18. Damage threshold data and theory vs. film thickness - II.

λ = 0.353 microns (measured in units of λ at 1.06 microns) (ThF_4 film; n = 1.3-i8): - - -, experimental data: ———, theoretical curve.

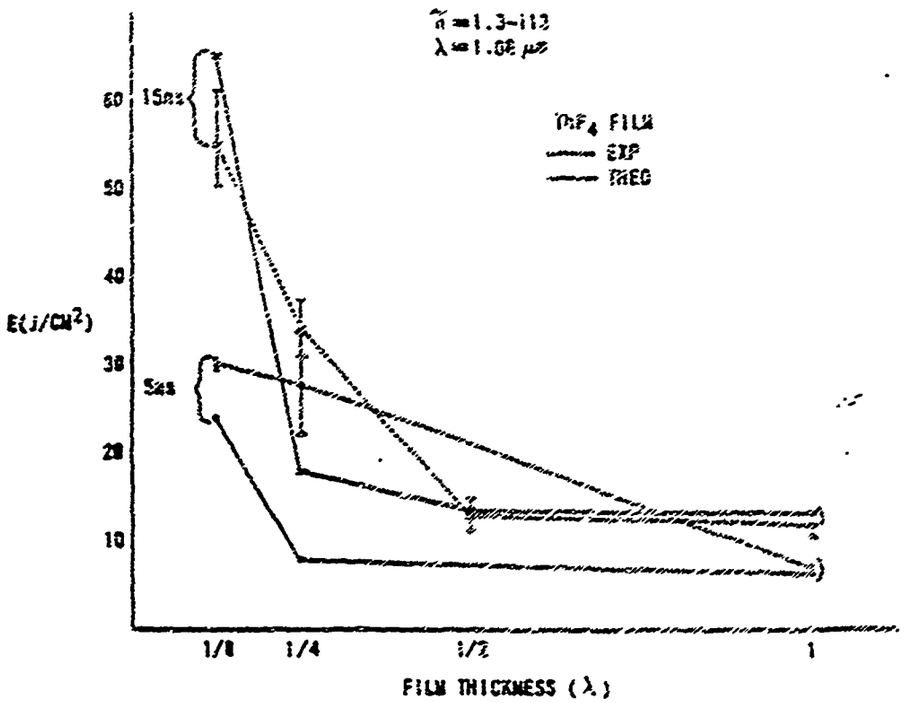

Fig. 19. Damage threshold data and theory vs. film thickness - III.

λ = 1.06 microns (measured in units of λ at 1.06 microns) (ThF_4 film; $\tilde{n}$ = 1.3-i13): - - -, experimental data; ———, theoretical curve.

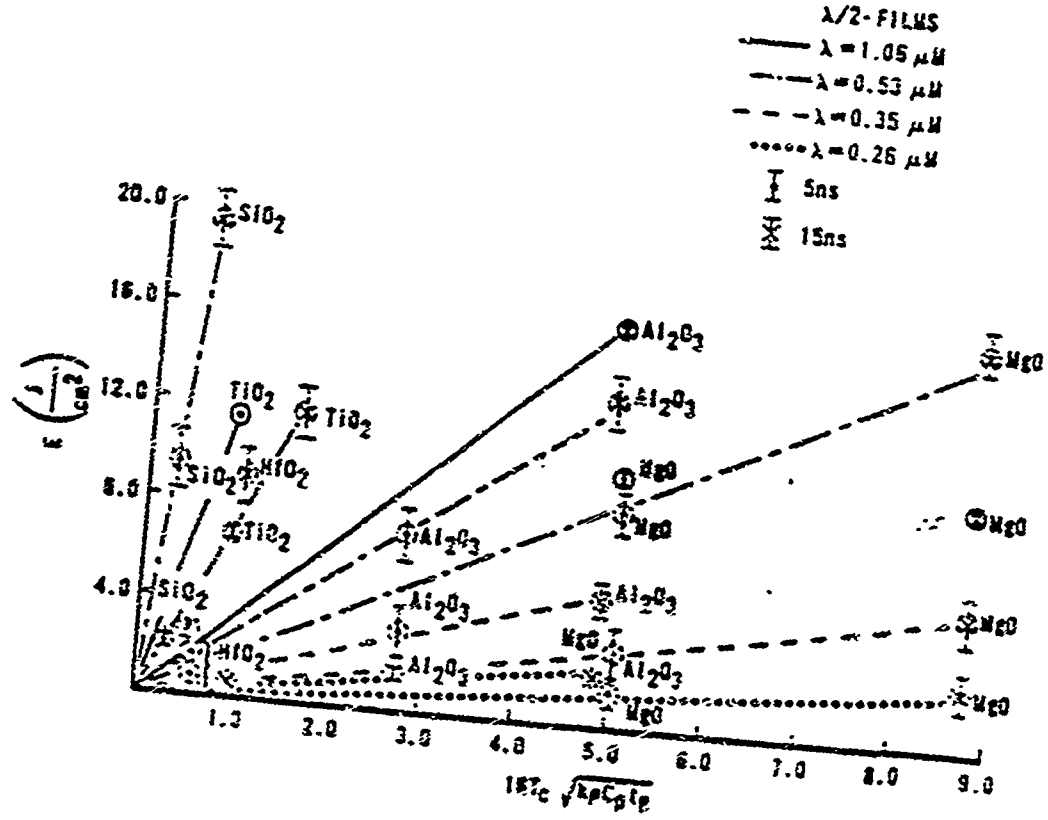

Fig. 20. Scaling of the experimentally measured damage threshold of oxides vs. a theoretically derived parameter.

The parameter contains the thermal properties and the data is for half-wave films at four different wavelengths measured at 5 ns (ǂ) and 15 ns (ǂ): ———, λ = 1.06 microns; — - —, λ = 0.53 microns; - - -, λ = 0.35 microns; ....., λ = 0.26 microns.

square root of the pulse length, but that some other material-dependent properties enter that are not strictly thermal (because of the wavelength dependence of the constant). In other words, the mechanisms for absorption in films of various fluorides are sufficiently similar that the thermal properties dominate the damage evolution, while oxides differ from film to film in some way other than the obvious thermal properties. This same behavior is also exhibited in Fig. 21 for fluoride and oxide data from a different source. Note how the fluorides group about a single line while the oxides spread. Note also that the order in which the oxide lines fall is the same in both data sets.

When the fluoride data are plotted against the scaling (Eq. (10)) for a given wavelength, films that are full-wave (at 1.06 μm) have damage thresholds that are similar to those of half-wave films, but as we consider quarter-wave or small films the difference becomes greater. This difference may be explained by reference to Figs. 17-19. These are plots of the exact solution of the diffusion equation using Mie scattering theory to compute the absorption cross section of these highly absorbing regions. That is, a combination of electromagnetic theory and thermal diffusion nicely explains the increase in damage threshold for thinner films at fixed incident wave lengths. This behavior may be simply understood. As the film, and therefore the absorbing regions, becomes small with respect to the wavelength, the regions absorb proportional to their volumes. However, regions of the order of a half wavelength or greater absorb in proportion to their geometrical cross section as shown in Chapter 2. Thus as the film

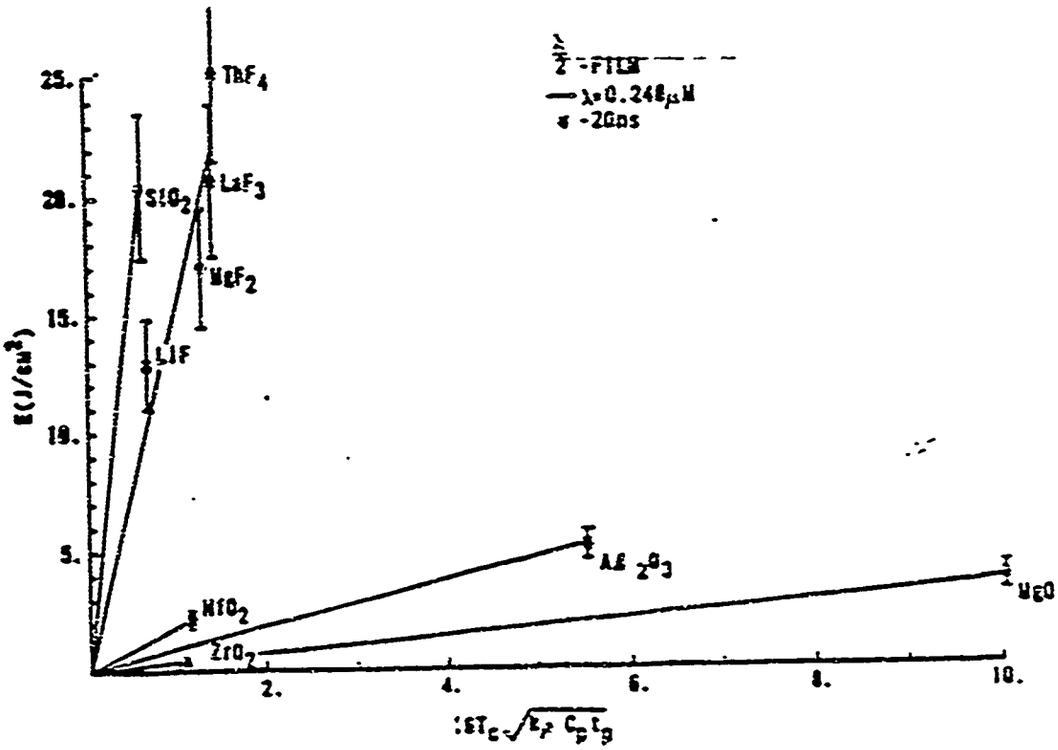

Fig. 21. Scaling of the experimentally measured damage threshold of both fluorides and oxides vs. a theoretically derived parameter.

The parameter contains the thermal properties and the data is for half-wave films at λ = 0.248 microns (* measurements taken at 20 ns).

thickness decreases, absorption decreases with the geometrical cross section of the absorbing region up to some point. Further decrease in the film thickness forces the absorption to decrease more like the volume, yielding higher damage thresholds.

This provides the relationship between the size of the absorbing region and the wavelength. In addition to that there is an increase in damage threshold due to the fact that the film becomes thinner than the diameter of the absorbing region of a size most likely to be damaged. Regions smaller than this require a larger amount of incident energy to be damaged.

The different behavior of oxides versus fluorides suggests at least one of three things. Either there is a major oxide-dependent difference in thin film properties as opposed to bulk properties, or there are structural or chemical complexities not accounted for or there is simply a mechanism for absorption in oxides such that the absorption appears to be highly material dependent. The last two seem more likely because of the wavelength dependence for the missing material constant.

It should be pointed out here that the more predictable behavior of the fluorides does not necessarily prove that an absorbing inclusion exists. However it strongly suggests a central absorbing region common to the various fluorides that thermally diffuses the absorbed energy such that damage thresholds for fluorides are thermally dominated. This region should have properties that either are initially different from the surrounding film or are quickly altered by an enhanced field, a mechanical or chemical process, or an increased

temperature in the region or possibly some combination of these. An enhanced field could be caused by a microcrack or a local defect [Bloembergen 1973].

The theoretical evidence that the size of the absorbing region that is damaged is of the order of the film thickness does not exclude the possibility that a smaller absorbing region expands to a size of the order of the thickness of the film as damage ensues. An expanding absorbing region has been suggested by Komolov [1982] and Anisimov and Makshantsev [1973] and expanding damage regions have been observed by Foltyn and Jolin [1983]. Also Babadzhan, et. al [1982] have suggested a mechanism for this process, although their assumptions leading to the absorption cross section appear to be in error.

It is interesting to note the stray ThF_4 points in Fig. 14 of the quarter-wave films. These same points are plotted on Fig. 19 for a damage threshold at $\lambda = 1.06$ microns versus film thickness. They are anomalously high on this plot also, indicating that they are unique points which do not follow the trends of the surrounding data.

It should be pointed out here that there are fundamental differences between oxides and fluorides which exhibit themselves through the macroscopic properties of the materials. For example, the index of refraction of fluoride films is usually less than that of oxide films. The melting temperature is also less for fluorides than for oxides. Furthermore the UV cut-off of absorption occurs for shorter wavelengths in fluorides than in oxides and thus multiphoton effects would appear sooner in oxides as the wavelength decreases. There are other possible differences such as the structural properties,

the elasticities or the thermomechanical response of the materials. One final apparent difference is the fact that fluorides probably have oxide impurities, but the nature of the impurities in oxide films is unknown. The implication or significance of these various differences is unknown. However, the fact that oxides tend to have lower damage thresholds yet higher melting temperatures indicates that some additional mechanisms may intervene in the damage evolution process for oxides.

One additional comparison of the thermal scaling is given purely for the sake of completeness (Fig. 22). This is plotted along with data from [Rainer, et al. 1982] for the purpose of comparison. Note that the data is plotted on different scales. Comparison of these scales for wavelength variation may or may not be meaningful since they are from two different experiments.

The final experimental comparison given is that of the work presented in Chapter 3. Some preliminary results from experiments currently being conducted by Kardach [1985] shows a scaling with the thermal conductivity of the substrate for single layer films. The results, shown in Fig. 23, are consistent with the findings in Chapter 3.

It is felt that significant correlation has been shown with experiment of the concept developed here. The transport scalings in Chapter 6 indicate that the absorption must be strong and localized. This is further supported by the morphology observed in the damage data. The next chapter concentrates on the development of the physical processes leading to the strong localized absorption.

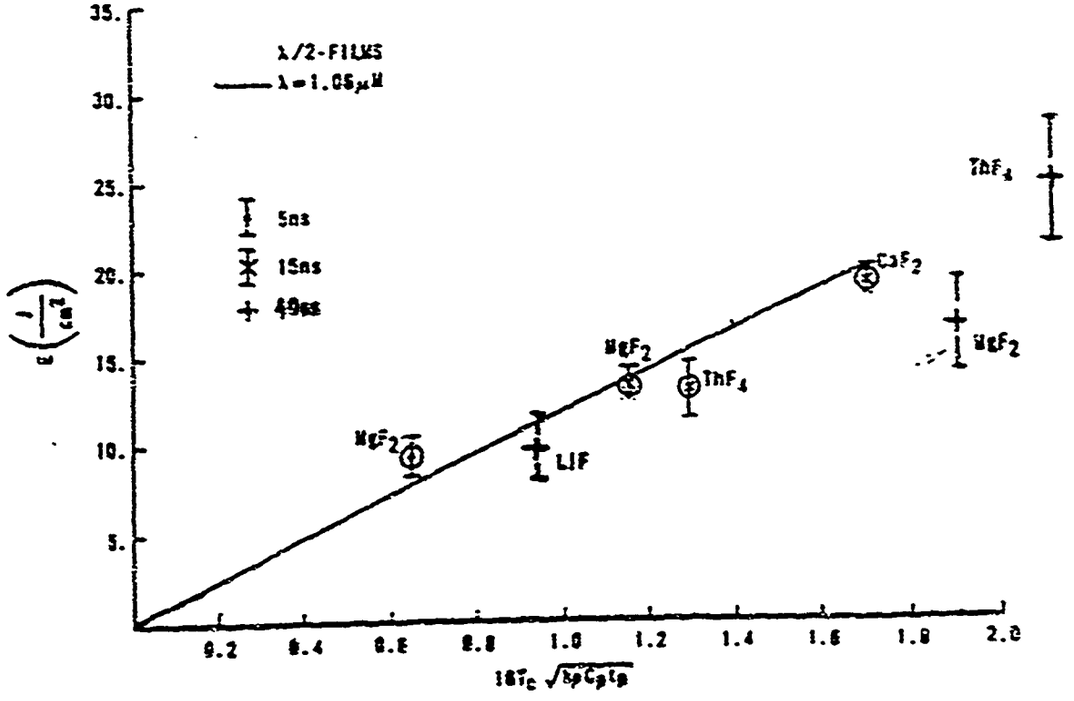

Fig. 22. Scaling of the experimentally measured damage threshold of fluorides vs. a theoretically derived parameter - IV.

The parameter contains the thermal properties and the data [Bettis, 1975] is for half-wave films at 1.06 microns and 40 ns. Some of the uncommon fluorides in the data set did not fit the scaling.

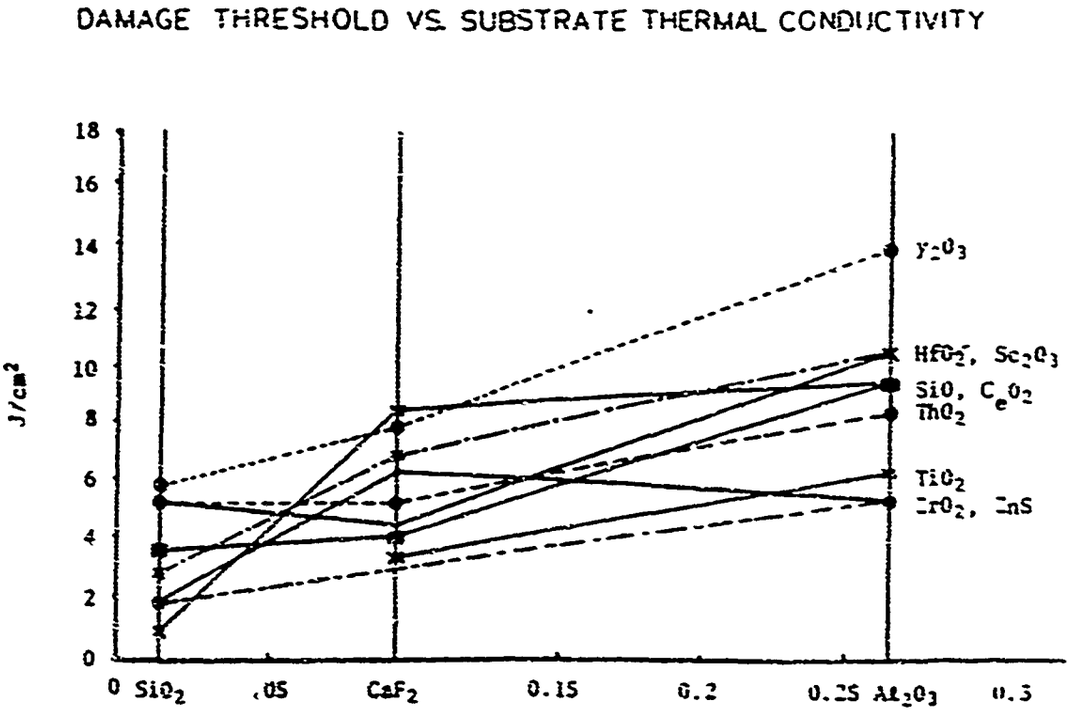

Fig. 23. Damage threshold vs. substrate thermal conductivity.

The data was taken at 1.06 microns and 5 ns on half wave films.

CHAPTER 6

FUNDAMENTAL ABSORPTION MECHANISMS

In the work set forth to this point, the concepts of a localized absorbing region within an optical thin film have been presented. These localized absorbing regions are assumed to be due to anomalies of some sort. Heat transfer equations were solved indicating trends in damage thresholds as a function of material and experimental parameters. Thermal diffusion was assumed as the dominant controlling mechanism in the damage process. Experimental data correlates quite well with this model. The thermal diffusion equations incorporate a nonhomogeneous thermal source, which is due to a localized electron density interacting with both the incident field and the lattice structure.

In actuality, there are two coupled nonhomogeneous diffusion processes involved. They are thermal diffusion due to the aforementioned thermal source, and electron diffusion due to a localized electron source. The electron source properties depend, in the main, upon the local optical field and local temperature. These coupled equations are generally untractable and as such are usually decoupled through assumptions which can apply in certain limits.

Assumptions that were made are that the operative coefficients and the source for thermal diffusion are independent of temperature, and the electron density has been assumed constant. That is, the electron density is modeled as a step function in time and space such

that it evolves instantaneously and does not diffuse. These assumptions are obviously not valid in all cases of interest. Certain refractory oxide film damage [Walker, Guenther and Nielsen 1981], for example, exhibits morphology, which grows spatially during irradiation to a size comparable to the incident beam diameter.

In addition to the short comings of these employed assumptions, the use of an instantaneous electron density must be justified. Thus, mechanisms for the evolution of an electron density have to be investigated.

Theory

In an attempt to refine the model of Chapters 2 through 4 in the direction of more comprehensive theory, the concentration of effort is placed upon the evolution of the localized electron density and the absorption processes involved. The approach taken to this end is to write down the classical equation of electron diffusion and solve it for a generalized electron source. Conservation of electromagnetic and thermal energy is then employed with the principal purpose of ascertaining useful scaling laws. The comparison of these scaling laws with experimental data implies certain preferred absorption mechanisms. These mechanisms are then further investigated via the appropriate expressions governing electron diffusion.

The principal findings are that; i) local metallic concentrations supplemented by color centers may be a viable mechanism for the initial electron production in certain optical thin films and

ii) very small regions of these anomalies (200 A) can possibly lead to damage when supplemented by an avalanche ionization. Avalanche ionization is only assumed to occur in optical coatings and serves to expand the region that is absorbing at the anomalously high rate.

The classical equation of electron diffusion is given as:

$$\frac{\partial n}{\partial t} = \frac{1}{r}\frac{\partial^2}{\partial r^2}(rD_e n) + g(n,T,|E|) - (n - n_i)\gamma(n,T) \quad , \tag{46}$$

where D_e = electron diffusivity (cm^2/S), $|E|$ = electric field strength (V/cm), g = electron carrier generation ($cm^{-3}S^{-1}$), n = electron carrier density (cm^{-3}), n_i = initial carrier density (cm^{-3}), T = temperature (K), and $\gamma(n,T)$ = free carrier decay rate (s^{-1}).

The assumptions made in solution of the above equation are that D_e is independent of n and T (which is not true in general), and g is independent of T. The dependence of g on n and E are incorporated iteratively and the other assumptions will be addressed in Chapter 7.

The solution of the above equation in all space is found via integral transform. n_i is absorbed in n so that n becomes $n = n - n_i$. The general solution is found to be

$$n(r,t) = \frac{2}{\pi}\int_0^\infty d\beta \sin(\beta r) e^{-(D_e\beta^2 + \gamma)t} \int_0^t dt' \int_0^\infty r'dr' \sin(\beta r') g(r',t') e^{(D_e\beta^2+\gamma)t'} \quad . \tag{47}$$

In order to decide upon a reasonable choice for the electron source generation term g(r,t), attention is diverted to a consideration

of the conservation of energy. The morphology of damage suggests a localized source of electron generation, however, it does not imply a mechanism. Scaling laws derived from the conservation of energy consideration may, though.

The Poynting theorem may be written as

$$\frac{\partial w}{\partial t} = \vec{\nabla} \cdot \vec{S} - (\vec{J} + \frac{\partial \vec{P}}{\partial t}) \cdot \vec{E} + \vec{M} \cdot \frac{\partial B}{\partial t} \tag{48}$$

where w is the field energy, $\vec{S}$ is the Poynting vector, $\vec{J}$ is the electron current flux, $\vec{P}$ is the material polarization and $\vec{M}$ is the magnetization vector. If the field is in approximate steady state with the absorption process and magnetic transitions are neglected, then

$$\vec{\nabla} \cdot \vec{S} = \vec{J} \cdot \vec{E} + \vec{E} \cdot \frac{\partial \vec{P}}{\partial t} . \tag{49}$$

The $\vec{J} \cdot \vec{E}$ term contains the energy stored in electron acceleration along with electron-phonon collisions and the $\dot{\vec{P}} \cdot \vec{E}$ term contains the energy stored in polarization along with electronic transitions. The $\vec{J} \cdot \vec{E}$ term is the dominant term in avalanche-ionization and inverse brehmsstrahlung processes while the $\dot{\vec{P}} \cdot \vec{E}$ term is assumed dominant in single and multiphoton transitions. All of these are possible mechanisms of absorption. In order to avoid restriction to any certain mechanism the $\vec{\nabla} \cdot \vec{S}$ term is used to represent absorption.

For simplicity an incident plane wave is assumed, which gives

$$\vec{\nabla} \cdot \vec{S} = - \frac{In_r \alpha}{u} e^{-\alpha z} = - \frac{In_r V \sigma}{u} e^{-\alpha z} \tag{50}$$

where I, n and μ are the incident field intensity, real index of refraction and magnetic permeability. α is the generalized absorption coefficient and σ is the generalized absorption cross-section with V the volume that is absorbing.

From the first law of thermodynamics the energy balance of an absorbing region is

$$\vec{\nabla} \cdot (-\vec{\nabla}(kT)) + \frac{\partial}{\partial t}(\rho c_v T) = -\vec{\nabla} \cdot \vec{S} , \qquad (51)$$

where k = thermal conductivity, c_v = specific heat at constant volume, and ρ = mass density, which leads to

$$E_D(J/cm^2) = \frac{\mu}{n_r}\int_0^{t_p} \frac{dt}{c} \left\{\frac{\partial}{\partial t}(\rho c_v T) - \vec{\nabla} \cdot (\vec{\nabla}(kT))\right\} , \qquad (52)$$

where E_D is the energy density of the incident pulse at which the region reaches a critical temperature which causes damage.

The energy depletion from the incident field occurs over a region represented by the length α^{-1} which includes absorption by electrons that immediately thermalize along with those that thermalize after electron diffusion of length δ_e. As pointed out by Meyer, Bartoli and Kruer [1980], the thermal diffusion may be incorporated in the same manner. That is, the energy that is deposited in the lattice is deposited in a region resulting from absorption and thermalization of electrons (both with and without diffusion) along with the thermal diffusion δ_T that occurs after deposition during the pulse. The thermal diffusion length is given by $\delta_T = \sqrt{Dt}$. The two parallel processes may be added to give

$$\delta_{eff} = \left[\frac{\chi_1}{\left[\alpha^{-1} + \delta_T\right]} + \frac{\chi_2}{\left[\alpha^{-1} + \delta_e + \delta_T\right]} \right]^{-1} . \quad (53)$$

Here χ_1 is the fraction of laser energy deposited directly into the Lattice and χ_2 is the fraction of energy that diffuses before being deposited.

Thus we can write

$$E_D(J/cm^2) \propto \frac{1}{n_r} \int_0^T dT \; c_v \delta_{eff} . \quad (54)$$

by substituting an effective diffusion length for the diffusion term.

The importance of this procedure is the demonstration of useful scaling laws. For example, when $\delta_T > \delta_e, \alpha^{-1}$,

$$E_D \propto \frac{1}{n_r} \int_0^T dT \sqrt{\rho c_v k t_p} \left[\frac{\chi_1}{\left[1 + \frac{\alpha^{-1}}{\delta_T}\right]} + \frac{\chi_2}{\left[1 + \frac{\alpha^{-1}}{\delta_T} + \frac{\delta_e}{\delta_T}\right]} \right]^{-1} , \quad (55)$$

and when $\delta_e, \delta_T < \alpha^{-1}$

$$E_D \propto \frac{1}{n_r} \int_0^T dT \rho c_v \alpha^{-1} \left[\frac{\chi_1}{\left[1 + \alpha\delta_T\right]} + \frac{\chi_2}{\left[1 + \alpha\delta_e + \alpha\delta_T\right]} \right]^{-1} . \quad (56)$$

The first case exhibits the same scaling law derived for a spherical absorbing region where thermal diffusion dominates (see Chapter 2). Here, it is much more general in that no specific geometry has been assumed and temperature variation of the constants is incorporated.

The second case demonstrates an absorption dominated process and implies that $E_D \propto \alpha^{-1}$. Thus the wavelength dependance of $\alpha(\lambda)$ should exhibit itself in the damage threshold data roughly as $E_D \propto \alpha^{-1}(\lambda)$.

In addition to the exhibition of wave length dependence in certain cases, an important point of the above scalings is the demonstration of the perspective which they lend to the all important energy transport process. The scales over which energy transformation and transport occur are solely responsible for whether the damage is absorption or diffusion dominated.

The wavelength dependence for damage from reference [Walker, et al. 1981] may be found by averaging the wavelength dependence of the films (λ and $\lambda/2$) for five and fifteen nanoseconds. When this is done it is found that between λ = 0.26 microns and 0.53 microns the fluorides damage as $\lambda^{1.95}$ while oxides damage as $\lambda^{2.49}$, and between λ = 0.53 microns and 1.06 microns fluorides damage as $\lambda^{0.24}$ and oxides $\lambda^{0.5}$. There is significant statistical deviation from film to film (i.e. for the various coating materials).

In all of the theories investigated, this increasing power of frequency in the absorption function with increasing photon energy was only noted in photo-ionization processes. However, the films and photon energies investigated [Walker, et al.,1981] should not be near band edge transitions. It should be noted that a large density of impurity states can exhibit this same behavior. In addition, the transition between different, but related, processes of absorption at different frequencies is a possibility (i.e., different sorts of

impurities). These may occur in the same, or even separate discrete regions.

The general α is constituted as $\alpha = \sum_n \alpha_n + \alpha_{Fc}$ where $\sum_n \alpha_n$ is the absorption coefficient for n-photon absorption and α_{Fc} is the absorption coefficient for free carriers. $\sum_n \alpha_n$ is related to α_{Fc} in that n-photon absorption produces free carriers.

Although these processes are generally considered intrinsic they also may apply to the obviously extrinsic damage processes which occur in optical coatings due to localized shallow or impurity states in the coating. These shallow impurity states support photo-ionization and impact ionization at threshold levels far below those expected of a pure material. These states may occur due to impurity atoms, ions, non-stoichiometric mixtures leading to metallic colloids, color centers or simply because of local disorder. Shallow states due to disorder have been confirmed for D.C. fields by conductivity measurements [Ovshinsky 1963]

Thus, due to the above possibilities and the observed morphology it is assumed that there exists the probability of very small localized regions of impurities.

One obvious choice for an electron source function is a uniform spherical region, of impurities or shallow states, of radius r_0. The origin of such a region may be a coagulation of centers resulting from dislocations, as discussed below.

This source term is given by

$$g(r',t') = f(t')\{s(r') - s(r'-r_0)\} . \qquad (57)$$

Where for single and multiphoton transitions of shallow states

$$f(t') = \left(\frac{\eta_Q \alpha_1 I}{h\nu} + \frac{I^2 \beta}{2h\nu}\right) \vartheta(t'). \tag{58}$$

Here I is the incident intensity (ev/cm^2-s), α_1 is the one photon coefficient (1/cm), β is the two photon coefficient (cm-s/ev), η_Q is the quantum efficiency (1), $h\nu$ is the photon energy (ev), and the ϑ's are step functions. This integral (Eq. (57) into Eq. (47)) is very similar to the one in Chapter 2 and affords a solution of

$$n(r,t) = \frac{2}{\pi} \frac{f(t_p) r_0^3}{D_e r}$$

$$\times \int_0^\infty \frac{dy \sin\frac{yr}{r_0} (\sin y - y\cos y)\left(1 - e^{-(D_e y^2/r_0^2 + \gamma)t}\right)}{y^2(y^2 + r_0^2\gamma/D_e)}. \tag{59}$$

For the region of parameter space of interest here, the above integral provides numerical problems in its evaluation. However the first term of the integral may be done analytically giving a solution of

$$n(r,t) = \frac{2}{\pi} \frac{f(t_p) r_0^3}{rD_e}$$

$$\times \left(A - \int_0^\infty \frac{dy \sin\frac{yr}{r_0} (\sin y - y\cos y)\left(e^{-(D_e y^2/r_0^2 + \gamma)t}\right)}{y^2(y^2 + r_0^2\gamma/D_e)}\right), \tag{60}$$

where

$$A = (\pi D_\epsilon \pi/(2r_0^3\gamma))\{1 - \frac{1}{2}\,(\exp[-(1+r/r_0)c]$$

$$+ \exp[-(1-r/r_0)c]\} - (r_0/(2cr))(1 + (1-r/r_0)c)$$

$$\times \exp[-(1-r/r_0)c] - (1+(1+r/r_0)c)\exp[-(1+r/r_0)c]\}\ , \qquad (61)$$

and where $c^2 = r_0^2\gamma/D_\epsilon$. This solution is numerically convergent, but only valid for the region of $0 < r/r_0 < 1$. A numerical plot from this solution is given in the next section.

In the far field ($r >> r_0$) the source may be described as

$$g(r',t') = \frac{\delta(r')\xi(t')V}{4\pi r'^2}\ . \qquad (62)$$

Where $\delta(r')$ is a delta function and V is the characteristic volume of absorption. This gives for the electron density,

$$n(r,t') = \int_0^t dt' \frac{Vf(t')}{8(\pi D_e(t-t'))^{3/2}}$$

$$\exp\ \frac{-r^2}{4D_e(t-t')}\ \exp(-\gamma(t-t'))\ , \qquad (63)$$

$f(t')$ is the same as before and α_1 and β are computed from the stimulated transition rates which can be found in terms of the oscillator strengths of the impurity states.

In alkali-halides the shallow impurity states may be provided by a distribution of metallic colloids resulting from poor stoichiometry and various aggregates of color centers. Colloids may be produced in the process of heating to 200 to 350 C [Schulman and Compton 1963; and Hayes 1974] or even by insufficient heating during film deposition. In addition, mild heating causes the coagulation of F-centers to colloidal particles [Schulman and Compton 1963]. With specific reference to alkaline earth fluorides, "F-centres in additively-colored alkaline earth fluoride crystals readily aggregate forming more complex structures" [Hayes 1974]. An example of the sort of distribution that may occur is shown in Fig. 24.

Where, in optical coatings, the possible localized concentrations of absorption centers such as these come from is not discussed here. Dislocation clusters and poor stoichiometry are quite likely in optical coatings. The assumption made is that the conditions of deposition and processing of coatings allow this to be true.

As an illustrative example of one of the materials of interest [Walker, et al. 1981], CaF_2 has an absorption peak at 521 nm in what is called the S band predominantly due to M-centers. It should be pointed out that in CaF_2 the F-centers peak at 376 nm and certain colloids peak at 550 nm. In addition to these are many other complex combinations of centers. [Schulman and Compton 1963; Hayes 1974; and Fowler 1968].

The oscillator strength may be assumed to be ~ 1 [Beaumont and Hayes 1969; and Fowler 1964] and the transition rate for single photon transitions is given as [Yariv 1[illegible] Gray 1973a]

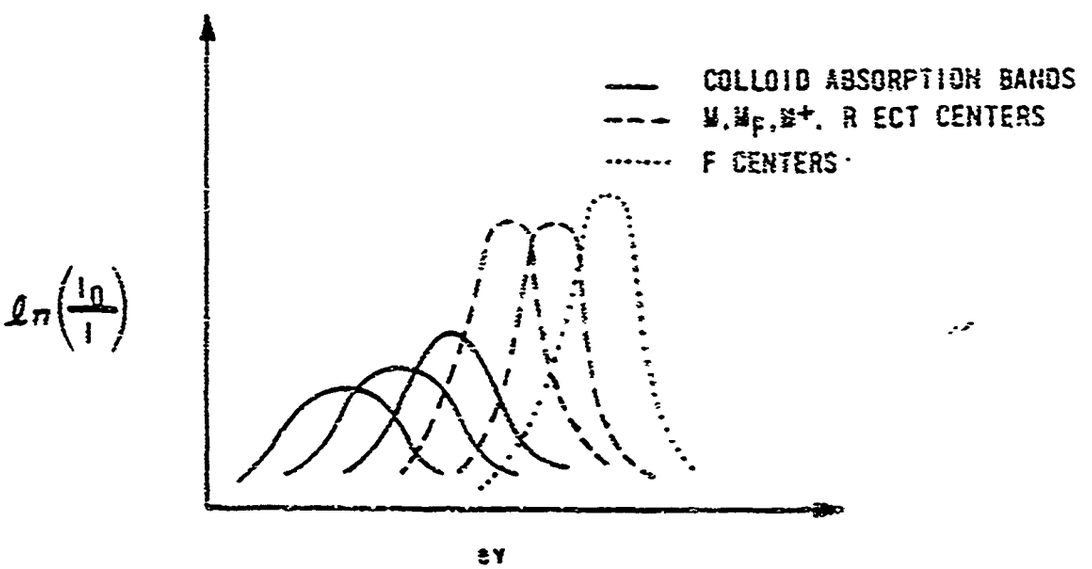

Fig. 24. A possible absorption distribution vs. photon energy for a complex aggregate of absorption centers.

$$W_{ik} = \frac{I\, g(\nu) e^2 f_{ik}}{mch\nu} , \tag{64}$$

where $g(\nu)$ is the normalized lineshape, f_{ik} is the oscillator strength and I is the laser intensity. $g(\nu)$ [Yariv 1967; and Gray 1973b] can be expressed as follow

$$g(\nu) = \frac{2(\ln 2)^{1/2}}{\pi^{1/2}} \exp[-4(\ln 2) \frac{(\nu-\nu_0)^2}{(\Delta\nu)^2}] . \tag{65}$$

One of the wavelengths of interest is 530 nm [Walker, et al. 1981], which is slightly off center of the transition line. Due to the large width of the lines [Schulman and Compton 1963; Hayes 1974; Fowler 1968; Gray 1973b; Sparks and Duthler 1975], we find $g(\nu) = 0.9/\Delta\nu$, however to be conservative a line shape factor of $0.1/\Delta\nu$ will be used.

From this computation it is found that $W_{ik} = 1.4 \times 10^{11} s^{-1}$ from ground state to the first excited state. This first excited state is long lived [Beaumont and Hayes 1969; and Fowler 1964] and will easily ionize deeply into the conduction band from here.

Results

Assuming an absorption center density of $n_a = 10^{17}$ cm^{-3} (which may be conservative for a thin film [Sparks and Duthler 1975])

$$\frac{n_0 \alpha_1 I}{h\nu} = \frac{n_a W_{ic}}{2} = 7 \times 10^{27} \text{ cm}^{-3} \text{ s}^{-1} . \tag{66}$$

Here a factor of 1/2 was included to account for the final ionization step, some of which may occur thermally. This factor may be placed

into the quantum efficiency $\eta_a = 1/2$ and can be considered conservative due to the ionization transition rate approximated from equations in references [Yariv 1967; Vaidyanathan, et al. 1977; Vaidyanathan, et al. 1979].

Several important points related to Table 4 should be mentioned. The results that follow are based upon classical diffusion which should not apply where small numbers of electrons are involved. If one multiplies the electron densities by the impurity region volume it is clear that rather small numbers of electrons are indeed involved. There is no attempt made here to model this situation rigorously. This aspect of the study is used to demonstrate relative orders of magnitudes, and the feasibility of very small local anomaly regions producing large electron densities in the conduction band.

Some of the numerical results from the integration of Eq. (59) are shown in Table 4.

α_1 = 4.91 (cm^{-1}), (for $n_a = 10^{17} cm^{-3}$, $\sigma = 2.1 \times 10^{-17}$)

β = 0.

η_Q = 1/2

D_e = 0.31 (cm^2/s)

f_{12} = 1.0 (oscillator strength)

$g(\nu)$ = $0.1/\Delta\nu$ (line shape factor)

$h\nu$ = 2.34 eV

t_p = 10^{-8} s

r_0 = radius of region of impurities

γ = conduction electron recombination rate (s^{-1})

σ = absorption cross section (cm^2)

P = probability of electron production within volume of interest

n(50A, 0.1ns) = electron density at 0.1ns and r = 50 A

Δt = time at which probability of electron production exceeds 1

For example, the initial color center density for the table below is chosen to be 10^{17} cm^{-3}, however the final electron densities produced from this exceed this number. This number is not chosen to be realistic as much as it is chosen to be conservative. In a region where trap centers are generated by polishing damage or some other process, the trap centers would probably be orders of magnitude greater than 10^{17} cm^{-3}. Thus, 10^{17} is chosen to provide a conservative transition rate, though it is not allowed to limit the number of electrons which transition. Conduction electrons are limited, however, by recombination, or decay. It may further be noted that if 10^{17} cm^{-3} color centers existed in a region of 100 Å in radius, at best one half of an available electron would be in this region. Clearly its only purpose is to give conservative transition rates. As such, the numbers in Tables 4 and 5 should not be taken as accurate. They are presented to demonstrate relative orders of magnitudes of conduction electrons that could be produced under the conditions of radiation, decay and diffusion. One primary point of Table 4 is the demonstration of the

Table 4. Electron densities achieved at 50 Å within an absorbing region due to photoionization of absorption centers.

$I \frac{GW}{cm^2}$	r_0(cm)	$\sigma(cm^2)$	$\gamma(s^{-1})$	P	n(50Å,0.1ns)	Δt
0.1	10^{-6}	2.1×10^{-17}	10^{12}	<1		
			10^{11}	<1		
			10^{10}	<1		
1.0			10^{12}	<1		
			10^{11}	<1		
			10^{10}	>1	4.2×10^{17}	40 ps
	2×10^{-6}	1.6×10^{-17}	10^{12}	<1		
			10^{11}	>1	6.5×10^{16}	10 ps
			10^{10}	>1	4.2×10^{17}	8 ps
	10^{-6}	1.6×10^{-16}	10^{12}	<1		
			10^{11}	>1	5.2×10^{17}	6 ps
			10^{10}	>1	3.4×10^{18}	4 ps

Table 5. Electron Densities achieved at $12.x10^{-6}$ cm from color center initiation due to an electron avalanche for various parameters. The avalanche is assumed to spread via diffusion.

α_a	$= 10^{10} (s^{-1})$	Avalanche coefficient
D_e	$= 0.01$ (cm^2/s)	Electron diffusion coefficient
f_{ik}	$= 1.0$	Oscillator strength
$g(\nu)$	$= 0.1/\Delta\nu$	Line shape factor
$h\nu$	$= 2.34$	Photon energy
t_p	$= 10^{-8}$	Pulse length
n_f^*	$= 10^{20}$	Limiting electron density

* The limiting electron density n_f^* was chosen as a reasonable value based upon [Burstein 1954].

$I \frac{GW}{cm^2}$	$\sigma/10^{-17}$	r(cm)	$\gamma(s^{-1})$	$\gamma_a(s^{-1})$	n(r,1ns)
1.0	2.1	$12.0x10^{-6}$	10^{10}	10^9	$4.7x10^{12}$
				10^{10}	$6.x10^{16}$
	16.4		10^{11}	10^9	$2x10^{10}$
				10^{10}	$1.2x10^{15}$
			10^{10}	10^9	$6.3x10^{12}$
				10^{10}	$6.x10^{16}$

fact that the size of a region and the intensity of radiation dictate a threshold condition due to competing probabilities of transition and decay in the region. What constitutes this region is not assumed here, other than the fact that it contains shallow centers. It may be an inclusion at the base of a nodule [Lao and Smith 1985] or at a grain boundary. It may be a dislocation cluster [Lewis, et al. 1985]. It should be noted here that colloidal particles deposit selectively at dislocations [Schulman and Compton 1963]. In addition, dislocations are the source of color centers.

This threshold is not, however the damage threshold. The important parameter in damage is the rate at which lattice energy builds in a local region. Even if the electron transition threshold is exceeded, the energy may be harmlessly conducted away by electron and phonon transport. Table 4 also serves to demonstrate that if sufficient numbers of electron trap centers (M-centers, in this case) are present, the transition is quick ($<< t_p$). The partitioning of such regions where the volume may be smaller than the volume between trap centers is very artificial. It is intended to generalize the table to weaker transitions at higher densities, or perhaps colloidal transitions. This is why the cross section is listed in Table 4. Whatever the source of electrons, if the cross section is as given, the table should remain valid in the region of the transitions.

Although the electron densities represented in these small regions are quite high, they could not alone transfer sufficient energy to the lattice to cause damage. Densities of this sort are required over regions approaching 0.1 to 1. micron in diameter [see Chapter

Twc]. Since anomaly regions of this size are not observed in optical coatings (except for nodules), these absorbing regions must evolve during irradiation. Since nodules are of the same material as the surrounding film the absorption in and around them must similarly evolve. Of the various mechanisms studied for this process, the only reasonable explanation found is the expansion of the absorbing region via impact ionization. That is, these small local high densities of conduction electrons ionize the surrounding off resonant electron trap centers and impurities. This is commonly termed avalanche ionization, though it usually applies to purely intrinsic processes (ionizing valence electrons). It should be noted that if the absorption center region is on the order of 0.1 to 1. micron, no avalanche is required to produce the appropriate region of high electron densities. This, however, is probably unlikely. A solution of this case is shown in Fig. 25 which emphasizes the effect of γ.

An avalanche due to impact ionization of impurity, colloidal or trap states would explain the observation of lower damage thresholds in doped materials regardless of whether or not the doping impurities are in resonance with the field. The photoionization of centers to initiate the process would explain qualitatively the wavelength dependence of damage thresholds in optical coatings.

Although specific numbers are used for a given case in a certain material, this is done for computational purposes. It is felt that the calculation of a specific example is desirable. The concepts are intended to be applied to more general cases through the use of absorption cross sections.

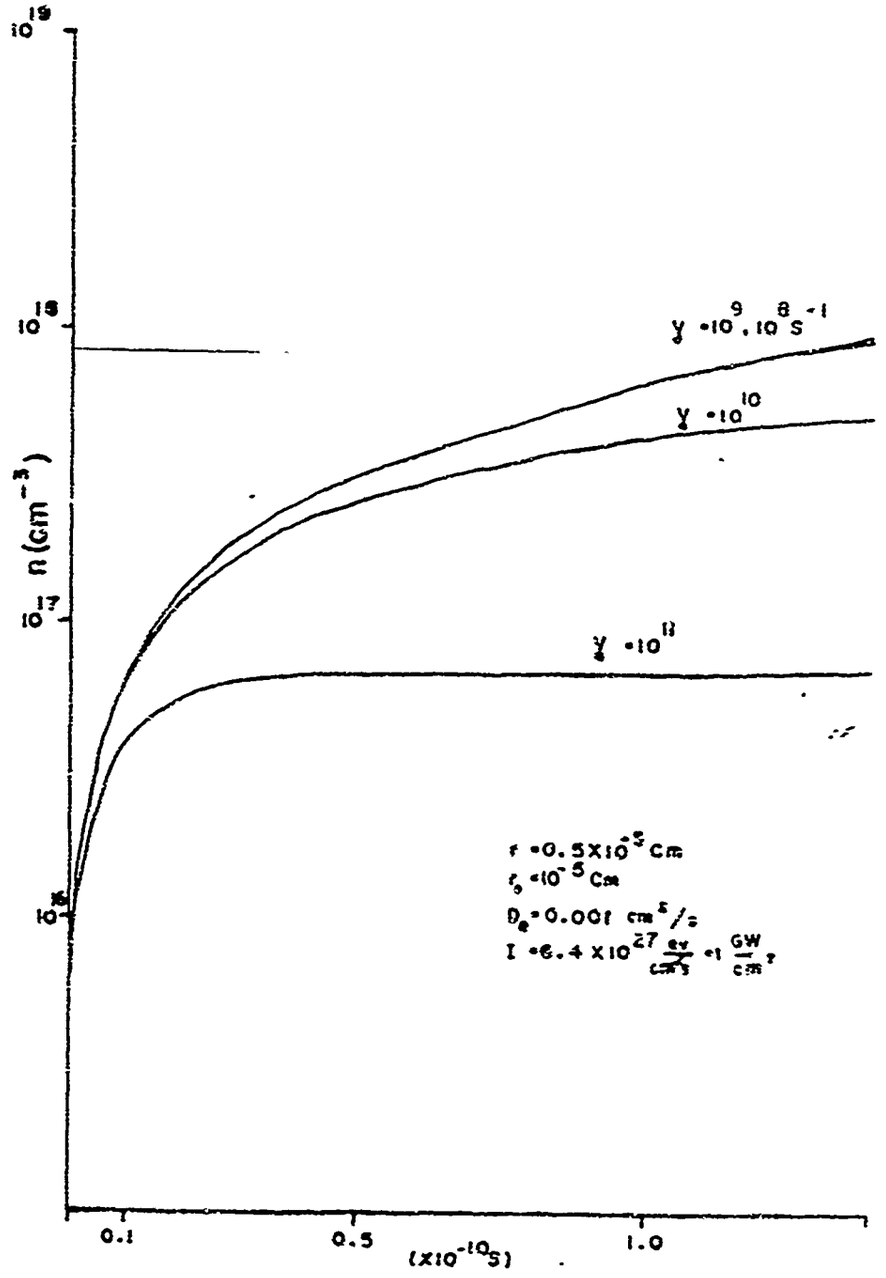

Fig. 25. The growth of the electron density.

The point of observation is at a radius of 500 Å within an absorbing regin of 1000 Å radius for various γ's and the parameters given. All unlisted parameters are those given for Table 4.

A detailed study of avalanche ionization will not be conducted here. That has been the topic of considerable research by authors such as [Sparks and Duthler 1975; Yablonovitch and Bloembergen 1972; Fradin, Yablonovitch and Bass 1973; Epifanov 1974]. As reference [Fradin, et al. 1973] implies, avalanche-ionization has been confirmed in solids, and as reference [Sparks and Duthler 1975] indicates, a computational competency has been achieved with the processes involved. It will simply be assumed here that due to shallow trap states, densities in excess of those required [Sparks and Duthler 1975] to initiate an avalanche have been provided. An exponential growth then follows, which is subsequently limited by ionization of a large fraction of the available atoms, carrier decay and the dynamic Burstein shift [Burstein 1954]. A simple calculation with Eq. (67) shows that at optical frequencies (~500 nm) and damage intensities (~1-2 GW/cm^2) in fluoride films a conduction electron can gain energies of one half to three eV in 10^{-10} seconds.

$$\frac{d\varepsilon}{dt} = |E|^2 \frac{e^2 \tau_k}{m^* (1+\omega^2 \tau_k^2)} \tag{67}$$

(In Eq. (67) ε is the energy transferred to the electron and τ_k is the time between collisions).

The spread in values is due to uncertainties in collision frequencies. These energies are sufficient to ionize many electron trap centers and some impurities [Sparks and Duthler 1977].

The simple model used herein will produce a conservative estimate of the growth of an electron density initiated by a small

region of absorption centers. This relates to the findings of Chapter 2 which demonstrate a requirement of isolated regions on the order of the film thickness with an average electron density on the order of 10^{18} cm^{-3}.

For this case, the form of g(r,t) chosen is

$$g(r',t') = f(t')e^{-p^2(t')r'^2} \tag{68}$$

where p(t') represents a spatial expansion of the electron source due to the avalanche process. It is assumed from previous studies [Fradin, et al. 1973] that an avalanche region's growth is nonlinear, however a conservative estimate of the region's size at a time t is $\delta_e = \sqrt{D_e t}$. That is, the distance electrons have travelled by diffusion from their initiation point. Thus; $p(t) = 1/\sqrt{D_e t}$ can be used as a trial parameter.

Subsequent integration of Eq. (47) affords

$$n(r,t) = \frac{1}{8}\int_0^t \frac{dt' f(t')(D_e t')^{3/2}}{(D_e((t-t') + \frac{1}{4D_e p^2}))^{3/2}}$$

$$\exp(-\gamma(t-t'))\exp\left(\frac{-r^2}{4\left(D_e(t-t') + \frac{1}{4D_e p^2}\right)}\right) \tag{69}$$

with

$$f(t') = n_i \alpha_a e^{\alpha_a t'} \tag{70}$$

where α_a is the avalanche coefficient. Equation (70) simply represents a means of generating electrons initially at an exponential rate. This growth is terminated at some point due to processes such as the dynamic Burstein shift and ionization of a large fraction of the available electrons.

A rigorous justification of Eqs. (69) and (70) above is not possible. These expressions are simply a reasonable choice for the purpose of a Gedanken study of a postulated process. It should also be noted that as shown in Braden, et al. [1973] avalanche is not a symmetric process. It in fact tends to propagate in the direction of the beam source due to an attenuation of the field. In optical thin films this propagation is modified by encounter of the film surface.

Some of the numerical results are presented in Figs. 26 and 27 and Table 4.

Discussion

The numerical results presented in the previous section indicate the feasibility of microdamage sites initiated by a localized absorbing anomally. An avalanche of electrons can produce large, densities of electrons expanding out to diameters on the order of the film thickness.

It should be noted that the field thresholds are lower than those reported previously for avalanche processes in similar materials. However, those were reported in bulk solids. The starting mechanism in thin films should provide lower thresholds for starting the process

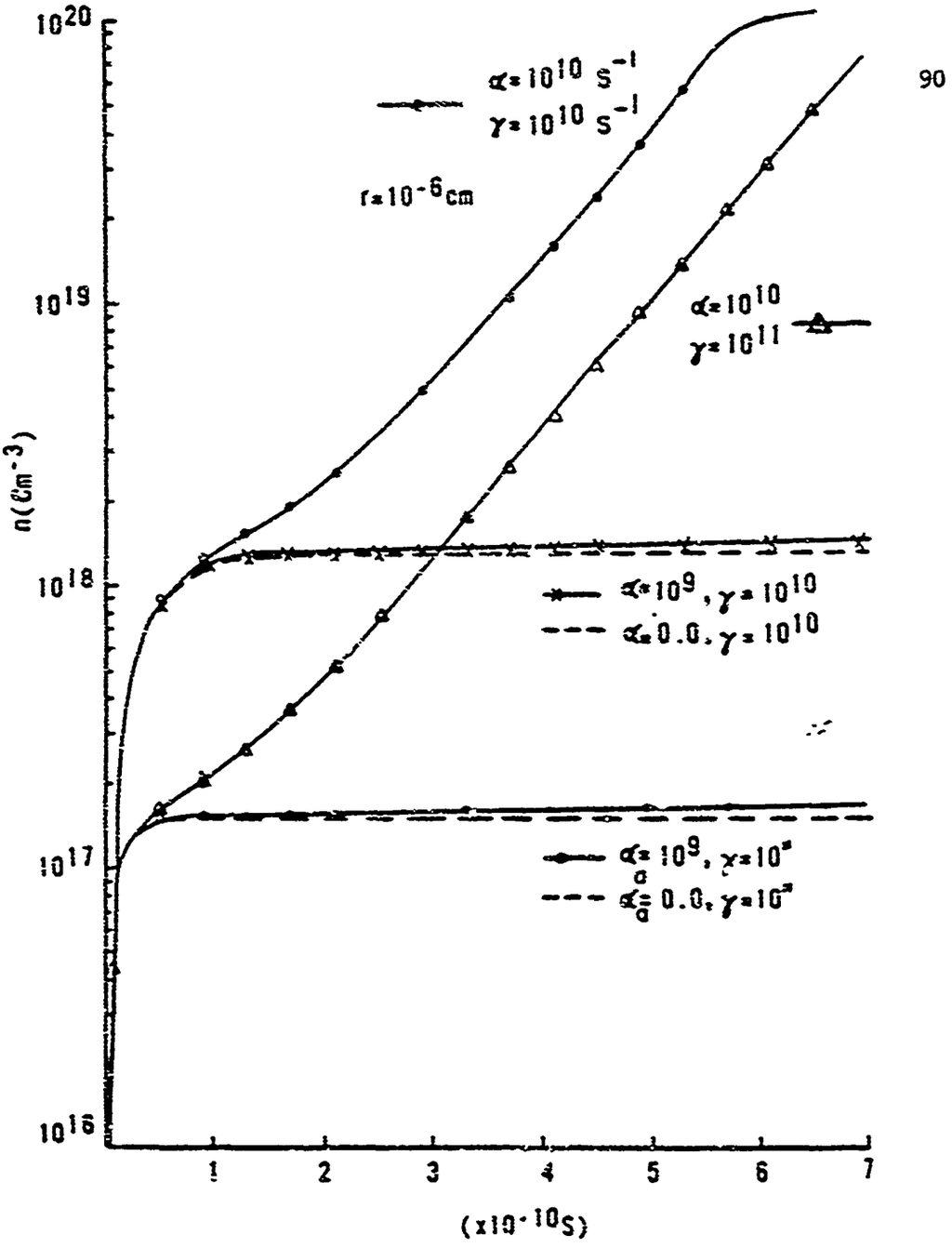

Fig. 26. The growth of the electron density - II.

The growth of the electron density at a radius of 100Å for various parameters. The parameters chosen are considered reasonable. Electron densities become very high at this radius both with and without avalanche ionization. D_e is assumed to be 0.01 cm^2/s.

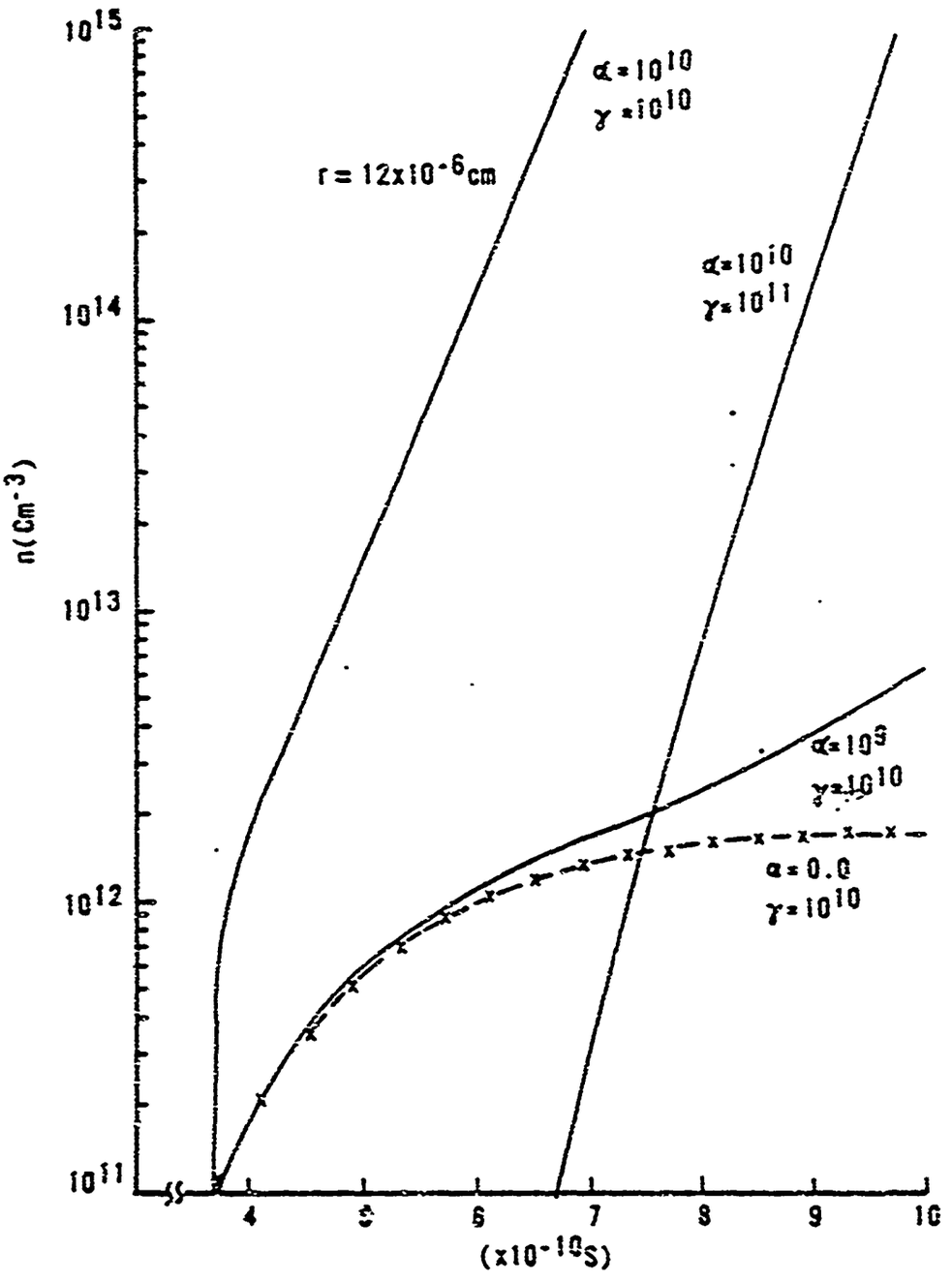

Fig. 27. The growth of the electron density - III.

The growth of the electron density at a radius of 1200 Å (1300 Å is the largest radius possible in a half wave film at 0.53 μM). Densities of the order of 10^{12} can be achieved by diffusion in the case considered if a sufficient number of electrons are available for photoionization. Otherwise an electron avalanche is required to reach and certainly to exceed this. The assumed D_e = 0.01 cm^2/s.

(colloids and aggregates of high density centers). The large density of shallow states (centers) which may coagulate about colloids, or coagulate about themselves, should provide lower levels required for a sustained avalanche process (i.e., the ionization of the off resonant centers requires significantly less energy than valence electrons).

The avalanche coefficients (10^9-10^{10}) were chosen by scaling data from Yablonovitch and Bloembergen [1972] using relations of Epifanov [1974] for 2.0 to 2.5 ev impurity states. These numbers were further supported by Eq. (67). It should be noted here that Eq. (67) is overly simplistic and may not be sufficiently conservative. In addition Epifanov [1985] believes that the coefficients determined in Yablonovitch and Bloembergen [1972] may be too high.

The approach taken here may not be considered rigorous. This is intended to be a feasibility study. The feasibility of this process or a similar one is considered sufficiently demonstrated. The exact processes involved are still considered unknown.

Conclusions

It has been shown that due to the non-ideal structure of an optical thin film, large local electron densities may be generated by non-stoichiometric colloids or aggregates of color centers. These are likely to exist in optical systems due to the conditions of deposition, substrate polishing and subsequent treatment. If avalanche ionization does occur in these films, regions as small as 100 Å in radius of colloids and centers may initiate the process. Otherwise regions

closer to the thickness of the film 10^3 - 10^4 Å of colloids and centers may be required.

It should be pointed out that colloids in the fluoride films would probably be oxidized due to ever present atmospheric oxygen. The process is thus further complicated. Band edge transitions may actually be occuring in oxidized metallic colloids in fluoride films. In addition to this, correct absorption cross sections of metal colloids in the optical region have yet to be computed. Errors or inappropriate assumptions have been found in those reported in the literature.

Measurements of colloidal absorption bands indicate that it is likely that colloidal absorption at λ = 1.06 micron is a strong competitor for the two-photon process which would be required for M-centers in CaF_2. The two-photon computation produces transition rates significantly less than the one photon at 0.53 micron. However, correct colloidal cross sections need to be computed for comparison. Also, more rigorous avalanche-computations need to be performed for this specialized case, if possible. It may not be possible due to the lack of knowledge of the thin film structure. In addition, complications such as oxidation and electron density variation of D_e and γ need to be accounted for.

Despite the details that have been neglected it is believed that feasibility has been shown.

CHAPTER 7

TEMPERATURE DEPENDENT EFFECTS

Theoretically, temperature dependence exhibits itself through several mechanisms. The first and most obvious is through the electron distribution. Increased temperature means increased phonon activity and increase in electrons statistically promoted to the conduction band, from either a shallow state or a valence band.

The second mechanism for temperature dependence is the band gap. The band gap invariably decreases with increased temperature.

A third effect of temperature is its affect on the material parameters. That is, the thermal diffusion, electron diffusion, electron recombination, etc.

One final role that temperature has is the secondary role that it plays in the primary processes, such as avalanche ionization. Here, the temperature, as above, exhibits itself via electron phonon collisions. The high energy phonons assist in promoting electrons up in energy in the conduction band. This role is considered of minor importance since it only requires a quantitative adjustment of the dominant processes. It is very important, however for quantitative calculation for comparison with data.

A model of the electron distribution in ideal solids is well known, and can be shown to be [Beam 1965]

$$n_e = \frac{8(\pi kT)^{3/2}}{h^3\sqrt{2}} m_n^{*3/4} m_p^{*3/4} e^{-E_g/2kT} . \quad (71)$$

In this relation, n_e is the conduction electron density, k is the boltzmann constant, m_n^* and m_p^* are the effective electron and hole masses and h is Planck's constant. This is, of course, directly related to the free carrier absorption coefficient by the Drude model

$$\alpha = \frac{\mu 4\pi e^2 \tau_k n_e}{Cn_r m_n^* (1 + \omega^2 \tau_k^2)} \quad (72)$$

where u is the magnetic permeability, τ_k is the momentum exchange (collision) time, ω is the incident field frequency and n_r and n_e are the real index and electron density.

Komolov [1982] finds experimentally that

$$\alpha(T) = \alpha_I + \alpha_0 e^{-u/T} \quad (73)$$

where for TiO_2 at optical frequencies

$$\alpha(T) = (80 \rightarrow 180) + (4.x10^7 \rightarrow 10^8) e^{-(21,000 \rightarrow 17,600)/T} (cm^{-1}) . \quad (74)$$

Since the band gap is at about 3eV = 2kT this yields a value of T = u = $1.8x10^4$. With a melting temperature of 2133 K this yields a maximum value at melting or $\alpha(T) = 180 + 10^8 \exp(-17,600/2133) = 2.6x10^4$. Although this is nearly on the order of the required absorption ($\sim 10^5$) it requires reaching the melting temperature to achieve this value.

The value of $\alpha_0 = 10^8$ is also about two orders of magnitude greater than theory predicts. However, the temperature dependence of the band gap will contribute to this process.

The band gap variation may be included as $E_g = E_{g0} - \gamma T$ where a relatively large value of γ from literature is 8 [Popov and Fedorov 1983]. To be liberal, the value $\gamma = 10$ is chosen. Thus $E_g = 3eV - 10(0.86x10^{-4})(2133) = 1.17$ at melting, so that $\alpha(T) = 1.7x10^5 cm^{-1}$. Under these liberal conditions it is clear that temperature dependence can be important. However, for temperature dependent absorption to dominate requires an initial absorbing impurity on the order of 10^{-4} cm to initialize the process [Komolov 1982]. Absorption centers in common oxide coating materials ($MgO, SiO_2 Al_2O_3$) are well known by those who study color centers [Schulman and Compton 1963]. It is also likely that many impurity transitions are within range of the conduction band in oxides. Thus if absorption centers of some sort start an isolated absorption in a film such as TiO_2 temperature dependent absorption may contribute via a spread by an absorption wave. This is an alternative to an avalanche ionization process. It is likely that if conditions are appropriate for an avalanche, it will dominate. It is a generally faster process than temperature dependent absorption and does not in theory demand such a significant initial absorption required to initiate a thermal instability involved in temperature dependent absorption. Furthermore, temperature dependent absorption may apply to only a select range of materials with small band gap [Komolov, 1982].

For example, if a typical fluoride film ($\sim CaF_2$) is considered, it can be found that $\alpha = 10^2 + 10^8 \exp(-5.8\times10^4/1775) = 10^2 + 8.35\times10^{-7}$. If the temperature dependence of the band gap is included $E_g = 10eV - 10(0.86\times10^{-4})\,.\,(1775) = 8.5$, $\alpha = 10^2 + 8.1\times10^{-5} cm^{-1}$. This is still an insignificant absorption at the melting temperature. In addition, it would require a very significant absorption to begin with in order to achieve a temperature near melting.

Thus, the only possible primary dependence on temperature for this case would be in the assist of the ionization of shallow trap centers and impurities. Since photoionization of resonant trap centers occurs on a scale of 10^{-11} seconds it is not likely that ionization of these is thermal. If temperature dependence does play a part in the absorption in large band gap coatings it is more likely that its contribution is in the assistance of impact ionization and photon absorption [Sparks and Duthler 1975]. Another way to look at this is to realize that for high intensity optical frequency interaction the electron temperature leads the phonon temperature. That is, the field interacts solely with electrons which impart their energy to phonons. It is less likely that electrons impart their energy to phonons and equilibrate with other phonons and then ionize valence or impurity bound electrons than it is that electrons are directly ionized. Trap centers, by their nature, have larger electron cross sections than the lattice ions. Any significant density of both trap centers and excited carriers necessitates impact ionization. Furthermore, simple computations (Eq. (67)) show that an optical field ($\sim$ 500 nm) at damage intensities ($\sim$ 1-2 (GW/cm^2)) for fluorides can generate one half to

three eV electrons in 10^{-10} seconds (depending upon the collisional frequency). These energies are sufficient to ionize many trap centers ($\sim$ 1 to 3 eV) along with some impurities [Sparks and Duthler 1977]. In this same time period even the most strongly absorbing ($\alpha = 10^5$ cm^{-1}) regions could increase at best a couple of tens of degrees K in temperature. If an absorption such as this exists there is no need for temperature dependent increase.

The temperature dependence of the material parameters may also be expressed theoretically. The thermal conductivity $k = \frac{1}{3} \sum_i c_i v_i l_i$, where i denotes the type of carrier, c is the contribution of carriers to the specific heat, v is the carrier velocity and l is its mean free path. At low temperatures $k \propto T^{i-n}$ where n = 0, 1, 2, or 3, due to the phonon frequency dependence of l and c [Touloukain 1970]. It generally has a positive slope at lower temperatures. At high temperatures k(T) is primarily governed by the temperature dependence of l (i.e. $l \propto 1/T$).

With the exceptions of SiO_2, HfO_2 and ZrO_2 the optical materials [Walker, 1981] are on the down slope of the conductivity curve at room temperature and above, with usually similar slopes [Touloukain 1970]. HfO_2 and ZrO_2 are approximately independent of temperature and SiO_2 is clearly positive ($\propto T^{1/2}$). Since the rate at which the heat is conducted away by the surrounding film is the point of interest, and in the problems of interest significant conduction takes place, it is felt that a relative measure of this rate is given by the room temperature conductivity. This is particularly true for materials where the behavior of the conductivity with temperature is

similar. It may be questioned as to whether materials which behave differently (SiO_2, HfO_2, ZrO_2) may be compared by this criterion.

The electron diffusivity is given theoretically by $D_e = \mu kT/e$, where mobility $\mu = e\tau/m^*$ [Beam 1965]. τ can be a complicated function of temperature. This occurs because it depends upon the energy of both the electrons and the phonons. Electron diffusivity as thermal diffusivity is a difficult quantity to determine for thin films. This quantity is used primarily to determine the rate of spread of the electron density. An order of magnitude value was chosen based upon theoretical considerations for this order of magnitude study and thus its dependence with temperature is not that significant to the feasibility of the process. This is true also of the other secondary effect rate constants.

In general, the part that temperature dependence plays in the material properties is not that important to the proposed process of electron density generation. The temperature effect is a quantitative correction. The feasibility of the process requires only order of magnitude values. The behavior of the thermal conductivity can affect the quantitative determination of damage threshold. However, due to the difficulty of a quantitative determination of the absorption process a qualitative (relative) measure of conductivities is adequate. The behavior of the thermal conductivity should not be important qualitatively. This is particularly true if the behavior is similar for various materials. The outstanding exception of the similar behaviors of conductivities is that of SiO_2. This may, in part, help

explain its anomalously high damage threshold with respect to other oxide coatings.

The temperature dependence in avalanche ionization may be dismissed as well. Avalanche ionization in optical thin films is a secondary process. The initial absorbing center would dominate the initiation of damage and an avalanche would simply provide a mechanism for the growth of an absorbing region. The basic temperature affect on avalanche ionization is to assist in promoting electrons to higher energies by collisions with more and higher energy phonons.

The basic conclusion of this study is that temperature dependence of absorption can play a part in the absorption of optical radiation in small band gap oxide coatings if avalanche ionization does not dominate. It is, however, probably a secondary effect which results in the growth of preexisting absorption center regions. Temperature dependent absorption cannot play any significant role of absorption in larger gap coatings, though.

CHAPTER 8

CONCLUSIONS

In Chapters 1 and 2 concepts of a localized absorbing region were introduced. Scaling laws were derived from the model in which thermal diffusion was the primary transport mechanism. These scalings related the macroscopic thermal material parameters to the damage threshold energy density of the incident laser field. The primary result from this work was that thermal transport through the region surrounding the absorption center dominated the rate at which damage occurred. Damage was assumed to occur when sufficient energy densities were present to melt the outside radius of the absorbing region. Thus, it is clear that the rate at which energy diffuses from this region is important.

In Chapters 3 and 4, the generality of integral transform techniques was exploited to investigate other forms of solutions. In particular, Chapter 3 dealt with the effects of the finite boundary due to a substrate on the film and Chapter 4 dealt with repetitively pulsed lasers. It was shown that the thermal conductivity of a substrate could make a difference in damage thresholds of a film under certain circumstances. These circumstances included the assumption that the film and substrate are in perfect thermal contact. This may be a poor assumption. However, if the absorption is at or sufficiently near the boundary, electron transport may occur. Electron transport across the boundary is not the assumed mechanism here. Thermal transport is the

mechanism assumed. The data indicates that thermal transport in the substrate is a contributing factor. The details of the boundary condition are not known. It was also shown that the laser field distribution in the film can be a significant factor.

Chapter 4 demonstrated that repetitively pulsed laser induced damage is more complicated than mere thermal effects. It also showed that thermal build up in optical coatings from repeated pulses should not, by itself, contribute to damage. However, a build up effect experimentally observed in optical components appears to be due to different mechanisms in different materials. The fact that an increase, as opposed to a decrease, in damage threshold occurs in certain films from the initial pulse supports this statement. It is possible that photo or thermal induced changes occur in the targets. Thus, subsequent pulses are incident upon a material that is in a different state from its state preceding the previous pulse. This state may be altered with every incident pulse leading to a build up phenomena. Such processes are not only complicated, but material and structure dependent. A thorough study of Multiple Pulse Damage Mechanisms, in itself should prove to be a fruitful exercise. It may very well contribute to the understanding of single pulse damage by demonstrating more apparently what occurs on the smaller scale of a single incident pulse.

Chapter 5 tied the findings of Chapters 1 through 3 to experimental damage data. The findings of these chapters were shown to agree remarkably well with the data. Furthermore, the morphology of damage corresponding to certain data (in particular, data on fluoride

films) was in support of the model. The scaling law derived in Chapter 2 scaled quite well with the experimentally measured damage threshold from several data sets. This scaling was shown to fit fluoride films best. A possible reason for the poor fit of oxides is that the absorbing region in some oxide films expands to large dimensions invalidating the application of a localized absorbing model. This expansion may be due either to an avalanche ionization, a temperature dependent absorption, or both. This does not occur in fluorides most probably because of their larger band gaps. In addition, experimental demonstration of increased substrate conductivities providing higher damage thresholds was given. This result was predicted in Chapter 3.

The investigation of a fundamental mechanism for providing the required absorption was the topic of chapter 6. Localized absorption on the order of 10^5 cm^{-1} does not exist prior to the damage shot and therefore it must evolve during the shot. A feasibility study demonstrated that absorption centers provided by collections of color centers were a clear possibility. Measurements and studies of absorption centers [Schulman and Compton 1963] indicate that colloids may also contribute to this absorption at the longer wavelengths. Multiphoton calculations of impurity atom transitions indicated that they were an unlikely source of large densities of conduction electrons, though multiphoton transitions of color centers may contribute.

The size of the region required for absorbing sufficient energy for damage indicates that it is likely that the initial absorbing region must expand. Of the mechanisms investigated for this process, avalanche ionization of the off resonant shallow states (including

impurity atoms) appears to be the most likely. Numerical calculations based upon this demonstrated the quantitative feasibility.

In Chapter 7 the effects of temperature were investigated. The effects of both temperature dependent absorption and the variation of material parameters with temperature were studied. Temperature dependent absorption was shown to be at best a secondary effect for most of the films of concern. It is clear, however, that the temperature behavior of the material parameters necessarily affects the quantitative calculations. The qualitative relations should not be affected significantly in most cases though. Thus, accounting of the temperature dependent behavior of the thermal parameters does not affect the feasibility of the processes and the generalized scalings. Any quantitative prediction attempts would require accounting for temperature dependence, particularly when more than order of magnitude values are of interest.

What has been presented in this text is a new model of laser induced damage in optical coatings. The idea of an absorbing inclusion is not new. The relations developed from the concept are, however, new. The explicit demonstration of scaling relations in various limits of transport is also new. In addition the demonstration of the relationship of thermal parameters to experimentally measured damage has not previously been done.

The wavelength dependence observed in optical coating damage lead to the formulation of a composite mechanism for laser induced damage evolution. This mechanism is also based upon the requirement of extraordinarily high localized absorption. The mechanism proposed is a

hypothetical construct based upon meeting requirements of the findings from thermal calculations. Comparison with data and numerical computation of microscopic phenomena support the model's feasibility. It is felt that feasibility has been sufficiently demonstrated for the process proposed.

The possible avenues of research implied in these findings are numerous. The most apparent are: the difference between oxides and flucrides, multiple pulse damage, measurement of the evolution and recombination kinetics of generated free carriers, measurement of thermal properties of thin films, the effect of material structure (crystalline, amorphous, etc.) on laser damage, measurement of color center concentrations in optical coatings, and the calculation of electron phonon and electron defect collision dynamics in intense fields. The answers to the questions associated with any one of these areas of research would contribute significantly to understanding the processes involved in pulsed laser induced damage. Efforts in a couple of these areas of research is presently underway at various institutions. It is the hope of this author that this present work has contributed to the understanding of the importance of these various processes.

APPENDIX A

SPHERICAL MODEL DERIVATION

In Appendix A the solution is derived for the spherical absorbing region using the integral transform method. This solution is then approximated in a certain region of behavior. This result (Eq. (10)) has provided tremendous insight into the processes, or at least the scale of processes, which occur in some cases of laser induced damage in thin films.

As stated in the text, the problem is modeled via Eqs. (A1) through (A5)

$$\frac{1}{D_i}\frac{\partial T_i(r,t)}{\partial t} = \frac{1}{r}\frac{\partial^2}{\partial r^2}(rT_i) + \frac{A}{K_i} \qquad r \leq a \tag{A1}$$

$$\frac{1}{D_h}\frac{\partial T_h(r,t)}{\partial t} = \frac{1}{r}\frac{\partial^2}{\partial r^2}(rT_h) \qquad a < r \tag{A2}$$

$$T_i(r,0) = T_h(r,0) = 0 \tag{A3}$$

where the subscripts i and h refer to the inclusion and the host respectively and A is the source term. The interface conditions between the impurity and the host is assumed to be

$$T_i(a,t) = T_h(a,t) \tag{A4}$$

$$K_i \left.\frac{dT_i}{dr}\right|_a = K_h \left.\frac{dT_h}{dr}\right|_a \tag{A5}$$

The integral transform technique involves expansion of the solution in appropriate eigenfunctions of the region which in this case are spherical Bessel functions. Because of the assumed spherical symmetry we need only consider spherical Bessel functions of order zero. These may be written as sines and cosines by the variable substitution U = rf. Thus Eqs. (A1) and (A2) become

$$\frac{1}{D_i}\frac{\partial U_i}{\partial t} = \frac{\partial^2 U_i}{\partial r^2} + \frac{rA}{K_i} \tag{A6}$$

$$\frac{1}{D_h}\frac{U_h}{t} = \frac{\partial^2 U_h}{\partial r^2} \tag{A7}$$

and the interface conditions become

$$U_i(a) = U_h(a) \tag{A8}$$

$$-K_i \left.\frac{\partial U_i}{\partial r}\right|_a + K_i \frac{U_i(a)}{a} = -K_h \left.\frac{\partial U_h}{\partial r}\right|_a + K_h \frac{U_h(a)}{a} \tag{A9}$$

We now have the auxiliary condition

$$U_i(r = 0,t) = 0 \tag{A10}$$

The appropriate eigenfunctions for this region are

$$F_i = \sin(\alpha r) \tag{A11}$$

and

$$F_h = B_1 \sin(\beta r) + B_2 \cos(\beta r) \tag{A12}$$

where α and β are continuous eigenvalues.

The overall temporal eigenvalue must be the same in both regions, i.e.

$$D_i\alpha^2 = D_h\beta^2 \equiv \lambda^2 \tag{A13}$$

The coefficients B_1 and B_2 may now be determined from the interface conditions for which we find

$$B_1 = \frac{1}{b\lambda}\left\{b\lambda \sin(\alpha a)\sin(\beta a) - \frac{D_h^{1/2}}{a} c \sin(\alpha a)\cos(\beta a) + \lambda \cos(\alpha a)\sin(\beta a)\right\} \tag{A14}$$

$$B_2 = \frac{1}{b\lambda}\left\{b\lambda \sin(\alpha a)\cos(\beta a) + \frac{D_i^{1/2}}{a} c \sin(\alpha a)\sin(\beta a) - \lambda \cos(\alpha a)\sin(\beta a)\right\} \tag{A15}$$

where

$$b = \frac{K_h D_i^{1/2}}{K_i D_h^{1/2}} \tag{A16}$$

and

$$c = 1 - \frac{K_h}{K_i} \tag{A17}$$

The eigenfunction normalization may be shown to be

$$N(\alpha) = \frac{2\pi^2 K_h}{(D_h D_i)^{1/2}} \left\{B_1^2(\alpha) + B_2^2(\alpha)\right\} \tag{A18}$$

which works out to be

$$N(y) = \frac{2\pi^2 K_i}{D_i b y^2} \{(c \sin y - y \cos y)^2 + b^2 y^2 \sin^2 y\} \qquad (A19)$$

with $y = \lambda a / D_i^{1/2} = \alpha a$.

The solution expanded in the eigenfunctions is of the form

$$U_R(r,t) = \int d\lambda C(\lambda,t) \nabla_R(\lambda,r) \qquad R = 1,h \qquad (A20)$$

The coefficients of the composite region then satisfy

$$C(\lambda,t) = \frac{1}{N(\lambda)} \sum_{R=i,h} \int dr_R \nabla_R(\lambda,r) U_R(r,t) \qquad (A21)$$

where use has been made of the orthogonality of the composite eigenfunction.

The time evolution of this coefficient is found by applying this transform operator to Eqs. (A6) - (A10). With the aid of Green's theorem the system and boundary conditions transform to an ordinary differential equation with the solution

$$C(\lambda,t) = \frac{\exp(-\lambda^2 t)}{N(\lambda)} \bar{\bar{A}}(\lambda,t) \qquad (A22)$$

where

$$\bar{\bar{A}}(\lambda,t) = \int_0^t dt' \exp(\lambda^2 t') \bar{A}(\lambda,t') \qquad (A23)$$

and

$$\bar{A}(\lambda,t') = 4\pi \int_0^a dr\, rA(r,t')\, \sin(\alpha r) \tag{A24}$$

Thus we find a solution of the form

$$T_R = \frac{U_R}{r} = \frac{1}{r} \int_0^\infty d\alpha C(\lambda,t) \Psi_R(\lambda,r)\} \tag{A25}$$

where for this case $\lambda = D_i^{1/2}\alpha$ and specifically for the impurity region

$$T_i(r,t) = \frac{D_i b}{2\pi^2 r a K_i} \int_0^\infty dy\{\frac{y^2 \sin(yr/a)\exp(-y^2 t/\gamma)\bar{\bar{A}}(y,t)}{(c\sin y - y\cos y)^2 + b^2 y^2 \sin^2 y}\} \tag{A26}$$

where $\gamma = a^2/D_i$. Now, if we assume that $A(r,t) = A(t)$ (i.e. absorption within the region is independent of the radius) $\bar{\bar{A}}$ becomes

$$\bar{\bar{A}}(y,t) = \frac{4\pi a^2}{y^2} (\sin y - y \cos y) \int_0^t dt' A(t') \exp(\frac{y^2 t'}{\gamma}) \tag{A27}$$

Thus

$$T_i(r,t) = \frac{2D_i ba}{\pi r K_i} \int_0^\infty dy F(y) \exp(\frac{-y^2 t}{\gamma}) \int_0^t dt' A(t') \exp(\frac{y^2 t'}{\gamma}) \tag{A28}$$

with

$$F(y) = \frac{(\sin y - y \cos y)\, \sin(yr/a)}{(c \sin y - y \cos y)^2 + b^2 y^2 \sin^2 y} \tag{A29}$$

It should be noted that no assumptions have been made as to the temporal behavior of the absorption profile.

The source term A is written in terms of the incident intensity I

$$\int_{V_i} dr^3 A(r,t) = Q(\frac{2\pi a}{\lambda}, n')I(t) \qquad (A30)$$

where Q is the absorption cross section computed from electromagentic theory and n' is the imaginary part of the index of refraction. The damage threshold is then defined as

$$E \equiv \int_0^{t_p} dt I(t) \qquad J\ cm^{-2} \qquad (A31)$$

where t_p is the pulse length required to reach the critical temperature T_c at the radius a of the absorbing region. Thus $T_c t_p = f(r,Q,E)$ is inverted to give $E = g(T_c,t_p,r,Q)$ for the damage threshold in Joules per centimeter squared.

Now, for a single square modeled pulse the integral becomes

$$T_i(r,t) = \frac{2D_i ba}{\pi r K_i} A\gamma \int_0^\infty dy \frac{F(y)}{y^2} \{1 - \exp(\frac{-y^2 t}{\gamma})\}. \qquad (A32)$$

The first term is shown to be analytically soluble by the LaPlace transform approach to this problem (Goldenberg, Tranter, 1952) or by multiple integration by parts when c = 0 and b = 1.

Thus, assuming $Q = \pi a^2$ and $E = It_p$,

$$Tt_p = \frac{3aE}{4K_i} \{\frac{K_i}{3K_h}$$

$$- \frac{2b}{\pi} \int_0^\infty \frac{\exp}{y^2} (\frac{-y^2 t_p}{\gamma}) \frac{(\sin y - y\cos y)\sin y dy}{[(c\sin y - y\cos y)^2 + b^2 y^2 \sin^2 y]}\} \qquad (A33)$$

Since for the region where $t_p/\gamma \geq 1$ the exponential dominates. The $F(y)/y^2$ may be expanded in a Taylor series about $y = 0$ and integrated term by term. The first term of the Taylor series is, for example,

$$\left.\frac{F(y)}{y^2}\right|_{y=0} = \frac{1}{3(c-1)^2} \tag{A34}$$

As stated in the text, the damage threshold has a minimum versus radius. That is, there is a size of absorbing region most likely to damage. This is found by taking $(dE/da) = 0$. In the first order approximation above, this is found to be

$$a = \frac{1}{2}\sqrt{D_h t_p \pi} \quad . \tag{A35}$$

Expanding to the next order and integrating, the solution is found to be

$$E_1 = 16T_c \frac{(\rho_h C_{ph} K_h t_p)^{1/2}}{\pi}$$

$$\left\{1 + \frac{\pi \rho_i C_{pi}}{120 \rho_h C_{ph}} \left(\frac{15 \rho_h C_{ph}}{\rho_i C_{pi}} - 10 - \frac{K_h}{K_i}\right)\right\}^{-1} \tag{A36}$$

where the second term in braces is usually quite small. Thus we may write

$$E_0 = 16Tc \frac{(\rho_h C_{ph} K_h t_p)^{1/2}}{\pi} \tag{A37}$$

Equation (A37) may be obtained directly by skipping the next order integration which lead to Eq. (A36). Performing the Next order integration allows one to see the validity of neglecting it.

APPENDIX B

CYLINDRICAL MODEL DERIVATION

In Appendix B the solution is derived for the cylindrical absorbing region using the integral transform method. This solution is then specified to a $\lambda/2$ standing wave between an insulating surface and an insulating substrate.

Mathematically the model is described by the following thermal diffusion equations:

$$\frac{1}{D_i}\frac{\partial T_i}{\partial t} = \frac{1}{r}\frac{\partial}{\partial r}\left(r\frac{\partial}{\partial r}T_i\right) + \frac{\partial^2 T_i}{\partial z^2} + \frac{A}{K_i} \qquad 0 \leq r < a, 0 \leq z < 1 \quad \text{(B1)}$$

$$\frac{1}{D_h}\frac{\partial T_h}{\partial t} = \frac{1}{r}\frac{\partial}{\partial r}\left(r\frac{\partial}{\partial r}T_h\right) + \frac{\partial^2 T_h}{\partial z^2} \qquad a < r, 0 \leq z < 1 \quad \text{(B2)}$$

$$\frac{1}{D_s}\frac{\partial T_s}{\partial t} = \frac{1}{r}\frac{\partial}{\partial r}\left(r\frac{\partial T_s}{\partial r}\right) + \frac{\partial^2 T_s}{\partial z^2} \qquad 0 \leq r, 1 < z \quad \text{(B3)}$$

$$T_i(r,z) = T_h(r,z) = T_s(r,z) = 0 \qquad t = 0 \quad \text{(B4)}$$

where A is the source term in watts per cubic centimeter.

Because there are no experimental data with which to assess the thermal impedance between the host and the inclusion (i.e. the heat transfer coefficient), ideal boundary conditions are assumed, i.e.

$$T_i = T_h$$

$$K_i \frac{dT_i}{dr} = K_h \frac{dT_h}{dr} \qquad \text{at } r = a, 0 \leq z < l \tag{B5}$$

$$T_i = T_s$$

$$K_i \frac{dT_i}{dz} = K_s \frac{dT_s}{dz} \qquad \text{at } 0 \leq r < a, z = l \tag{B6}$$

$$T_h = T_s$$

$$K_h \frac{dT_h}{dz} = K_s \frac{dT_s}{dz} \qquad \text{at } a < r, z = l \tag{B7}$$

and

$$\frac{dT}{dz} = 0 \qquad \text{at } z = 0 \tag{B8}$$

For the special cases of the infinite and the nonconducting substrates the problem reduces to Eq. (B1) and (B2) together with Eq. (B5) where Eq. (B6) and (B7) go to $T = 0$ at $z = l$ for an infinitely conducting substrate and $dT/dz = 0$ at $z = l$ for a nonconducting substrate. Exact solutions are found for these cases.

It should be noted that many common substrates employed in high energy laser reflectors are very poor conductors (e.g. SiO_2). Furthermore, as was shown for the common half-wave film the temperature at the boundary with the substrate does not change significantly for sufficiently short pulse lengths. The case of the nonconducting substrate therefore becomes an important one to consider.

The solution to this particular case may be developed by considering corresponding homogeneous equations for the combined system. The obvious eigenfunctions for the regions are

$$\psi_i = J_0(\alpha r)\ \cos\left(\frac{n\pi z}{l}\right) \tag{B9}$$

and

$$\psi_h = \{AJ_0(\beta r) + BY_0(\beta r)\}\ \cos\left(\frac{n\pi z}{l}\right) \tag{B10}$$

where J_0 and Y_0 are the Bessel functions of the first and second kind respectively and of order zero, and α and β are eigenvalues. Thus, we find solutions of the form

$$T_R(r,t) = \sum_n \int d\alpha\ \alpha\ C_n(\alpha,t)\psi_{Rn}(\alpha,r) \qquad R = i,h \tag{B11}$$

where the overall temporal eigenvalue must be the same in both regions, i.e.

$$D_i\{\alpha^2 + (\tfrac{n\pi}{l})^2\} = D_h\{\beta^2 + (\tfrac{n\pi}{l})^2\} \tag{B12}$$

The coefficients A and B may easily be solved for by satisfying boundary condition (B6) for the functions and their derivatives. We find that

$$A = \frac{\pi a}{2K_h}\ \{K_i\alpha J_1(\alpha a)Y_0(\beta a) - K_h\beta J_0(\alpha a)Y_1(\beta a)\} \tag{B13}$$

$$B = \frac{\pi a}{2K_h}\ \{K_h\beta J_1(\beta a)J_0(\alpha a) - K_i\alpha J_1(\alpha a)J_0(\beta a)\} \tag{B14}$$

and the eigenfunction normalization may be shown to be

$$N_n(\alpha) = \frac{1}{2}\{A_n^2(\alpha) + B_n^2(\alpha)\}\frac{K_h}{D_i} \tag{B15}$$

The coefficients $C_n(\alpha,t)$ may be found via orthogonality as

$$C_n(\alpha,t) = \frac{1}{N_n(\alpha)} \sum_{R=i,h} \int_r dr\, r \int_0^1 dz \frac{k_R}{D_R} \phi_{Rn}(\alpha r) T_R(r,t). \tag{B16}$$

Thus, to solve for $C_n(\alpha,t)$ explicitly the above transform is applied to the governing differential Eqs. (B1) and (B2). With the aid of Green's theorem the system and boundary conditions transform to an ordinary differential equation with a solution of

$$C_n(\alpha,t) = \frac{a}{N_n(\alpha)} \exp\{-D_i\{\alpha^2 + (\tfrac{n\pi}{l})^2\}t\} \frac{\hat{\bar{A}}_n(\alpha,t) J_1(\alpha a)}{\alpha} \tag{B17}$$

where

$$\hat{\bar{A}}_n(\alpha,t) = \int_0^t dt' \int_0^1 dz \cos(\tfrac{n\pi z}{l}) \exp[D_i\{\alpha^2 + (\tfrac{n\pi}{l})^2\}t']A(z,t') \tag{B18}$$

The resulting solution for the temperature at some point in the impurity and at a certain time then becomes

$$T_i(r,t) = \sum_n \int d\alpha\, \alpha\, C_n(\alpha,t) J_0(\alpha r)\cos(\tfrac{n\pi z}{l}) \tag{B19}$$

The source term $A(z,t')$ which describes the spatial and temporal absorption of radiation within the inclusion is quite general. No functional dependence on z and t has been assumed. This solution, therefore, can take into account the spatial dependence of standing

waves in the film and such temporal dependence as a repetively pulsed laser. Any spatial dependence can be repetitively pulsed by forming a sum of integrals over time, integrating from $(n-1)t_p + (n-1)t_d$ to $nt_p + (n-1)t_d$ where t_p is each pulse length, t_d is the delay time between pulses and n is the pulse number.

For the realistic case of a single-pulse sine-squared standing wave (half-wave film) the source term is

$$A(z,t) = A_0 \sin^2\left(\frac{\pi z}{l}\right) = \frac{A_0}{2}\left\{1 - \cos\left(\frac{2\pi z}{l}\right)\right\} \tag{B20}$$

In this case the coefficients become

$$C_n(\alpha,t) = \frac{A_0 a}{2N_n(\alpha)} \frac{1 - \exp\{-D_i\{\alpha^2+(n\pi/l)^2\}t\}}{D_i\{\alpha^2 + (n\pi/l)^2\}}$$

$$\times \frac{1}{2}\frac{J_1(\alpha a)}{\alpha}\left(\delta_{n0} - \delta_{n2}\right) \tag{B21}$$

so that

$$T_i = \sum_n \lambda_{ni} = T_{0i} + T_{2i} \tag{B22}$$

The source term A(z,t) can also be written in terms of the incident laser intensity $I(W\ cm^{-2})$ and the absorption cross section $Q(cm^2)$ by realizing that

$$\int_R dr^3\ A(r,t) = QI(t) \qquad 0 < t < t_p$$

$$A = 0 \qquad t_p < t \tag{B23}$$

where t_p is the duration of the laser pulse. In this case

$$\frac{A_0}{2} \pi a^2 l = IQ \tag{B24a}$$

or

$$A_0 = \frac{2IQ}{\pi a^2 l} \tag{B24b}$$

APPENDIX C

REPETITIVE PULSE DERIVATION

In Appendix C the process for extending all solutions in this text to the multiple pulse case is demonstrated. By integral transform, one is left with an ordinary differential equation in time which has the general solution of

$$\hat{\bar{A}} = \exp(-\xi t) \int_0^t dt' \exp(\xi t') F(\alpha) A(t') \tag{C1}$$

(see, for example, Eq. (39)). For the repetitively pulsed case where only thermal effects result,

$$\hat{\bar{A}} = \exp(-\xi t) F(\alpha) A \left\{ \int_0^{t_p} dt' \, e^{\xi t'} + \int_{t_d+t_p}^{t_d+2t_p} dt' \, e^{\xi t'} \right.$$

$$\left. + \ldots \int_{(N-1)(t_d+t_p)}^{(N-1)(t_d+t_p)+t_p} dt' \, e^{\xi t'} \right\} \tag{C2}$$

$$t_d + t_p = \tau \tag{C3}$$

$$\{\ \} = \int_0^{t_p} dt' e^{\xi t'} \left[1 + e^{\xi\tau} + \ldots + e^{(N-1)\tau\xi}\right] \tag{C4}$$

$$= \left(\frac{e^{\xi t_p} - 1}{\xi}\right) \sum_{n=0}^{N-1} (e^{\xi\tau})^n \qquad (C5)$$

$$= \frac{(e^{\xi t_p} - 1)}{\xi} \frac{(1 - e^{N\xi\tau})}{(1 - e^{\xi\tau})} \qquad (C6)$$

multiply by $e^{-\xi t} = e^{-\xi[(N-1)\tau + t_p]}$ to find

$$\hat{A} = (A_0 F(\alpha)) \left(\frac{(1 - e^{-\xi t_p})}{\xi} \frac{(1 - e^{-N\xi\tau})}{(1 - e^{-\xi\tau})}\right) \qquad (C7)$$

REFERENCES

Anisimov, S. I. and Makshantsev, B. I., "Role of Absorbing Inclusions in the Optical Breakdown of Transparent Media", Sov. Phys. Tech. Phys., 15, 1090 (1973).

Babadzhan, E. J., Kosachev, V. V., Lokhov, Yu. N. and Ryazanov, M. I., "Theory of the Absorption of Laser Radiation by Metalized Microinclusions in Transparent Materials", Fiz. Khim. Obrab. Mater., 17, 12 (1982).

Balitskas, S. K. and Maldutis, E. K., "Bulk Damage to Optical Glasses by Repeated Laser Irradiation", Sov. J. Quant. Elect. 11, 541 (1981).

Barna, P. B, Radoczi, G. and Reicha, M., "Surface Growth Morphology of Grain Boundaries in Al Thin Films", Int. Conf. on Thin Films, Stockholm, Sweden, (1984).

Bass, M. and Barrett, H. H., "Laser-Induced Damage Probability at 1.06 and 0.69 micron", Proc. Sym. Opt. Mat. High Pow. Las., NBS Spec. Publ. 372 58, (1972).

Bass, M. and Barrett, H. H., "Laser-Induced Damage Probability at 1.06 and 0.69 Micron", Appl. Opt. 12, 690 (1973).

Beam, W. R., Electronics of Solids, McGraw Hill (1965).

Beaumont, J. H. and Hayes, W. "M Centres in Alkaline Earth Fluorides", Proc. Roy. Soc. A. 309, 41, (1969).

Becker, M. F., Domann, F. E., Stewart, A. F. and Guenther, A. H., "Charge Emission and Related Precursor Events Associated with Laser Induced Damage", Proc. Sym. Opt. Mat. High Pow. Las., NBS Spec. Publ. 688 (1983).

Bettis, J. R., "Laser-Induced Damage as a Function of Dielectric Properties at 1.06 Micron", Dissertation, Air Force Inst. of Tech. (1975).

Bliss, E. S., Milam, D. and Bradbury, R. A., "Dielectric Mirror Damage by Laser Radiation over a Range of Pulse Durations and Beam Radii", Appl. Opt. 12, 677 (1973).

Bloembergen, N., "Role of Cracks, Pores and Absorbing Inclusions on Laser Induced Damage Threshold at Surfaces of Transparent Dielectrics", Appl. Opt., 12, 661 (1973).

Bordalon, M., Walser, R. M., Becker, M. F. and Jhee, Y-K., "A Study of the PRF Dependence of the Accumulation Effect in Multiple Pulse Laser Damage of Silicon", Proc. Sym. Opt. Mat. High Pow. Las., NBS Spec. Publ. 669, 427 (1982).

Born, M. and Wolf, E., Principles of Optics, 6th ed., 1980, Pergamon Press.

Burstain, E. "Anomalous Optical Absorption Limit in In Sb, Phys. Rev. 93, 632 (1954).

Epifanov, A. S. "Avalanche Ionization Induced in Solid Transparent Dielectrics by Strong Laser Pulses", Sov. Phys. JETP, 40, 897 (1974).

Epifanov, A. S., Lebedev Institute, Moscow, Private Communications, Nov. (1985).

Foltyn, S. R. and Jolin, L. J., "Catastrophic Versus Microscopic Damage: Applicability of Laboratory Measurements to Real Systems", Proc. Sym. Opt. Mat. High Pow. Las., NBS Spec. Publ. 688 (1983).

Fowler, W. B. "Relaxation of the Excited F Center," Phys. Rev. 135, 1725 (1964).

Fowler, W. B. Physics of Color Centers, Academic Press, N.Y., (1968).

Fradin, D. W.; Yablonovitch, E. and Bass, M. "Confirmation of an Electron Avalanche Causing Laser-Induced Bulk Damage at 1.06 Micron", App. Opt., 12, 700 (1973).

Goldenberg, H. and Tranter, J. C., Br. J. Appl. Phys., 2, 296 (1952).

Goldsmith, A., Waterman, T. E. and Hirchhorn, H. J., Handbook of Thermophysical Prof. of Solid Mat., MacMillan Co., New York (1961).

Gorshkov, B. G., Danileiko, Yu. K., Nikolaev, V. N. and Sidorin, A. V., "Effects of Multiple Interaction in Laser Damage to Optical Materials", Sov. J. Quant. Elect. 13, 388 (1983).

Gray, D. E., ed., A.I.P. Handbook, Sec. 7; 3rd ed.; McGraw Hill (1973a).

Gray, D. E., ed., A.I.P. Handbook, Sec. 9; 3rd ed.; McGraw Hill (1973b).

Guenther, K. H., "Nodular Defects in Dielectric Multilayers and Thick Single Layers", Appl. Opt. 20, 1034 (1981).

Hayes, W. Crystals with Fluorites Structures, Oxford: Clarendon Press (1974).

Hurt, H. H. and Decker, D. L., "High Resolution Electron Microscopy of Defects in Optical Materials", 1984 Proc. Sym. Opt. Mat. High Pow. Las., NBS Spec. Publ. to be published.

Kardach, J., Dissertation Research conducted at Air Force Weapons Lab., Air Force Inst. of Tech. (1985).

Komolov, V. L., "Optical Breakdown Produced by Intense Light in Thin Films Having Spatially Varying Absorption", Sov. Phys. Tech. Phys. 27, 311 (1982).

Koumvakalis, N., Lee, E. S. and Bass, M., "Single and Multiple Pulse Catastrophic Damage in Cu and Ag Diamond Turned Microns at 10.6, 1.06 and 0.532 Microns", NBS Spec. Publ. 669, 186 (1982).

Kovalev, A. A. and Makshantsev, B. I., Pilipetskii, N. F., Sidorin, Yu V. and Stonik, O. G., "Cumulative Effects and Time Dependence of the Optical Damage Threshold of Solid Transparent Dielectrics Exposed to Coherent Radiation", Sov. J. Quant. Elect. 10, 736 (1980).

Lao, B. and Smith, D. "The Development of Nodular Defects in Optical Coatings", 1985 Proc. Sym. Opt. Mat. High Pow. Las., NBS Spec. Pub., to be published.

Lewis, K. L., Pitt, A. M., Cullis, A. G., Chew, N. G. and Charlwood, L., "Laser Induced Damage in Dense Optical Thin Films", 1985 Proc. Symp. Opt. Mat. High Pow. Las., NBS Spec. Pub., to be published.

Manenkov, A. A., Matyushin, G. A., Nechitailo, V. S., Prokhorov, A. M. and Tsaprikov, A. A., "On the Nature of Accumulation Effect in Laser-Induced Damage to Optical Materials", NBS Spec. Publ. 669, 436 (1982).

Merkle, L. D., Bass, M. and Swimm, R. T., "Multiple Pulsed Laser-Induced Bulk Damage in Crystalline and Pulsed Quartz at 1.06 and 0.53 Microns", Proc. Sym. Opt. Mat. High Pow. Las., NBS Spec. Publ. 669, 50 (1982).

Meyer, J. R.; Bartoli, F. J. and Kruer, M. R. "Optical Heating in Semiconductors" Phys. Rev. B. 21, 1559 (1980).

Milam, D., Lawrence Livermore Laboratory, personal communication (1984).

Nathan, V., Walker, T. W., Guenther, A. H., Air Force Weapons Laboratory, Albuquerque, Private Communications (1983).

Ovshinsky, S. R. "Reversible electrical Switching Phenomena in Disordered Structures," Physical Review Letters, 21, 1450 (1968).

Ozisik, N., Heat Conduction, Wiley, New York, 1st edn., (1980).

Popov, S. P. and Fedorov, G. M., "Influence of Narrowing of Energy Gapwidth of the Velocity of Ionization Waves in Transparent Dielectrics", Sov. Phys. Tech. Phys. 28 494 (1983).

Rainer, F., Lowdermilk, W. H., Milam, D., Carniglia, C. K. Tuttlehart, T. and Lichtenstein, T. L., "Damage Thresholds of Thin Films Materials and High Reflectors at 248 nm", NBS Spec. Publ. 669, 274 (1982)

Schulman, J. H. and Compton, W. D, Color Centers in Solids, Pergamon Press (1963).

Sparks, M. and Duthler, C. J. "Theoretical Studies of High-Power Ultra Violet and Infrared Materials," Fifth Tech. Rep. Xonics, Corp. Contract DAHC15-73-C-0127 (1975).

Sparks, M. and Duthler, C. J., "Theoretical Studies of High-Power Ultra Violet and Infrared Materials," 8th Tech. Rept. Xonics, Corp., Contract DAHC15-73-C-0127 (1976).

Sparks, M. and Duthler, C. J., "Theoretical Studies of High-Power Ultra Violet and Infrared Materials," 9-10 Tech. Rep. Xonics, Corp. Contract DAHC15-73-C-0127 (1977).

Touloukain, Y. S., Dir., Thermo Physical Properties of Matter, N. Y. Plenum Press (1970).

Vaidyanathan, A., Mitra, S., Narducci, L. and Shatras, R. "One-Photon Absorption in Direct Gap Semiconductors," Sol. Stat. Com. 21, 405 (1977).

Vaidyanathan, A., Walker, T., Guenther, A., Mitra, S., Narducci, L. "Comparison Keldysh and Perturbation Formulas for One-Photon Absorption," Phys. Rev. B20, 3526 (1979).

Walker, T. W., Air Force Weapons Laboratory, Private Communication (1983).

Walker, T. W., Guenther, A. H. and Nielsen, P., "Pulsed Laser-Induced Damage to Thin-Film Optical Coatings-Part I and II", IEEE J. Quant. Electron, QE-17, 2041 (1981).

Wiscombe, W. J., "MIE Scattering Calculations: Advances in Technique and Fast Vector-Speed Computer Codes", NCAR Tech. Note, NCAR/TN-140+STR (1979).

Wood, R. M., Sharma, S. K. and Waite, P., "Variation of Laser Induced Damage Threshold with Laser Pulse Repetition Frequency", Proc. Sym. Opt. Mat. High Pow. Las., NBS Spec. Publ. 669, 44 (1982).

Yablonovitch, E. and Bloembergen, N. "Avalanche Ionization and the Limiting Diameter of Filaments Induced by Light Pulse in Transparent Media," Phys. Rev. Let. 29, 907 (1972).

Yariv, A., Quantum Electronics, John Wiley (1967).